Role of Polycomb repressive complex 2 in thymic epithelial development and function

Inauguraldissertation

zur

Erlangung der Würde eines Doktors der Philosophie
vorgelegt der
Philosophisch-Naturwissenschaftlichen Fakultät
der Universität Basel

von

Hong Ying Teh
aus Singapur

Basel, 2017

Genehmigt von der Philosophisch-Naturwissenschaftlichen Fakultät
auf Antrag von

Prof. Dr. Georg A. Holländer
Prof. Dr. Daniela Finke
Prof. Patrick Matthias

Basel, den 21. Februar 2017

Prof. Dr. Martin Spiess
Dekan

TABLE OF CONTENTS

ABSTRACT

Thymic epithelial cells (TEC) make up a majority of the thymic stroma and can be classified into cortical (c) and medullary (m) compartment. TEC are responsible for generating a self-tolerant T cell repertoire and thus potentially self-reactive thymocytes are induced to undergo apoptosis in the process termed negative selection. For this purpose, TEC express over 19,000 protein-encoding genes to represent almost the entire repertoire of protein-encoded antigens of the host. Many of these genes are typically expressed only in specific organs and are referred to as tissue-restricted antigens (TRA). The autoimmune regulator (Aire) facilitates the expression of a subset of TRA and these Aire-regulated TRA occupy chromatin regions enriched with the trimethylation of 27th lysine on histone 3 (H3K27me3), an epigenetic mark is catalysed by the methyltransferase activity of Polycomb Repressive Complex 2 (PRC2). However, the physiological significance of H3K27me3 in TEC biology remains to be elucidated. To address this issue, mice with TEC-targeted PRC2 deficiency were generated. These mice displayed severely hypocellular thymi but yet maintained intact tissue architecture and total TEC cellularity. Within the TEC population, mTEC cellularity was drastically reduced and the maturation of mTEC was also hindered. Furthermore, the decrease in number of early T lineage progenitors recruited correlated with the reduced expression of chemokines by the cTEC. The deficiency of PRC2 in TEC also interfered with efficiency of negative selection and T_{reg} production. Single cell transcriptome and flow cytometric data demonstrated that the deficiency of PRC2 activity also provokes mTEC development along a novel lineage differentiation path. Taken together, these data provide experimental proof that PRC2 plays crucial roles in the regulation of TEC differentiation and the capacity to carry out negative selection.

ACKNOWLEDGEMENT

First and foremost, I would like to thank Professor Georg A. Holländer for his great support and mentorship during the past four years. As a supervisor, you have taken much time and effort to introduce me to the scientific arena. You have given me invaluable insights and guidance consistently throughout the PhD years for which I feel deep gratitude. You have also encourage me to keep learning and widen my horizon in the many discussions at work and as well giving me the chance to take part in several international conferences abroad. Thank you so much for allowing the chance to grow under your mentorship.

I would also like to express my sincere gratitude to Doctor Saulius Zuklys and Doctor Thomas Barthlott for being always keen to lend a helping hand. You both have provided me with patient guidance and much needed advices towards my thesis. I would also like to acknowledge Professor Daniela Finke and Professor Patrick Matthias as members of my PhD committee.

A big thank you to Carlos Mayer and Sanjay Gawade for the friendship and companionship in and out of the laboratory. You have given me immense support through out the years. I deeply cherish the moments we have shared. I would also like to thank Katrin Hafen, Rodrigo Recinos and Elli Christen for the great support for the technical support and advices that I have will never take for granted. I am also grateful for the time with all the past and present laboratory members: Angela Bosch, Marco Catucci, Simone Dertschnig, Martha Gaio, Noriko Shikama and Saule Zhanybekova.

I would also like to thank all my friends for the companionship, the kitchen dinners and adventures, which have filled the past years with wonderful memories to be cherished for the years to come.

Last but definitely not the least, I would like to express my gratitude to my family for the unwavering love and support. To my mother and father, who have made countless sacrifices in life to provide the best in life for my sister and I.

ABBREVIATIONS

Aire	Autoimmune regulator
CCL #	CC-chemokine ligand #
cTEC	Cortical thymic epithelial cells
dGuo	deoxyguanosine
DN	Double negatives
DP	Double positives
E #	Embryonic day #
Eed	Embryonic ectoderm development
EpCAM	Epithelial cell adhesion molecule
ETP	Early T lineage progenitor
Ezh1/2	Enhancer of Zeste 1/2
fl or floxed	Flanked by LoxP sites
FPKM	Fragments Per Kilobase of transcript per Million
gMFI	Geometric mean fluorescence intensity
H&E	Haematoxylin and eosin
H3K#	Lysine at position # of histone 3
HSC	Haematopoietic stem cells
i.p.	Intraperitoneal injection
IHC	Immunohistochemistry
IL	Interleukin
ISP	Immature CD8 single positives
K #	Cytokeratin #
LTi	Lymphoid tissue-inducer
MHC	Major histocompatibility complex
mTEC	Medullary thymic epithelial cells
PCA	Principle component analysis
PCR	Polymerase chain reaction
PHD	Plant homeodomain
PRC2	Polycomb repressive complex 2
qPCR	Quantitative PCR
RANKL	Receptor activator of nuclear factor kappa-B ligand
SP	Single positives
TCR	T cell receptor
TEC	Thymic epithelial cells
TEPC	Thymic epithelial progenitor cells
TRA	Tissue restricted antigen
T_{reg}	Regulatory T cells
TSS	Transcriptional start sites
tSNE	t-Distributed Stochastic Neighbor Embedding
UEA	*Ulex europaeus* agglutinin

1. INTRODUCTION

1.1. History of Thymus

"Seat of the soul" was what the ancient Greek physicians believed the thymus to be due to its close proximity to the heart. As early as 100-200AD, descriptions of the thymus have been recorded by Greek physicians Rufus of Ephesus and Galen of Pergamum. From the Middles Ages to the Baroque Age, the thymus was disregarded and thought by some to be merely a tissue filling up the chest cavity (*1*). The tipping point in unraveling the thymus physiology came along in 18th century with the invention of optical microscopy, when the anatomists William Hewson and Arthur Hill Hassall drew the link between thymus and the lymphatic systems through histological studies. By the 1950s, the lymphopoietic role of the thymus was well recognised (*2*). But the significant breakthrough in the understanding of the importance of thymus in the context of the immune system came only to light in 1961 when Jacques Miller observed the deficiency of a lymphocyte population, subsequently named T cells, as a consequence of surgically removing the thymus in newborn mice (*3*). In the following years, tremendous and combined efforts by numerous scientists have unravel the central role of thymus in processes such as positive selection of developing thymocytes (*4*), negative selection of self-reactive T cells (*5*) and the development of regulatory T cells (T_{reg}) (*6*). A detailed understanding of the thymus physiology has therefore evolved over an extended period of time and the ever-growing advances in modern technologies have spurred ongoing efforts to discover the yet unknown intricacies of the exact cellular and molecular functions of the thymus.

1.2. Anatomy of the Thymus

The thymus is a primary lymphoid organ and consists of 2 lobes. It is located anatomically in the anterior superior thoracic cavity, anterior to the heart and posterior to the sternum. The main bulk of the thymus cellularity consists of thymocytes while only a small fraction constitutes the stromal compartments. These stromal cells play the crucial role in supporting thymopoiesis through the production of both soluble and cell-bound factors (*7*). The stromal cells comprise a group of heterogeneous cell types whereby thymic epithelial cells (TEC) form the main bulk and contributions made of dendritic cells, macrophages, B cells.

The thymus can be divided into 2 structurally and functionally distinct compartments, a central medullary region surrounded by an outer cortical region. Most developing T cells, known as thymocytes, are situated in the peripheral cortical region and this compartment is highly dense with cells. The cortical thymic epithelial cells (cTEC) have mesh-like architecture thus providing an extensive surface area for simultaneous interaction with multiple thymocytes (**Figure 1**). In comparison, the thymic medulla is significantly less densely populated as only a small fraction of thymocytes survive the developmental processes in the cortex (**Section 1.5**) and attain the capacity to migrate into the medulla. The medullary thymic epithelial cells (mTEC) have a less mesh-like structure in comparison to cTEC (**Figure 1**) and express a vast array of tissue-restricted antigens for the final stages of thymocyte development (**Section 1.5.2**). The macrophages present among the thymic stroma play an important role of clearing cellular debris generated by the programmed cell death (apoptosis) of negatively selected thymocytes (*8*). As professional antigen-presenting cells, the dendritic cells are able to acquire tissue-restricted antigens from TEC and present these antigens to developing thymocytes (*9*). The dendritic cells acquire tissue-restricted antigens from

either mTEC undergoing homeostatic turnover (*10*) or exosomes containing tissue-restricted antigens released by TEC (*11*). Collectively, the thymic stroma provides a scaffold, and hence microenvironment, crucial for the development and egress of thymocytes.

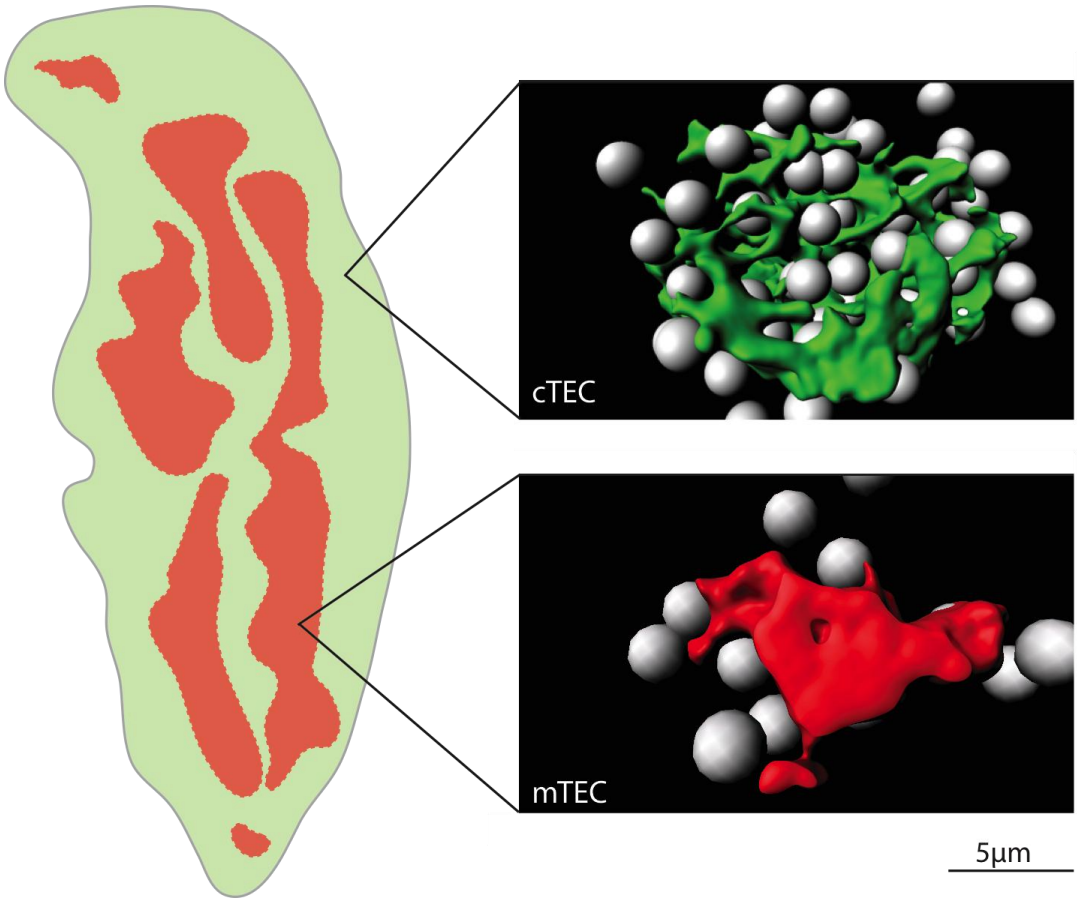

Figure 1. *Images of 3D-reconstructed thymic epithelial cells*. A schematic representation of the thymus, on the left side of the panel, shows the cortical region in the periphery (*green*) and the central medullary regions (*red*). The 3D-reconstruction of a singular cTEC (top right) shows a mesh-like architecture that forms extensive surface area for interaction with thymocytes (*grey*). While the mTEC (bottom right) has a much less complex structure and interact with relatively fewer thymocytes. The 3D images of the TECs were reconstructed from series of z-stacked confocal images using the Imaris®.

1.3. Thymus Organogenesis

Organogenesis of the thymus in mouse and man follows a series of bilateral developmental steps and are intimately tied to the formation of the parathyroid (**Figure 2**). These two organs form at about embryonic day 10.5 (E10.5) from a single primordium in the ventral aspect of the third pharyngeal pouch that is surrounded by neural crest cells that providing signals to support the primordium outgrowth. Parallel to this extension, expression of Foxhead box protein N1 (Foxn1) begins in the dorso-ventral region of the primordium from E11.25 onwards (*12*). Concurrently, the adjacent aspect of the primordium initiates the expression of Glial cells missing 2 (Gcm2). The expression of these two distinct transcription factors demarcates the distinct segment of the primordium with different developmental potential; Foxn1 determines the formation of the thymus epithelial scaffold while cells expressing Gcm2 are precursors of the parathyroids (*13*). However, the expression of Foxn1 is not necessary to determine thymic fate of the distal region as Foxn1 deficient mice (designated nude; *nu*/*nu* mice) are still able to form a rudimentary thymus anlage visibly segregated from the parathyroid glands (*13*). By E12.5, the organ primordia separate from the pharynx and migrate towards the anterior thoracic cavity with guidance from the neural crest cells (*14*).

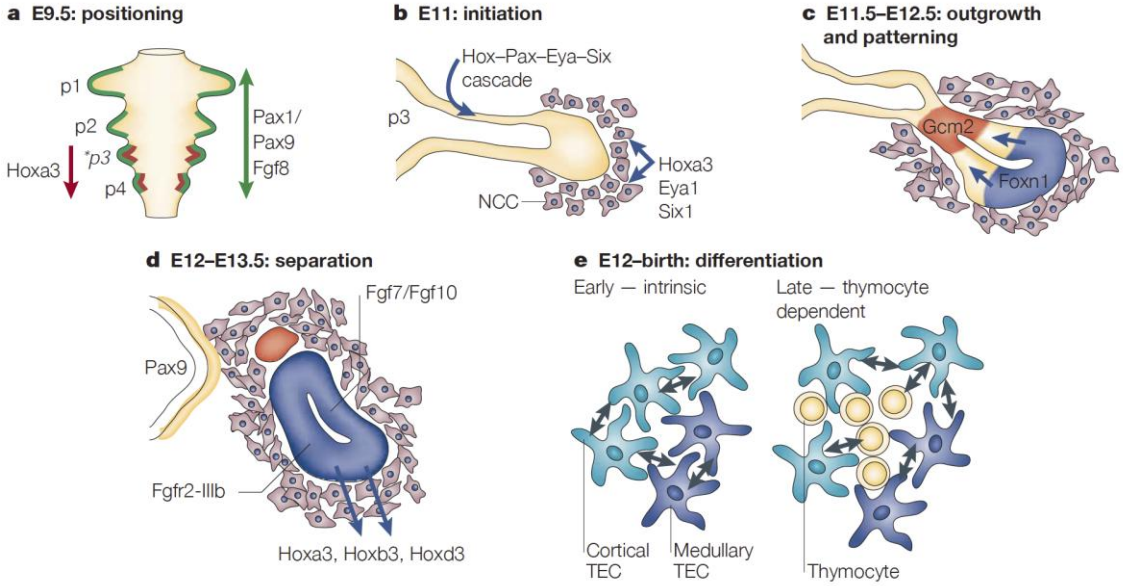

Figure 2. *Illustration of the current model of the early thymus organogenesis.* The thymus and parathyroid develop from a common anlage derived from outgrowths of the third pharyngeal pouch. The distal portion of the outgrowth initiates the expression of Foxn1 on E11.25 and eventually pinches off to form the thymus. The interactions of the thymus organ primordia with various factors from surrounding cells and subsequently recruited thymocytes are crucial for the development of a functional thymus. (*Image from Blackburn et al, 2004*)

1.4. Common thymic epithelium progenitor cell

The endodermal origin of TEC was experimentally proven when pharyngeal endoderm cells isolated from embryos at E9 and grafted under the kidney capsule of *nu/nu* mice was sufficient to give rise to a functional thymus (*15*). The differentiation of endodermal cells to functionally competent TEC requires however signals from the neural crest cells and recruited haematopoietic precursor cells and also depends on the intrinsic expression of Foxn1 (*7*) whose regulation of expression is only incompletely understood.

The distinct cTEC and mTEC lineages are derived from a common thymic epithelial progenitor cells (TEPC). Clues for the existence of these precursor cells came from the presence of cells stalled in an immature state found in thymic rudiments of the *nu/nu* mice (*16*). These cells are

phenotypically identified by their reactivity to either MTS20 or MTS24 antibodies and compose 50% of the epithelial cells in E12 thymus primordial (*16*). Using histochemistry, the majority of cTEC and mTEC stain positively for cytokeratin8 (K8) and cytokeratin5 (K5) respectively. K5 and K8 double positive cells are found to be abundant in E12 thymus primordia and also preferentially located in the postnatal mice at the cortico-medullary junction (*17*). These K5 and K8 double positive cells have therefore been postulated to be TEPC but cell transfer experiments have not yet proven this assumption. Nevertheless, the existence of a common source of TEPC was demonstrated when immature TEC isolated from E12 were able to contribute to both TEC compartments (*18*, *19*).

The relationship between the seemingly separate cortical and medullary TEC lineages was recently further detailed. Ohigashi and colleagues showed the expression of β5t in the TEPC and that the TEPC first acquire the cTEC phenotype but later diverge via asymmetrical differentiation to form also mTEC. β5t is a subunit of the proteasome and is exclusively expressed only in the cTEC (**Section 1.5.2**). Using transgenic mice, TEC that have expressed β5t at any stage of their development will be genetically marked to express enhanced green fluorescence protein (eGFP) in their progeny independent of whether these cells continue to express β5t or not. Under these experimental conditions, more than 90% of mTEC express eGFP despite the lack of active β5t expression. This suggests that the majority of mTEC are indeed derived from β5t-expressing progenitors (*20*) that may be localised in the postnatal thymus at the cortico-medullary junction (*21*).

After differentiation of TEPC into either cTEC or mTEC, the immature TEC begin to up-regulate MHC-II and CD40 and attain a mature state and only in the mTEC is Aire subsequently unregulated (*22*). The immature mTEC pool largely consists of slow cycling fraction while the mature mTEC pool has a turnover rate of 3 weeks (*23*).

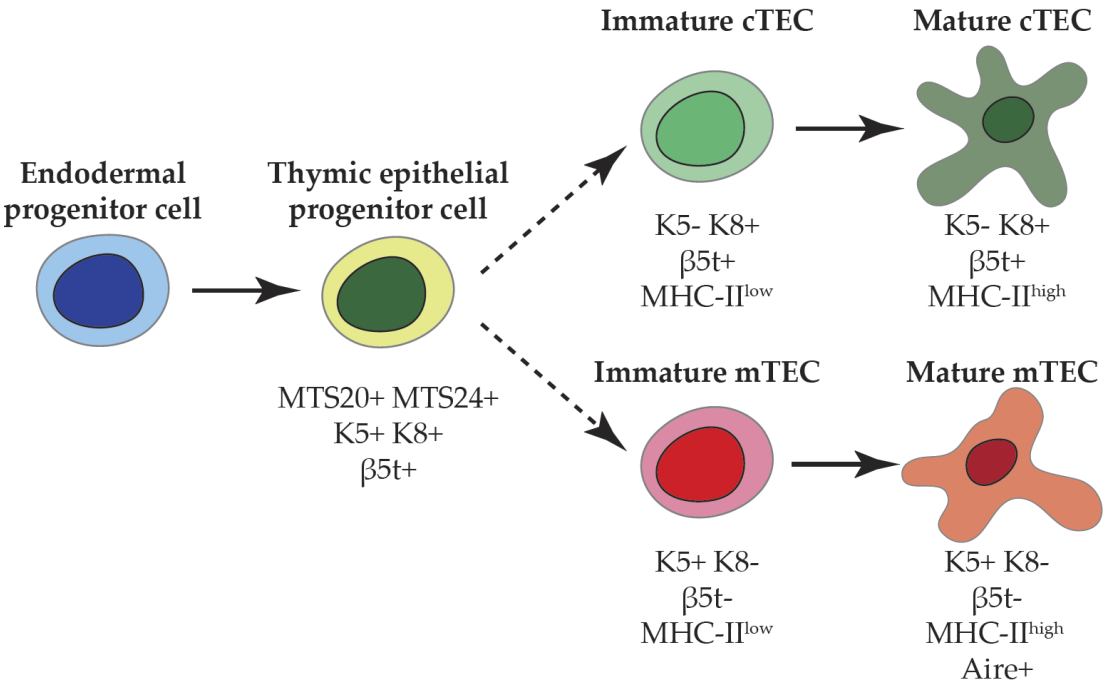

Figure 3. *Illustration of the model of thymic epithelial cell lineage development.* An endodermal progenitor gives rise to a common β5t-expressing TEC progenitor that is also positive for K5, K8, MTS20 and MTS24. This common TEC progenitor is likely to be restricted to thymic epithelial cell lineage and subsequently differentiates into either cTEC or mTEC.

1.5. Thymic epithelial cell function

1.5.1. T cell development in thymus

The primary role of the thymus is to support the differentiation and selection of T cells. The commitment to a T cell fate within the thymus microenvironment and subsequent maturation comprises a series of processes and is initiated with the recruitment of blood-borne T cell progenitors, also termed thymus-settling progenitors (*24*). Also the thymus does not contain a self-renewing progenitor pool, hence the thymus needs to have a continuous progenitor recruitment process to sustain T cell production. These blood-borne progenitors are rare with about only 200 cells per mouse and are lineage negative (markers to exclude B cells, myeloid and red blood cells) with high expression of stem cell antigen 1 (Sca1) and c-kit (*25*). Progenitor

recruitment occurs as early as E11.5 and is guided by the expression of CC-chemokine-ligand 21 (CCL21) and CCL25 in the embryo before vascularisation of the thymus (*26*). The chemokines continue to play a role in the recruitment of the T cell progenitors in the adult thymus (*27*). In addition to chemokines, T cell progenitors are also recruited through engagement of platelet-selectin glycoprotein ligand 1 (PSGL1) and P-selectin expressed on the thymic endothelial cells located mostly in the cortico-medullary junction (*28*). The level of expression of P-selectin on the endothelial cells can be regulated to control the rate of progenitor recruitment (*29*) and this receptivity can be influenced by the availability of niche within the thymus (*30*).

Upon recruitment, the thymus-settling progenitors then give rise to the early T lineage progenitor (ETP), a population that constitutes the most immature T-cell precursors within the thymus and that is phenotypically part of the DN1 sub-population (*31*). In these early stages, the thymocytes are termed double-negatives (DN) due to the lack of expression of two prominent T cell co-receptors, CD4 and CD8. The DN population is commonly separated into distinct and sequential cell stages based on their expression profile of CD44, a surface glycoprotein involved in cell interactions and migrations, and CD25, the α-chain of IL2-receptor. The cTEC express Delta-like 4, which commits ETP to T cell lineage through the engagement with Notch1-receptor on the ETP (*32*). cTEC also produce interleukin 7 (IL-7) that supports the survival of ETP (*33*). These two signals promote the development of DN1 (CD44+CD25-) to the DN2 stage (CD25+CD44+), and subsequently DN3 stage (CD25+CD44-) as they down-regulate CD44 expression. Thymocyte maturation is coupled by the migration of cells towards the capsular region of the thymus and the expression of recombination activating genes (RAG) 1 and 2, which drives the rearrangement of the gene locus encoding for T cell receptor β chain (TCRβ). This process forms unique combinations of

individual genes of variable (V), diversity (D), and joining (J) gene segments within the TCRβ gene locus and thus enables the generation of a sequence that encodes TCRβ chains with unique antigen-binding capabilities. At this stage, the DN3 express rearranged TCRβ together with a surrogate TCRα chain to form a pre-TCR on the cell surface and then complexes with CD3 to enable its signaling competency. Only about half of all thymocytes at this step manage to rearrange either of their two TCRβ loci to generate a functional pre-TCR to receive survival signals. This checkpoint in the early thymocyte development is termed as β-selection. Thymocytes passing the β-selection checkpoint undergo strong proliferate to expand clones of thymocytes expressing functional TCRβ (*34*). After the pre-TCR is expressed and begins signal transduction, the cells down-regulate CD25 and progress to DN4 stage (CD25-CD44-). In mice, these cells also being to express CD8 to become immature CD8 single positives (ISP) (*35*) and then later also express CD4 to attain a double-positive (DP) phenotype. During this process, the TCRα gene locus is being rearranged and the TCRα/TCRβ complex is then expressed on the cell surface (*36*).

At this stage, the thymocytes are probed for the functionality of their TCR by binding to peptide-major histocompatibility complex (MHC) complexes (*37*) expressed on surface of cTEC and also other cells in the cortex. This constitutes the second checkpoint in the thymocyte development, whereby the avidity of TCR binding to peptide-MHC complex will determines the further fate of DP thymocytes and is termed the positive/negative selection. Only thymocytes binding with sufficient affinity above a certain threshold will be positively selected for further maturation into single positives (SP). The vast majority of thymocytes have none or very low avidity for the peptide-MHC complexes and will undergo programmed cell death due to the lack of TCR-mediated survival signal, a process termed "death by neglect" (*38*). This process ensures that only thymocytes with a

functional TCR and capable of eliciting an immune response will proceed in the developmental process. Positively selected thymocytes transiently up-regulate an activation marker, CD69 (*39*) and then depending on whether the thymocytes recognise MHC-class-I (MHC-I) or MHC-class-II (MHC-II), the thymocytes further mature into CD8 SP or CD4 SP respectively (*40*). However, thymocytes possessing TCR with a high-avidity are able react against self-antigens to induce autoimmunity and thus must be deleted. Thymocytes binding to the peptide-MHC complexes on the stromal cells with high-avidity will undergo apoptosis in a process named "negative selection" (*41*). The first round of negative selection in the cortex is termed "Wave 1" and the cells can be identified by the co-expression of Helios and PD1 (*42*, *43*). Thymocytes surviving the first wave of deletion then up-regulate CC-chemokine-receptor 7 (CCR7) and migrate into the medulla to undergo further development. In the medulla, the SP thymocytes undergo further negative selection to fine tune the TCR repertoire and delete any self-reactive thymocytes that escaped negative selection in the cortex. This second round of negative selection is also referred to as "Wave 2" and the cells can be identified by the co-expression of Helios and Ox40 (CD134) within the medullary (CCR7+) CD4 SP (*42*, *43*). The cellular mechanism of the negative selection is dependent on the compartmentalisation of the Ras and mitogen-activated protein kinase (MAPK) signaling intermediates, which can be significantly shifted with small changes in affinity for peptide-MHC complexes at the threshold of negative selection (*44*). This allows the conversion of the TCR affinity values into a binary response. The outcome of this stringent selection process results in the survival of only about 5% of thymocytes with a low to intermediate avidity to proceed with the final stages of development (*45*).

However the deletion of self-reactive thymocyte is incomplete and thus, instead of undergoing apoptosis, undeleted self-reactive thymocytes

express Foxhead box protein P3 (Foxp3) and differentiate into regulatory T cells (T_{reg}). This constitutes the non-deletional tolerance whereby self-reactivity is averted via the development of undeleted self-reactive thymocytes into thymic-derived $Foxp3^{+}$ T_{reg} (*46*). Thymic T_{reg} produced in the first 3 postnatal days of the mice is crucial for the prevention of autoimmunity (*47*) and the development of thymic T_{reg} is dependent on the availability of niches in the medulla (*48*).

It takes ETP approximately 4 weeks to complete their development to a post selection stage of mature and functionally competent T cells that are now ready to exit the thymus. This is facilitated by the up-regulation of sphingosine-1-phosphate receptor 1 ($S1P_1$) that enables the process of egress of naïve T cells into the periphery (*49*).

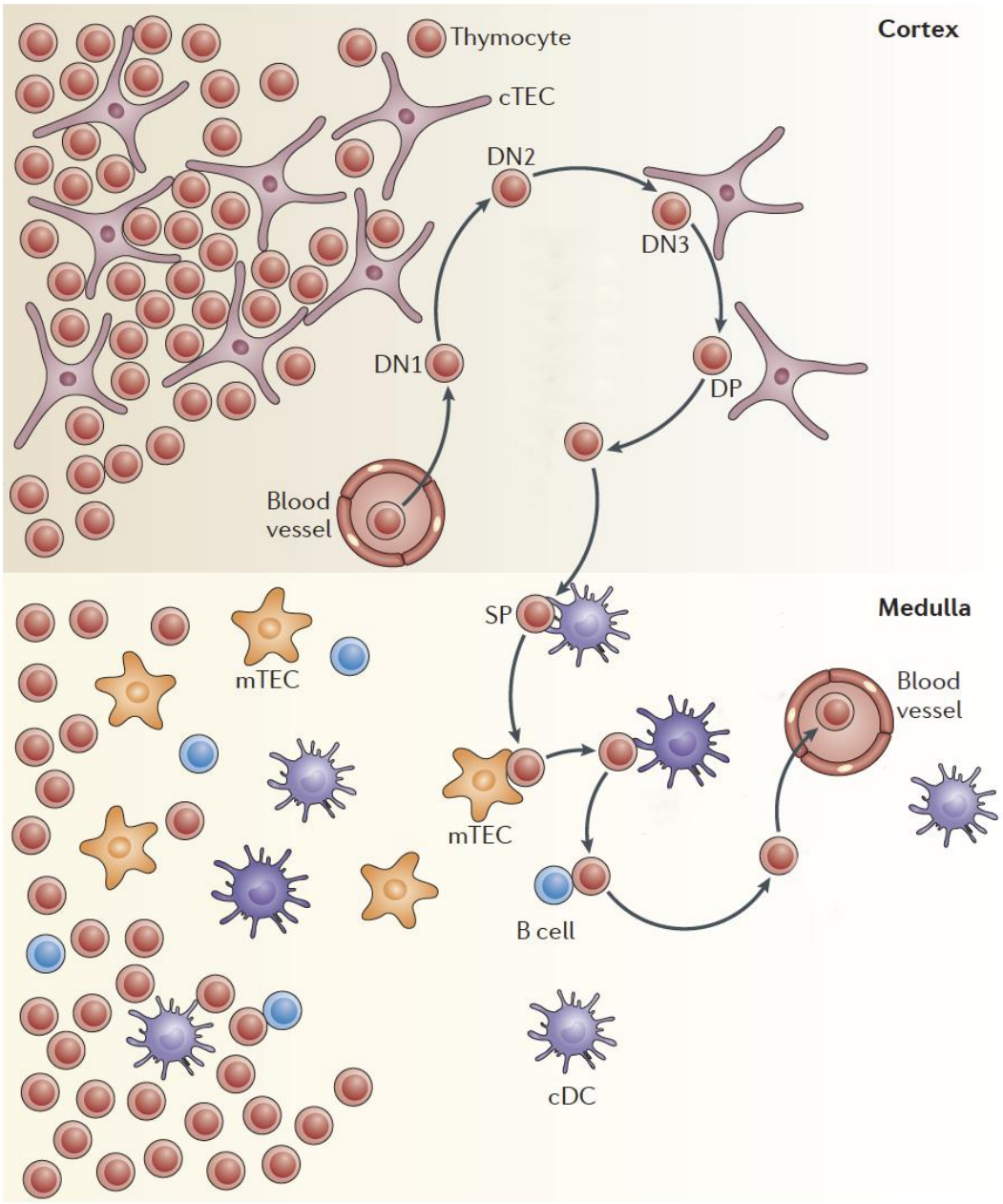

Figure 4. *Schematic diagram of T cell development in the thymus.* T cell progenitors are recruited to the thymus though blood vessels localised near the cortico-medullary junction. Guided by chemokines signals, these progenitors migrate to the cortex, commit to T cell fate, and initiate TCR gene rearrangement. The initial stages of T cell development are double negative for both CD4 and CD8 and hence are termed DN 1 to DN4. Upon successful TCR rearrangement, the thymocytes receive survival signal, up-regulate both TCR co-receptors, CD4 and CD8, and enter the DP stage. However, auto-reactive thymocytes with strong avidity to the tissue-restricted antigens presented on stromal cells are induced to undergo apoptosis in a process termed negative selection. As thymocytes continues to develop, they down-regulate one of the TCR co-receptors and enter the SP stage. SP cells then migrate to medullary region, where the remaining auto-reactive thymocytes undergo further negative selection or develop into T_{reg} cells. Finally, the cells complete the T cell development and exit the thymus as MHC restricted and self-tolerant naïve T cells. *(Image from Klein et al 2014.)*

1.5.2. Establishment of self-tolerance T cell repertoire

TEC express on their cell surface co-stimulatory and MHC molecules, the latter displaying a wide range of peptides including those derived from tissue-restricted antigens (TRA). These peptide-MHC complexes are essential for shaping the correct TCR repertoire and the TRA are defined as genes that are expressed in 5 or less tissues within entire body and contrast the group of housekeeping genes that are typically expressed in most if not all tissues (*50*). As a cell population, TEC hold unique capacity (in striking contrast to any other somatic cell population) of being able to express over 19,000 protein-coding genes (*50*), and are thus able to provide an almost complete range of the molecular signature of all cells in the body.

TEC possess, as professional antigen presenting cells, sophisticated cellular processes that allow the presentation of TRA-derived peptides in the context of MHC and co-stimulatory molecules (*51*). However, TEC specific mechanisms are in play to generate a uniquely shaped repertoire of self-peptides. Most notably, cTEC possess proteasomes composed of a unique subunit, β5t, which replaces the other components β5 and β5i found in proteasomes of all other cell types (*52*). This cTEC-specific (i.e. β5t-containing) proteasome produces peptides with high affinity to MHC-I molecules essential in fostering the selection of CD8 T cells (*52*). Other TEC-specific components involved in TRA processing for antigen-presentation by MHC-II molecules are Cathepsin L (Ctsl) and the thymus specific serine progease (TSSP). Both proteins determine the efficiency by which CD4SP T cells are selected (*53*–*55*).

One of the key factors crucial for the regulation of establishing central (i.e. thymic) immune tolerance concerns the function of the transcriptional facilitator autoimmune regulator (Aire). Expressed within the thymus most prominently in a population of mature mTEC (MHC-II^{hi} CD80^{+}), Aire

expression controls in mouse mTEC the expression of 3980 TRA (*50*). Complementary to the role of Aire, FEZ family zinc finger 2 (Fezf2) has recently been claimed as a transcription factor in mTEC that drives the expression a subset of Aire-independent TRA (*56*) although this finding could not yet be independently verified. Though most of the TRA expression appears to be stochastic, genomic single cell and population studies with subpopulations of mature mTEC indicate that some co-expression patterns may exist, possibly creating non-mutually exclusive sets of TRA patterns in specific mTEC populations (*57*). The underpinning mechanism for this observation has been suggested to be based on localised changes in chromatin structure on spatially placed adjacent but separate chromosomes creating 3D proximity within the nucleus of a single cell. How "fixed" these patterns are is at the moment a point of contention (*58*, *59*) and will need to be tested using refined chromatin analyses at single cell resolution, a method which is yet to be robustly established.

The exact molecular mechanism by which Aire drives expression of the TRA and other proteins remain incompletely defined. The reasons for this limited understanding lie, in part, in the complexity of the mechanism itself but also in the fact that primary mature mTEC and their Aire expression cannot be modeled in *in vitro* culture systems as Aire expression requires "cross-talk" with thymocytes and depends on a 3D-growing environment. Nonetheless, advances in technology, such as single cell RNA sequencing, have recently revealed intriguing insights into Aire's molecular mechanisms as a transcriptional facilitator.

1.5.3. Role of epigenetics in TRA expression

To elucidate the molecular mechanisms enabling TEC to express a very large number of TRA is challenging and TRA expression has to overcome the

tissue-specific mechanisms that enforce transcriptional silencing. It is therefore not surprising that TRA expression has been linked to epigenetics, which describes the heritable modifications to the genetic material without changing the underlying DNA sequences. Indeed, epigenetics mechanisms determine the temporal and spatial control of gene activity during development and therefore co-define cellular identity (*60*). To initiate and sustain epigenetic changes, at least three systems are currently considered that may operate in parallel to modify gene expression: DNA methylation, histone modifications and non-coding RNA-associated gene silencing (*61*).

Aire carries out its function of facilitating TRA gene expression in a complex with a large set of proteins that physically associated with it. The binding partners fall into four major functional classes: nuclear transport, transcription, pre-mRNA processing but also chromatin binding/structure (*62*, *63*). For example, Aire binds to MBD1 (methyl-CpG-binding domain protein), which associates with ATF7ip (activating transcription factor 7-interacting protein) and recognises methylated CpG dinucleotides, a repressive epigenetic marker enriched in promoters of inactivated genes (*64*). Thus, Aire coopts the normally repressive MBD1-ATF7ip complex and utilises the preferential recognition of specific methylated CpGs provided by MBD1 to localise and target TRA loci. This preferential recruitment of Aire to sites of selective repression likely works in concert with the PHD1 domain-mediated recognition of unmethylated 4th lysine residue on the histone H3 (H3K4me0) and may also involve other Aire binding partners such as the chromodomain-helicase-DNA-binding proteins, Chd4 and Chd6. Both of these proteins physically associate with Aire (*62*, *63*) and can bind to H3K4me0, trimethylated 27th lysine residue on the histone H3 (H3K27me3) and trimethylated 9th lysine residue on the histone H3 (H3K9me3) (*65*–*68*) to influence nucleosome mobilization (*69*), DNA repair (*70*), and transcriptional regulation (*71*). Additional evidence suggests that Aire complexes localise to

genes encoding TRA by recognizing repressive epigenetic marks (*50*, *refer to next section*) because the transcriptional start sites of Aire-controlled genes are typically (albeit not exclusively) marked by H3K72me3 and H3K9me3 but devoid of trimethylated 4th lysine residue on the histone H3 (H3K4me3) (*50*, *unpublished data from Holländer lab*). Thus, the expression of Aire-controlled TRA is very likely to be determined, at least in part, by the recognition of post-translational histone modification via Aire itself and its binding partners.

1.6. Histone modifications

1.6.1. Introduction to epigenetics

Epigenetic changes to the genome such as post-translational histone modifications, the presence of different forms of non-coding RNA sequences as well as DNA methylation constitute the main regulators of gene expression. These epigenetic modifications can induce changes in gene promoters thus regulating the accessibility for transcription factors and consequently transcription of the genes (*72*). Post-translational modifications of amino acid residues in the histone tail by methylation, acetylation, phosphorylation, ubiquitylation, and sumolyation play an essential role in regulating transcription via structural modifications consequent to changes in the state of chromatin compaction. Histone modifications can be broadly classified into either permissive (allowing transcription) or repressive (inhibiting transcription) marks (*73*). A typical example of a permissive histone mark is the H3K4me3 whereas the comparable modification at position 27 of the same molecule (H3K27me3) imposes a repressive mark instead. These two histone marks, albeit of opposing function, can co-exist on the same histone molecule resulting in a bivalent histone code, a feature commonly found with developmental genes where rapidly induced changes

in transcription are required in response to developmental cues (*74*). For example, the genes encoding the lineage-defining transcription factors Gata3, Tbet, Rorc and Foxp3 are marked with bivalent histone codes, which impart CD4 T cells with the plasticity to differentiate into different subsets in response to environmental cues (*75*–*77*).

1.6.2. Polycomb repressive complex 2

The Polycomb repressive complex 2 (PRC2) is a chromatin remodeling complex that mediates silencing of gene expression in the context of cell pluripotency and differentiation by establishing H3K27me3 marks. The crucial role of PRC2 plays in the control of gene expression is highlighted by the observation of early embryonic lethality in mice lacking any of the core PRC2 components (*78*–*80*). PRC2 is a dynamic complex composed of four core components: embryonic ectoderm development (Eed), enhancer of zeste homolog 1/2 (Ezh1/2), suppressor of zeste 12 (Suz12), and retinoblastoma protein associated protein 46/48 (RbAp46/48). In addition to these core components, PRC2 can also interact with other co-factors that modulate its activity under specific cell-contextual conditions. One such example is jumonji and AT-rich interaction domain 2 (Jarid2) that acts as a demethylase regulating enzymatic activity of PRC2 (*81*). Another example is the adipocyte enhancer-binding protein 2 (Aebp2), an evolutionarily well conserved protein and isoforms of this protein are expressed in a developmental stage-specific pattern. Aebp2 binds to the close proximity to known target loci of PRC2 suggesting a targeting role for this complex in cells where Aebp2 is co-expressed with the PRC2 core components (*82*). Finally, the polycomb-like (PCL) proteins compose another group of co-factors of the PRC2 (*83*, *84*). PRC2 therefore acts as a holoenzyme with the contributions by additional components that procure the complex's maximum activity (*85*). However, it is

unclear whether the same mechanisms are also involved in the initial recruitment of PRC2 to a specific gene locus and maintaining its presence there.

PRC2 maintains the repressive chromatin state via the ability of Eed to recognise and bind to pre-existing H3K27me3 and consequently depositing more H3K27me3 marks on tails of neighbouring H3 histones (**Figure 5**) thus acting in a "forward" positive feedback mode (*86*). Furthermore, PRC2 also recruits PRC1, which monoubiquitylates lysine 119 of histone H2A (H2AK119ub), and jointly these two complexes cooperatively maintain the repressive state of the chromatin. Although many evidences have supported that recruitment of PRC1 and PRC2 are inter-dependent (*87*, *88*), more recent observations argue that neither H3K27me3 nor H2AK119ub are required for PRC targeting (*89*). Thus, the binding of either PRC complex could take place independently without any specific hierarchical order.

The PRC2 imposes a transcriptional repression on many gene loci including those that are identified for their role in developmental processes (*90, 91*). This activity is cell-contextual and may therefore differ between different cell types. In a mouse embryonic stem cell line, PRC2 is required for the silencing of pluripotent factors so as to allow the cell to differentiate (*83*, *92*). Under other conditions, PCR2 is needed for adipogenesis (*93*) or lymphopoiesis (*94*), whereas PRC2 inactivation initiates myogenesis (*95*) and epidermis formation (*96*).

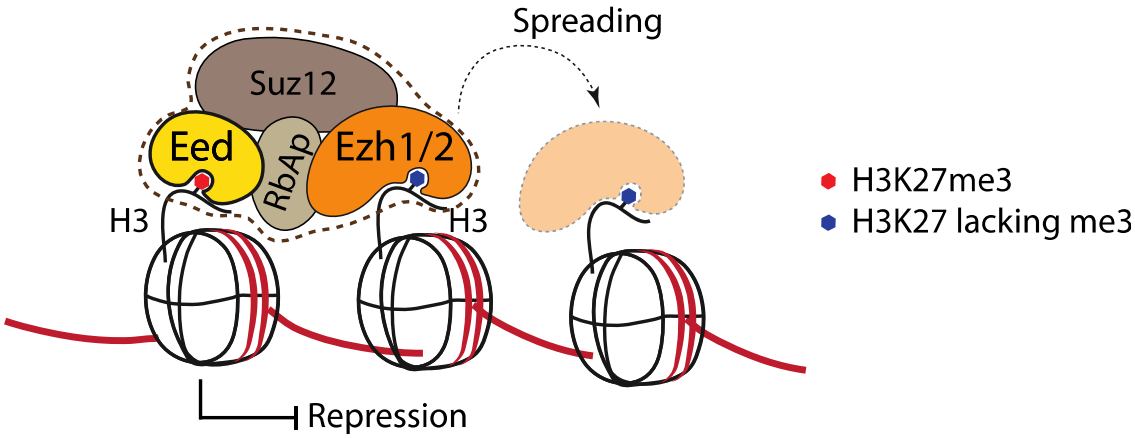

Figure 5. *Illustration of Polycomb Repressive Complex 2*. The holoenzyme PRC2 is represented by the 4 core components, Suz12, RbAp, Eed and Ezh1/2. The histone H3 amino-end tail can have either 27th lysine residue with (*red*) or without (*blue*) trimethylation modification. The Eed binds to pre-existing H3K27me3 while Ezh1 or Ezh2 catalyses the trimethylation of H3K27 of neighbouring histone H3 molecules. This mechanism allows PRC2 to deposit H3K27me3 marks on the chromatin in a positive feedback mode.

1.6.3. Eed

Eed physically associates with both Ezh1/2 via its WD (tryptophan-aspartic acid) domain (*97*) and with H3K27me3 modifications via its second WD domain (*86*, *98*). The latter interaction enables Eed to maintain a transcriptionally repressed chromatin state as described in the previous section (*86*). Deletion of Eed drastically precludes the trimethylation of 27th lysine residue of histone 3 (*99*). If the deletion of *Eed* is constitutive, embryogenesis is terminated on E9 due to a gastrulation failure and the lack of axial structures (node, notochord, somties) (*79*). These developmental defects are already clearly discernable by E8.5 with homozygous mutant mice demonstrating smaller and undifferentiated embryonic ectoderm and meager embryonic mesoderm. Nevertheless, Eed-deficient embryos have extensive development of extra-embryonic structures albeit not completely normal with the allantois being larger as compared to the wild types. Moreover, Eed is essential for the repression of the Homeobox (Hox) genes (Hoxa4, Hoxa7, Hoxb6, Hoxc8) during embryogenesis (*90*). The de-repression of these Hox

genes is also the consequence of the loss of PRC1 function (*100*, *101*) implying that both PRC1 and PRC2 possibly regulate the same homeotic genes. The function of Eed is not restricted to only early and mid-gestational developmental but has also been documented in postnatal life where a loss of Eed exhausts adult bone marrow haematopoietic stem cells (HSC) despite a normal production of fetal liver HSCs (*102*).

1.6.4. Ezh1 and Ezh2

Enhance of zeste (E(z)), or the mammalian homolog Ezh, is one of the founding member of the family of SET domain family of proteins. The domain's acronym derives from the identification of conserved structure in 3 *Drosophila melanogaster* proteins, namely Suppressor of variegation 3-9, E(z), and Trithorax (*103–105*). The SET domain, within the Ezh subunit, imparts the histone lysine methyltransferase activity and requires interaction with Eed for its catalytic activity (*106*, *107*). Two homologs of Ezh have been identified in mammalian cells, whereby Ezh1 and Ezh2 exert only partial redundancy that are not interchangeable (*99*). Both genes will therefore have to be deleted to achieve a complete loss in H3K27me3 marks in many cell types (*96*, *102*, *108*). The Ezh homologs also have different expression pattern with Ezh1 present in both dividing and differentiating cells while Ezh2 expressed only in actively dividing cells (*109*). Ezh1 has a lower methyltransferase activity in comparison to Ezh2 (*109*), which may account for the differential activity of PRC2 complex that contain either Ezh1 or Ezh2. This difference in level of enzymatic activity has lead to the postulation that PRC2-Ezh2 complex establishes the cellular H3K27me3 through the stronger Ezh2-mediated methyltransferase activity while PRC2-Ezh1 complex restores and maintains H3K27me3 lost after histone exchange or demethylase activity (*85*). Moreover, Ezh1 and Ezh2 exert their individual functions in a differential and age-

sensitive fashion. For example, Ezh2 is essential in fetal but dispensable in adult HSC (*110*). On the other hand, Ezh1 is critical for postnatal HSCs as these proteins control self-renewal, differentiation and apoptosis (*102*).

The deletion of both Ezh1 and Ezh2 leads to the loss of Sox2 expression and consequently altered the cell fate of the epidermal progenitor cells. Thus, this reveals the important role of Ezh1 and Ezh2 for skin epithelial cell differentiation (*96*). In addition, Ezh2 methylates the transcription factors Stat3 and Gata4 resulting in a functional activation of the former but a repression of the latter (*96*, *111*). The precise role of either of these PRC2 subunits for thymic development and PGE remains, however unknown and is the focus of my research.

1.7. Importance of histone modifications to TRA expression

Experimental evidences linking the Aire molecular structure to the recognition of specific epigenetic modifications and TRA expression have accumulated to suggest that Aire's function is mainly related to cues provided by specific epigenetic marks present in mTEC. This postulation is supported by structural data demonstrating that plant homeodomain 1 (PHD1) domain on Aire binds directly and with sufficient affinity to H3K4me0 (*112*, *113*). The importance of epigenetic landscape in defining Aire targets was revealed when Aire was found to induce expression of different sets of genes when etopically expressed in the pancreatic islet β cells as compared to primary mTEC (*114*). The variable severity of autoimmunity observed in Aire-deficient human (*115*) and mouse (*116*) also highlights the importance of epigenetic, and possibly genetic background, in Aire-driven TRA expression. Furthermore, the transcriptional start sites of genes transcriptionally controlled by Aire are enriched for the repressive histone mark H3K27me3

whereas marks indicating a permissive chromatin state such as H3K4me3 and H3K79me3 appear to be reduced (*50, unpublished data from Holländer's lab*).

It is therefore conceivable that Aire controls transcription of gene loci with a repressive state though the precise molecular mechanism how this may be achieved remains not yet defined. Two opposing models have been suggested to account for this seemingly contradictory phenomenon (*50*). The first model suggests that Aire is able to recognise repressive marks and "over-rides" this chromatin configuration due to its non-classical capacity to initiate transcription. The alternative model proposed that upon binding of Aire to a repressive chromatin configuration the epigenetic landscape of this locus is temporarily altered to a permissive state to allow the subsequent transcription to occur. Another challenge of elucidating the mechanisms driving TRA expression is that analysis of mTEC on population level might result in the under-representation of epigenetic marks since an individual TRA is expressed only in 1% to 3% of mTEC. Hence, evidence for either model is presently missing as analyses at single cell resolution of both transcriptional activity at a given locus and its precise histone marks are required to derive an unequivocal conclusion regarding the precise mechanism in play. This methodological tool is however not yet available rendering any conclusions unfounded as to how Aire and repressive epigenetic marks may co-opt for the purpose of driving TRA expression.

2. HYPOTHESIS AND AIMS

The main catalytic function of PRC2 is the trimethylation of histone 3 at lysine 27 (H3K27me3), which constitutes a repressive epigenetic mark for gene transcription. This modification is preferentially associated in medullary thymic epithelial cells (TEC) with transcriptional start sites (TSS) of Autoimmune regulator (Aire)-controlled loci. In contrast, H3K27me3 marks are lacking at these sites in genes that encode other genes, including Aire-independent tissue-restricted antigens (TRA). It has remained not only unknown but also not further investigated whether this correlation of H3K27me3 marks with TSS of Aire-controlled loci is coincidental or, alternatively, required for Aire-mediated transcription and thus for the molecule's capacity for TRA expression.

The hypothesis underpinning the experimental works presented in this thesis postulates that PRC2 function is essential for the regular differentiation of epithelial precursors into functional competent TEC able of expressing TRA in an Aire-dependent fashion.

This thesis addresses specifically the following aims:

1. The effects of PRC2-deficiency upon the differentiation and developmental processes of TEC.
2. The effects of PRC2-deficiency upon TEC function, including the integrity of the negative selection process that is dependent on the expression of TRA.

3. MATERIALS AND METHODS

3.1. Conditional targeted knockout mouse models

Eed^{tm1Sho}/J (Eed$^{fl/fl}$) mouse line was obtained from Stuart Orkin (Harvard) (*102*) and Ezh1^{tm1Jnw}Ezh2^{tm1Tara} (Ezh1^{KO}::Ezh2$^{fl/fl}$) mouse line was obtained from Elena Ezhkova (Mount Sinai) (*108*) with the permission of Thomas Jenuwein and Alexander Tarakhovsky. These 2 mouse lines were crossed with the mouse line carrying the transgene β5tCre to achieve TEC-targeted knockout of the lox-flanked genes, *Eed* and *Ezh2*, via the Cre-lox system. The heterozygous F1 generation is then crossed amongst littermates to obtain a subsequent offsprings homozygous for the lox-flanked transgene (either Eed$^{fl/fl}$::β5tCre or Ezh1^{KO}::Ezh2$^{fl/fl}$::β5tCre). The Eed$^{fl/fl}$::β5tCre mouse line was further crossed with Cg-*t(ROSA)26Sor*$^{tm6(CAG-ZsGreen1)Hze}$/J (ZsGreen) mouse line to achieve triple transgenic mouse line with Eed targeted knockout and ZsGreen expression in cells that have expressed β5tCre (Eed$^{fl/fl}$::β5tCre::ZsGreen). All mouse strains were kept in accordance with federal regulations.

3.2. Mouse Genotyping

Toes from the mice were clipped at the age of 1 to 2 weeks old. The toes were subsequently lysed using lysis buffer [0.1M Tris adjusted to pH8.5 (Sigma, St. Louis, USA), 5mM EDTA (Sigma, St. Louis, USA), 0.2M NaCl (Sigma, St. Louis, USA), 0.4% SDS (Sigma, St. Louis, USA), 0.1mg/ml Proteinase K (Amresco, Solon, Ohio, USA)] and incubation for at least 2 hours at 56°C and 750rpm. To purify the DNA, an equal volume of isopropanol (Sigma, St. Louis, USA) is added to precipitate the DNA, then spun down at

14000rpm for 3min, washed with 70% ethanol (Sigma, St. Louis, USA) and subsequently dissolved in TE buffer (Ambrion, Minneapolis, USA). To determine the mouse genotype, the PCR reactions were carried out with primers at final concentration of 0.4mM, 1x PCR buffer (Sigma, USA), 0.2mM dNTP (Sigma, USA) and 0.5U Taq polymerase (Sigma, USA). The reactions were then placed in PCR machine (Eppendorf, CH) with a hot start of 94°C for 5min, followed by 35 cycles of 95°C for 30sec, 58°C for 30sec, 72°C for 30sec and finally 72°C for 10min. The resulting PCR reaction products were resolved by gel electrophoresis with 1.5% agarose and 90V for 40min.

Table 1. *List of primers used for PCR genotyping*

Gene	Forward Primer	Reverse Primer
Cre (β5t)	GGCCTTTGAACGCACTGAC	GACAGGGCCTTCTCCACAC
Eed floxed	CTACGGGCAGGAGGAAGAG	GGGGGAGAGGGAGTTGTC
Eed deleted	CTACGGGCAGGAGGAAGAG	CCACATAGGCTCATAGAATTG
Ezh1 - KO	CTCCTGTCCTCATAGCAAGAC	GTACTCTTAACCACTGGACTG
Ezh2 floxed	CTGCTCTGAATGGCAACTCC	TTATTCATAGAGCCACCTGG
Ezh2 deleted	CTGCTCTGAATGGCAACTCC	ACGAAACAGCTCCAGATTCAGGG

3.3. Flow cytometry analysis reagents

For multi-coloured flow cytometry analyses, the monoclonal antibodies directed against specific murine antigens are summarised in the following table. These antibodies were conjugated to biotin, fluorescein isothyocyanate (FITC), phycoerythrin (PE), cyanin 5 (Cy5), allophycocyanin (APC), Alexa Fluor® 700, BrilliantViolet® dyes (421, 510, 605, 650, 786) or tandem dyes PE-Cy7, PerCP-Cy5.5, APC-Cy7, PE-TexasRed. In cases where biotin-conjugated primary monoclonal antibody is used, streptavidin conjugated to a specific fluorochrome was used for its detection. While for unconjugated primary monoclonal antibody, anti-rabbit IgG conjugated to Alexa Fluor® 555 or Alexa Fluor® 647 (Life Technologies, Oregon, USA) was used for its detection.

Table 2. *List of antibodies*

Antigen	Clone	Isotype	Manufacturer
Thymocytes / T cells			
CD4	RM4-5	Rat IgG2a, k	eBioscience
CD5	53-7.3	Rat IgG2a, k	eBioscience
CD8a	53-6.7	Rat IgG2a, k	BioLegend
CD19	6D5	Mouse IgA, k	Molecular Probes
CD24	M1/69	Rat IgG2b, k	eBioscience
CD25	PC61	Rat IgG1, λ	BioLegend
CD44	IM7	Rat IgG2b, k	BioLegend
CD62L	MEL-14	Rat IgG2ak	BioLegend
CD69	H1.2F3	Armenian Hamster IgG	BioLegend
CD73	TY11.8	Rat IgG1, λ	BioLegend
NK1.1	PK136	Mouse IgG2a, k	BioLegend
TCRβ	H57-597	Armenian Hamster IgG	BioLegend
c-kit (CD117)	2B8	Rat IgG2b, k	BioLegend
Foxp3	FJK-16s	Rat IgG2a, k	eBioscience
Helios	22F6	Armenian Hamster IgG	eBioscience
PD1	29F.1A12	Rat IgG2a, k	BioLegend
FR4	eBio12A5	Rat IgG2b, k	BioLegend
CCR7 (CD197)	4B12	Rat IgG2a, k	BioLegend
Ox40 (CD134)	OX-86	Rat IgG1, k	BioLegend
CD45.1	A20	Mouse IgG2a, k	eBioscience
γδTCR	GL3	Armenian Hamster IgG	eBioscience
Lineage markers for Thymocytes staining panel			
CD11b	M1/70	Rat IgG2b, k	BioLegend
CD11c	N418	Armenian Hamster IgG	BioLegend
PanNK (CD49b)	DX5	Rat IgM, k	BioLegend
CD31	390	Rat IgG2a, k	BioLegend
B220	RA3-6B2	Rat IgG2a, k	BioLegend
F4/80	BM8	Rat IgG2a, k	BioLegend
Gr1 (Ly6G/Ly6C)	RB6-8C5	Rat IgG2b, k	BioLegend
NK1.1	PK136	Rat IgG2a, k	BioLegend
TER119	TER-119	Rat IgG2b, k	Self-made
γδTCR	GL3	Armenian Hamster IgG	eBioscience
TECs			
EpCAM	G8.8	Rat IgG2a,k	BioLegend
UEA1	-	-	Reactolab/Self-made
Ly51	6C3	Rat IgG2a,k	BioLegend
CD45	M1/9.3.3.HL	Rat IgG2a	Self-made
IA/IE (MHC class II)	M5/114.15.2	Rat IgG2b, k	BioLegend
Aire	5H12	Rat IgG2c	eBioscience
H3K27me3	C36B11	Rabbit IgG	Cell Signalling
Total H3	ab1791	Rabbit IgG	AbCam
IgG2a control	-	Rabbit IgG	AbCam
Eed	ab4469	Rabbit IgG	AbCam

3.4. Analysis with flow cytometry

For analyses on TEC, thymic lobes were dissected and diced into small pieces and then incubated in PBS containing 200μg/ml Liberase™ (Roche Diagnostics, CH) and 30μg/ml DNaseI (Roche Diagnostics, CH) at 37°C for 60min with occasional pipetting to obtain single cell suspensions. Due to the scarcity of TEC, samples were enriched for TEC using AutoMACS (Miltenyi Biotec, USA) according to manufacturer's protocol. The enriched cell samples were then subsequently stained with monoclonal antibodies at 4°C for 45mins in PBS containing 2% (w/v) FCS (Perbio, UK). For intracellular staining, TEC first stained for surface antigens and thereafter fixed and permeabilised by using Cytofix/Cytoperm kit (Becton-Dickson, USA) according to manufacturer's protocol. The fixed cells are then stained with antibodies.

Single-cell suspension of haematopoietic cell samples were obtained from thymus and spleen by smashing the organs in between 2 sheets of nylon mesh with pore size of 100μm (Sefar Nitex, CH). The samples were then stained with monoclonal antibodies at 4°C for 45mins. For intracellular staining, cells were first stained with surface antigens then fixed and permeabilised by using Cytofix/Cytoperm Kit (eBioscience, USA) according to manufacturer's protocol.

Flow cytometric analysis and cell sorting were carried out using FACS Aria or FACS Fortessa. Data analyses were subsequently done using FlowJo software (Treestar, USA).

3.5. Real time quantitative PCR analysis

RNA samples were extracted from sorted cells by using RNeasy Micro Kit (Qiagen, CH) according to manufacturer's protocol. The RNA samples were then reverse transcribed into cDNA with SuperScript III Reverse

Transcriptase (Invitrogen, USA) according to instructions provided by the manufacturer. Subsequently, real time quantitative PCR was carried out on Rotor-Gene 3000A (Qiagen, CH) using SensiMix SYBR kit (Bioline, USA) to ascertain the relative gene expression levels.

Table 3. *List of primers used for quantitative PCR*

Gene	Foward Primer	Reverse Primer
GAPDH	TGAAGCAGGCATCTGAGGG	CGAAGGTGGAAGAGTGGGAG
Foxn1	TTGTGGAACTGGAGTCCACG	TGTTGGGCATAGCTCAAGCC
Rag2	CTGACTGCCTACCCCATGTT	GTGCGTTCTTCCAAATCCAT
Chemokines		
CXCL12	AAATCCTCAACACTCCAAAC	GCTTTCTCCAGGTACTCTTG
CCL19	CCTGGGTGGATCGCATCATCCG	AGAGCATCAGGAGGCCTGGTCCT
CCL21	AGAAAGCTTGCTGCCCTCCAA	GGCGCATCAGGTTCTGCACCCA
CCL25	CCACCCTAGGTCATCCCAGG	CCTAGGAAGTTCAGGGTATG
Cytokines		
IL7	CTTGCTTTTTCCAGCCACGT	AGGCATGGCTACCACACATG
c-kit Ligand	CACAAAACCATTTATGTTACCC	TTACAAGCGAAATGAGAGCC
IL15	GAATACATCCATCTCGTGCT	CCAGGTCATATCTTACATCTATCC
TSLP	ACGAATTGTACTTGTCCTGGGT	ACGAATTGTACTTGTCCTGGGT
Apoptotic Genes		
Bax	CTCAAGGCCCTGTGCACTAA	CACGGAGGAAGTCCAGTGTC
Bid	GACTCTGAGGTCAGCAACGG	CCTCCCAGTAAGCTTGCACA
Bcl-xl	CGCCGGAGATAGATTTGAATAACC	CCCGGTTGCTCTGAGACATT
Bak	CCAAGATCGCCTCCAGCCTA	CACGCTGGTAGACGTACAGG
Eed deletion		
Exon1-2	ATGTCCGAGAGGGAAGTGTC	TGTGTTTGTGCCACTCTCAA
Exon3-4	CTGCTCTGAATGGCAACTCC	GGACTGCAATAACCGTATCTCC
Exon5-6	TTTACACTTGTGCATGGACCT	CATTTCCATGGCCAACATAG
Exon7-8	CTCTTGTGGCAATATTCGGA	TGCATTTCATCATCCTCTTTGA

3.6. Histology and immunofluorescence confocal microscopy

The thymi were isolated and frozen immediately in the Optimal cutting temperature compound (OCT) (Cell Path, UK). Tissue sections of 8μm were sliced on a cryostat, dried and fixed with acetone (Sigma, USA) for both haematoxylin and eosin (H&E) and immunofluorescence staining. For H&E

staining, the tissue sections were subsequently dehydrated with increasing concentrations of ethanol, 50%, 75%, 95%, 100% (w/v), then stained with Mayer's haematoxylin (Réactifs RAL) and eosin (J.T. Baker). For immunofluorescence histology, the tissue sections were first fixed with 4% paraformaldehyde (Sigma, USA), then stained with antibodies (refer to *Table 2.3-1*) and subsequently detected using anti-IgG antibodies conjugated to Alexa Flour® fluorochrome. The section images were subsequently acquired with Leica SP5 confocal microscope.

3.7. T cell *in vitro* proliferation assay

T cells were first stained with appropriate fluorescence-labelled antibodies and then sorted flow cytometer. These cells were then stained with 2.5μg/ml of CFSE in PBS at room temperature. Following that, the cells were then cultured in triplicates with gamma-irradiated (2500cGy) spleenocytes extracted from RAG-/- mice and 1μg/ml of anti-CD3 antibody for 72hours in IMDM culture medium (Life Technologies, USA) with added 10% fetal bovine serum (Hyclone, Perbio, Belgium) and 1% Gentamycin (Life Technologies, USA). The supernatant were then aspirated and kept at -20°C until use for ELISA assay. To acertain the rate of proliferation, the cells were then stained with fluorescence-labelled antibodies and analysed with a flow cytometer for the proliferation rates. The proliferative index is calculated by following formula,

$$\text{Proliferative index} = \frac{\text{Total cell count}}{n_0 + \frac{n_1}{2} + \frac{n_2}{4} + \frac{n_3}{8} + \cdots + \frac{n_a}{2^a}}$$

a = number of cellular division as indicated by serial CFSE dilution

3.8. ELISA assay

The ELISA kit from eBioscience (USA) was used to determine the concentration of IL2 in the supernatant of the in vitro T cell culture. First, the 96-well-plates (Corning, USA) were coated with 5μg/well of capture antibody (anti-IL2 antibody) overnight at 4°C. The wells were then blocked with 1xELISASPOT diluent (eBioscience, USA) for 1 hour at room temperature. Next, the standards and samples were added to respective wells and incubated for 2 hours at room temperature. The biotinylated detection antibody was then added to each well and incubated for 1 hour at room temperature. 100μl of avidin-HRP (horseradish peroxidase) was then added to each well and incubated for 1 hour at room temperature. In between each steps, the wells were washed 4 times with PBS-0.05%Tween-20 (Sigma, USA). For detection, 50μg/well of TMB (tetramethylbenzidine) substrate solution was added and incubate for 15 minutes at room temperature followed by the addition of 100μl of 5N sulphuric acid stop solution. The absorbance values of each well were then acquired using an absorbance reader at 450nm.

3.9. BrdU Analysis

For analysis of proliferation in TEC, mice were injected intraperitoneally (i.p.) with 1mg BrdU (BD Pharmingen, USA) diluted in sterile phosphate buffered saline and analysed 16 hours later by flow cytometry (**Section 3.4**).

3.10. Fetal thymic organ culture

Thymic lobes were dissected from E15.5 embryos obtained from timed mated female mice. The thymic lobes were first placed on a 0.45 micro pore size filter (Milipore, USA) floating on culture medium (IMDM culture medium (Life Technologies, USA) plus 10% fetal bovine serum (Hyclone, Perbio, UK)) with added 1.35mM of 2'-deoxyguanosine (Sigma, USA) for 5 days to deplete the thymus of thymocytes. The filters were then transferred onto fresh medium (without 2'-deoxyguanosine) for 1 day. After that, the filters were transferred to fresh culture medium containing 10μg/ml of recombinant RANKL (obtained from Finke's Lab) for an additional 5 days. The thymic lobes were then incubated in PBS containing 200μg/ml Liberase™ (Roche Diagnostics, CH) and 30μg/ml DNaseI (Roche Diagnostics, CH) at 37°C for 60min with occasional pipetting to obtain single cell suspensions. The cells were stained with fluorescence-tagged antibodies for FACS analysis.

3.11. Cytospin

Single cell suspension of thymus tissue was obtained using the same method as described in **Section 3.4**. The cells were then stained with fluorescence-tagged antibodies for extracellular antigens and fixed with Cytofix/Cytoperm kit (Becton-Dickson, USA) according to manufacturer's protocol. The cells were then sorted using the FACS Aria to obtain specific cell populations and attached onto glass slides using the Cytospin (Thermo Scientific, USA) at 800g for 5min. The cells were then stained with monoclonal anti-Eed antibody (**Table 2**) and incubated overnight at 4°C. Subsequently, anti-rabbit IgG antibody conjugated to Alexa Flour® 555 was added to detect the anti-Eed antibody and images were acquired using SP5 Leica SP5 confocal microscope.

3.12. T-cell depletion

Two-weeks-old $Eed^{fl/fl}$ and $Eed^{fl/fl}$:: β5tCre mice were injected i.p. over 3 consecutive days with 200μg anti-CD4 (GK1.5), 100μg anti-CD8 (53-67) and 50μg anti-Thy1.2 (T24) per dose. All antibodies used were homemade and tested for the sufficient dosage to peripheral T cell population.

3.13. Statistical analysis

The values of all experimental data presented are mean ± standard deviation. The two-tailed unpaired Student's t-test was performed using GraphPad Prism version 5 (San Diego, USA). The p-values are indicated in each figures and classified in four categories: $p>0.05$ (not significant), $p>0.01$ (*), $p>0.001$ (**), $p>0.0001$ (***).

3.14. Single cell transcriptomic analysis

Single cells were obtained from 4-weeks-old $Eed^{fl/fl}$:: β5tCre and wild type B6 control mice and sorted into individual wells of a 96-well plate containing 2.3μl of lysis buffer (0.2% Triton, 2units/μl RNase inhibitor, RNase-free water). The samples were then sent to collaborator for the construction of a cDNA library for every individual cell and subsequently transcriptomic analysis using the Smart-Seq2 method (*117*).

For quality control, cells were eliminated from further analysis if the proportion of aligned reads was < 75%; if the number of detected genes was < 2000 or > 10000; if the proportion of fragments mapping to ERCC (External RNA Controls Consortium) spike-ins was > 75% or < 1%; if the proportion of fragments mapping to mitochondrial genes was either an outlier or > 20%; if the proportion of fragments mapping to rRNA was an outlier; if the cell was

classified as an outlier by PCA; if the GC content of the library was < 40% or > 60%; or if the 5′ to 3′ bias was ≤ 0.2 (as assessed by Picard tools). Outlier analysis was conducted in R using the boxplot function. PCA outliers were those where the ratio of MAD to median distance from the plate centroid was > 2. The proportion of fragments was estimated as $\Sigma y_{1 \rightarrow j} / (\Sigma y_{1 \rightarrow j} + \Sigma x_{1 \rightarrow i})$, where y is the gene set of interest (e.g. ERCC spike-ins), x is the set of protein-coding genes, j is the number of genes in the gene set of interest and i is the number of protein-coding genes.

The size-factors (i.e. sample amount) were calculated for each cell passing quality control on protein-coding genes and ERCC spike-ins using DESeq (*118*). Counts were adjusted by two-factor correction: $([x_{1 \ldots i}] / sf_x) / sf_{ERCC}$, where sf_x is the size-factor of protein-coding genes and sf_{ERCC} is the size-factor of ERCC spike-ins.

Analysis of the number of detectable genes in different numbers of cells was conducted by randomly sampling 100 combinations of cells with replacement at each number of cells (apart from 1 cell - at which point all cells were analysed separately). Empirical 95% confidence intervals were calculated from these sampled data and multiple different FPKM (Fragments Per Kilobase of transcript per Million mapped reads) thresholds were used. Counts were converted into the absolute number of molecules by linear modelling of the amount of ERCC spike-ins against the detected FPKM (with the fitted line forced through the origin).

Clustering was conducted using PCA (principal component analysis) and t-SNE (t-distributed stochastic neighbor embedding; implemented in the tsne R package). In the case of clustering, genes were included in the model only if the standard deviation was > 0 and the gene was expressed in > 20% cells.

Differential expression was analysed using single-cell differential expression (scde) analysis package on genes with standard deviation >0 and

detectable at >10 reads per cell (*119*). The level of significance was set at an FDR < 0.05. Gene ontology enrichment was estimated using DAVID (*120*).

4. RESULTS

4.1. Introduction to mouse model used in the study

Deficiency of PRC2 function is lethal to mice in the early embryonic stages (*79*). Therefore, the gene ablation of *Eed* was achieved conditionally by using the Cre-lox system to probe the functional role of PRC2 complex in TEC development and function. Tissue specific expression of Cre is achieved by placing the coding sequence of Cre under the transcriptional control of a tissue specific promoter. The gene to be conditionally ablated is modified by recombinant DNA technology so that recognition sequences for Cre, so called loxP sites, are placed at the 5′ and 3′ ends of the genomic DNA segment to be excised (*121*). To target the loss of gene functions exclusively to TEC, Cre expression was placed under the transcriptional control of *Psmb11* that encodes β5t, a thymic specific subcomponent of the proteasome complex (*52*, *122*). The use of *Foxn1* transcriptional controlled Cre expression (*123–125*) was omitted as transcript of Foxn1 is also significantly detected in skin keratinocytes (*123*, further eloborated in **Discussion**). β5t expression is initiated at E12.5 in the thymus that, at the early stage, constitutes of TEC precursors that eventually give rise to both cortical and medullary lineages (*122*). Hence, the placing of Cre expression under transcriptional control of β5t instead of Foxn1 enables the gene deletion specific to only TEC and eliminates potential confounding factors to the mouse model phenotype due to off target deletion in other organs such as the skin.

To achieve a loss of PRC2 function specific to TEC, $Eed^{fl/fl}$::β5tCre mouse line was generated whereby exon 3 to exon 6 of the *Eed* gene locus is flanked by to loxP sites (fl) (**Figure 6**). These exons contain sequences encoding the WD domain that enables Eed to interact with Ezh1/2 (*97*). The

presence of Cre recombinase, specifically in TEC, will result in the excision of the loxP flanked exons of *Eed* leading to the functional loss of Eed and subsequently PRC2 function. Littermates lacking the β5tCre transgene (referred to as $Eed^{fl/fl}$) will serve as the wild type control mice.

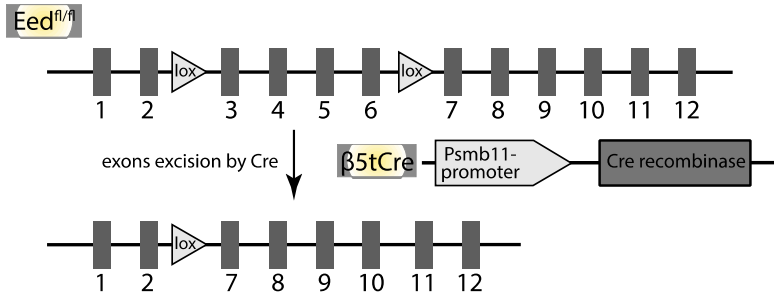

Figure 6. *Schematic representation of the recombinant Eed and Psmb11 loci used to generate $Eed^{fl/fl}$::β5tCre mice*. The lox P sites are inserted into the *eed* locus flanking the exon 3 to 6. Upon the co-expression of Cre controlled by *Psmb11* locus, the intervening sequence of *Eed* is excised in the genome.

A second experimental model to probe the functionality of PRC2 was developed in parallel. For this purpose, mice deficient in the expression of either one or both homologs of the catalytic component Ezh were created. Mice with a conditional *Ezh2* gene locus, with loxP sites flanking exons 16-19 that encodes the SET domain, were crossed to mice that carry the transgene β5tCre and were conventionally deficient of Ezh1 to obtain mice designated $Ezh1^{KO}$::$Ezh2^{fl/fl}$::β5tCre. The TEC of these mice are devoid of both Ezh1 and Ezh2 and thus provide an alternative approach to assess the function PRC2.

A third mouse model was designed to visualise TEC in $Eed^{fl/fl}$::β5tCre mice that had recombined their loxP modified loci. This was achieved by breeding into $Eed^{fl/fl}$::β5tCre mice a modified *Rosa26* locus which expresses ZsGreen fluorescence protein in a tissue specific fashion upon removal of a stop cassette flanked by loxP sequences. The design of these mice, designated $Eed^{fl/fl}$::β5tCre::ZsGreen, is displayed in **Figure 7**. Since the Cre recombinase mediated process of DNA recombination is irreversible, modifications to the

genome will be inherited to all subsequent daughter cells and thus serves also conveniently as a lineage tracer tool.

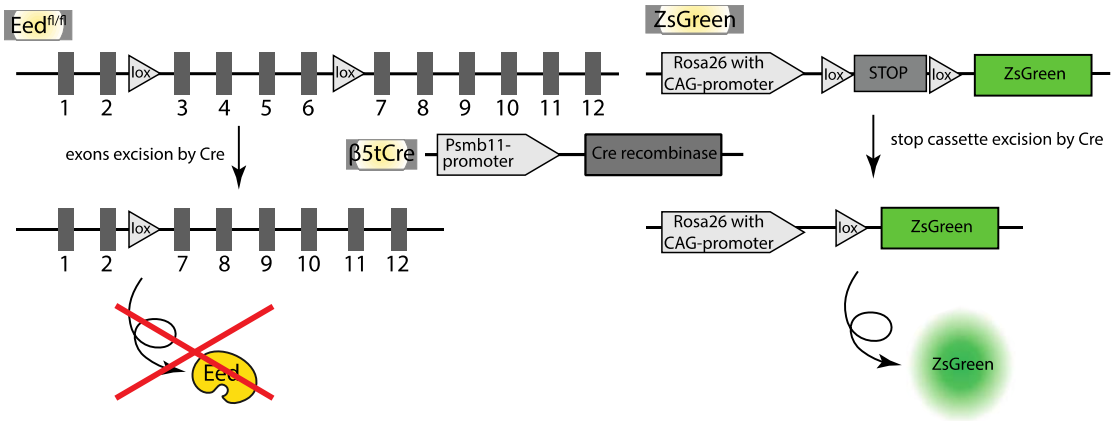

Figure 7. *Schematic representation of gene construct in Eed$^{fl/fl}$::β5tCre::ZsGreen*. The loxP sites flank exons 3 and 6 of the *Eed* locus and the stop cassette downstream of the *Rosa26* locus and upstream of transgene encoding ZsGreen. Following Cre expression under TEC-specific *Psmb11* promoter, both exons 3-6 of *Eed* and stop cassette are deleted by targeted recombination and, as a consequence, the cells cease to express Eed and are also rendered green fluorescent.

4.2. TEC Phenotype of Eed$^{fl/fl}$::β5tCre

4.2.1. Diminished thymus cellularity but unchanged tissue architecture

I first investigated the consequences of a loss of PRC2 function, resulting from the deficiency of Eed expression, in TEC for thymus cellularity and tissue architecture. Thymus organ size and overall cellularity following physical tissue disruption were significantly reduced in Eed$^{fl/fl}$::β5tCre mice when compared to the Cre negative control Eed$^{fl/fl}$ mice (**Figure 8A,B**). The reduction of thymus cellularity was significantly diminished at all time points tested between the newborn age and 4 weeks of life (**Figure 8B**). Progressive thymus involution precluded any further analysis beyond 5 weeks of age. These results clearly demonstrate that PRC2 function is required for the regular development and maintenance of the thymus.

Using haematoxylin and eosin (H&E) staining, tissues from control Eed$^{fl/fl}$ mice displayed a characteristically segregated, cell-dense cortical and less compact medullary region. In contrast, cross section of the thymus of Eed$^{fl/fl}$::β5tCre demonstrated a thymus largely reduced in size (**Figure 8A**), reflecting the overall diminished cell count of the organ (**Figure 8B**). In addition, the cortex was significantly reduced in depth and displayed a "broken" appearance with small islands at its periphery that appeared less dense with cells. Regions with reduced cellular density, similar to that of the medulla, were also observed in the sub-capsular region adding to an overall altered appearance of the thymus histological morphology (**Figure 8C**). However, a thymic architecture with segregated cortex and medulla and a clearly defined cortico-medullary junction was overall maintained in Eed$^{fl/fl}$::β5tCre mice (**Figure 8D**).

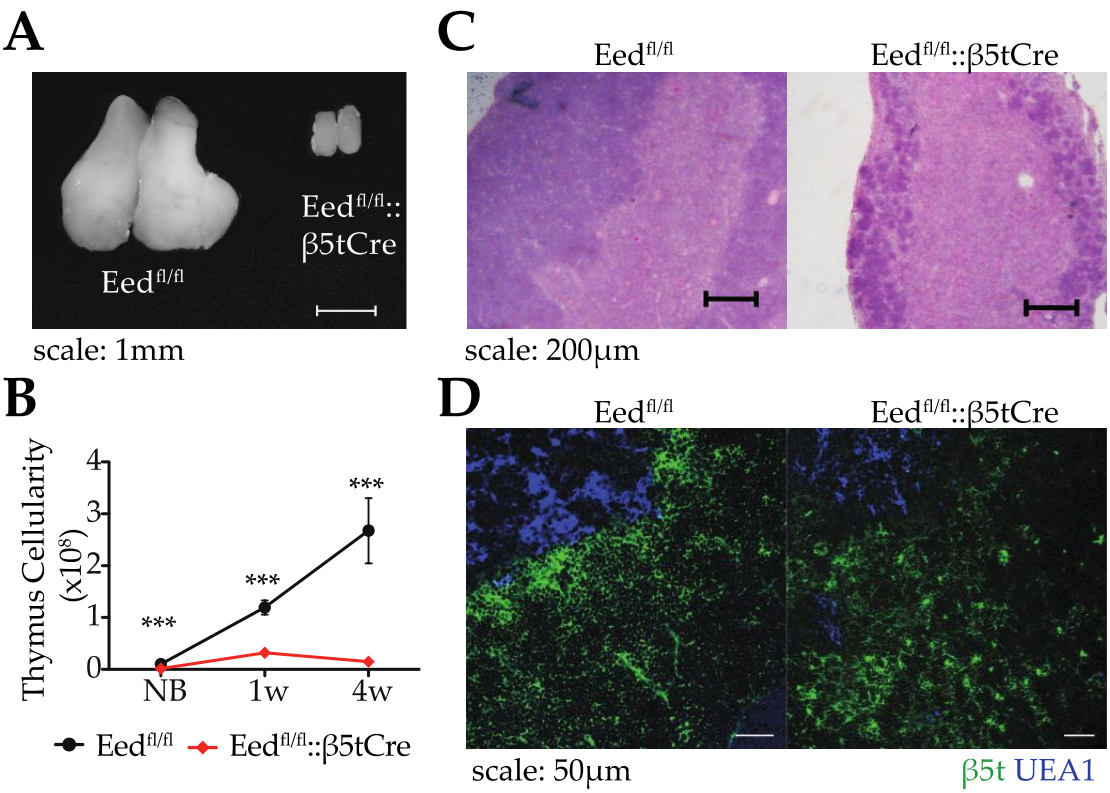

Figure 8. *Thymus morphological features*. (**A**) The macropathological analysis of thymic lobes from 4-weeks-old Eed$^{fl/fl}$::β5tCre and control Eed$^{fl/fl}$ mice. (**B**) Total thymic cellularity following physical disruption at the indicated time points: newborn (NB), 1 and 4-weeks-old (w). (**C**) H&E staining of thymic lobes isolated from Eed$^{fl/fl}$::β5tCre

and control Eed$^{fl/fl}$ mice at age of 4 weeks. (**D**) Immunohistology of thymus tissue sections of 4-weeks-old Eed$^{fl/fl}$::β5tCre and control Eed$^{fl/fl}$ mice using antibodies specific for β5t (*green*) and reactivity to UEA1 (*blue*) identifying cTEC and mTEC, respectively. Note, a distinct cortico-medullary junction can be observed in both Eed$^{fl/fl}$::β5tCre and control Eed$^{fl/fl}$ mice. Data are representative of at least 2 independent experiments with 3 to 5 mice per group. ***$p<0.001$, two-tailed paired Student's T test.

4.2.2. Decreased mTEC but increased cTEC cellularity

I next analysed the thymic tissue using flow cytometric analysis to characterise the phenotypes of thymic epithelia and quantify their respective cellularity. In this analysis, TEC were positively identified by their expression of the cell surface marker EpCAM and their consistent lack of expression of the pan-haematopoietc marker CD45. Within this population of epithelial stroma (EpCAM$^+$ CD45$^-$) cells, cTEC were identified by their expression of the cell surface marker Ly51 whereas mTEC were classified as being reactive with the lectin *Ulex europaeus* agglutinin 1 (UEA1). The frequency of TEC was relatively increased in thymic single cell suspensions of Eed$^{fl/fl}$::β5tCre mice (2%) when compared to controls (0.16%) which was approximately 12-fold higher than the age-matched controls (**Figure 9A**). The further analysis of the TEC subpopulations in 4-weeks-old Eed$^{fl/fl}$::β5tCre mice showed that mTEC were greatly reduced but cTEC – in contrary to what was expected from the H&E analysis – were paradoxically increased consequent to Eed deficiency (**Figure 9A**). To test whether these changes correlated with a change in post-translational histone modifications resultant from the absence of PRC2's catalytic activity, I measured H3K27me3 marks in the nuclei of cTEC and mTEC and related their extent of detection to the overall level of histone H3. While a loss of Eed expression did not impact on the global detection of histone H3, the H3K27me3 mark was however significantly altered; all cTEC displayed an unvarying reduction of H3K27me3 marks revealing a uniform

change in this repressive mark (**Figure 9B**). In contrast, mTEC subjected to the same flow cytometric analysis showed two populations, one in which the level of H3K27me3 mark was comparable to that observed in Eed-deficient cTEC and a second, albeit smaller population, that failed to display such a reduction and stained identical to the $Eed^{fl/fl}$ control mice. (The analysis of the lesser population of mTEC maintaining seemingly regular H3K27me3 marks will be further described in **Section 4.4**.) Despite the significant reduction in overall thymus cellularity in $Eed^{fl/fl}$::β5tCre mice, TEC absolute cellularity was identical to that of $Eed^{fl/fl}$ control mice irrespective of the specific age measured within the first 4 weeks of life (**Figure 9C**). The relative increase of TEC without a change in its absolute cellularity implies that a stark reduction in thymocytes will have most likely accounted for these observed changes, as thymocytes constitute the most abundant cell population in the thymus. Within the TEC compartment of $Eed^{fl/fl}$::β5tCre mice, cells with a medullary phenotype ($EpCAM^{+}CD45^{-}UEA1^{+}$) constituted a minority as compared to cells with cortical phenotype ($EpCAM^{+}CD45^{-}Ly51^{+}$) (**Figure 9D, E**). These differences were most striking at 4 weeks of age and suggested that a loss of PRC2 function impacted differentially on mTEC and cTEC; the former was reduced in both frequency and absolute cellularity in PRC2-deficient mice at 4 weeks of age whereas the latter was more abundant for both measures. Moreover, the level of MHC-II expression was typically reduced in TEC largely independent of their cortical and medullary phenotype (**Figure 9F, G**). However, there was again a subpopulation of mTEC that displayed a cell-surface MHC-II expression level identical to that of the $Eed^{fl/fl}$ controls. The frequency of these cells was similar to that of mTEC that maintained unchanged H3K27me3 marks (**Figure 9F**).

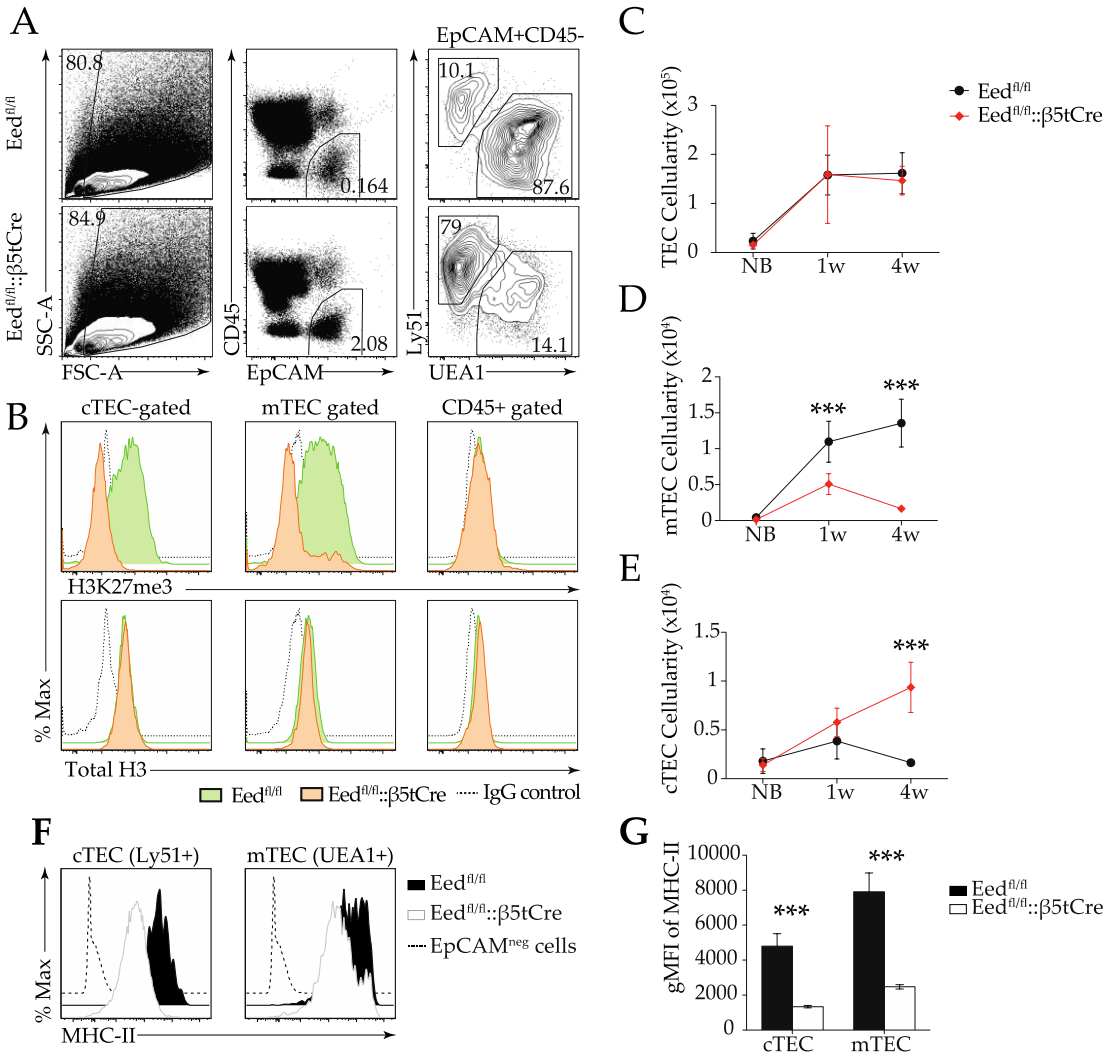

Figure 9. *Phenotypic TEC analysis.* (**A**) Gating strategy to identify TEC (EpCAM+CD45-) using flow cytometry. Forward scatter (FSC), side scatter (SSC). Note the differences in cTEC and mTEC between 4-weeks-old Eed$^{fl/fl}$::β5tCre and Eed$^{fl/fl}$ control mice. (**B**) Detection of H3K27me3 and total histone H3 in TEC nuclei of Eed$^{fl/fl}$::β5tCre and Eed$^{fl/fl}$ control mice. (**C-E**) Absolute TEC, cTEC and mTEC cellularity at different postnatal time points: newborn (NB), 1 and 4-weeks-old (w). (**F**) MHC-II expression and their (**G**) geometric mean fluorescence intensity (gMFI) on cTEC and mTEC of Eed$^{fl/fl}$::β5tCre and Eed$^{fl/fl}$ control mice. Data are representative of at least 2 independent experiments with 3 to 5 mice per group and experiment. *** p<0.01, two-tailed paired Student's T test.

4.2.3. Altered mTEC maturation consequent to lack of PRC2 activity

The mTEC maturation was staged by the up-regulation of MHC-II on the cell surface and the subsequent expression of Aire in a subpopulation of mTEC with high level of MHC-II (*23*, *126*). The frequency of mature mTEC (expressing high level of MHC-II; designated $mTEC^{hi}$) was reduced in $Eed^{fl/fl}$::β5tCre mice and also fewer $mTEC^{hi}$ expressed Aire (**Figure 10A, B**). Hence, the absence of PRC2 function impeded the regular maturation of epithelia in the mTEC lineage. This observed change may either be the direct consequence of the loss of PRC2 function that could be required for mTEC terminal differentiation, or alternatively, may indirectly be caused by the paucity of single positive thymocytes as these cells induce mTEC maturation via their expression of lymphotoxinβ, CD40 ligand or receptor activator of nuclear factor kappa-B ligand (RANKL) (*127*). To further interrogate the mechanism possibly responsible for the decreased mTEC cellularity in $Eed^{fl/fl}$::β5tCre mice, fetal E15.5 thymic lobes were harvested from mutant and control mice, treated with deoxyguanosine to deplete thymocytes and then cultured in the presence of exogenously added RANKL to substituted for signals otherwise provided by single positive thymocytes (*128*). RANKL was unable to restore in these cultures a normal mTEC (UEA1+) frequency (**Figure 10C**) thus demonstrating an intrinsic incompetence of PRC2-deficient TEC to respond adequately to a signal typically associated with mTEC maturation.

The observed decrease in mTEC cellularity in mice with TEC devoid of PRC2 function could be the consequence of: i) the decreased cellular proliferation; ii) the result of an increased rate of apoptosis in the absence of PRC2 function; iii) or, alternatively the change in asymmetrical TEC differentiation since fewer mTEC were contrasted by an increased cTEC cellularity. To test the first explanation, mice were exposed *in vivo* to BrdU to quantify DNA neo-synthesis in distinct TEC subpopulations (**Figure 10D**).

This analysis revealed that both cTEC and mTEC proliferation were significantly decreased in 4-weeks-old $Eed^{fl/fl}$::β5tCre mice. Given the stark reduction in BrdU incorporation in both epithelial compartments, it remained unclear why the cellularity of mTEC was reduced while the cTEC increased in mice with the TEC-specific loss of PRC2 function (**Figure 9D, E**). Upon closer analysis of the mTEC subpopulations, the proliferation of immature mTEC was severely reduced in the mutant mice yet these cells constitute approximately two thirds of all mTEC. In contrast, the proliferation of the mature mTEC, with upregulated MHC-II expression, was not different to that of the controls (**Figure 10D**). Moreover, the altered frequencies of both cTEC and mTEC are unlikely accounted for by difference in rate of apoptosis, and for this reason survival rate, as both populations when analysed by qPCR displayed a comparable relative expression levels in apoptosis-related genes (*Bak, Bax, Bid, Bcl-xl*; **Figure 10E**). In addition to these observations, the stark reduction of mTEC cellularity (**Figure 9D, 10B**) despite of an unchanged total TEC cellularity (**Figure 9C**) suggested a shift in the lineage commitment towards a cTEC fate. Hence, a likely explanation for the observed changes in cellularity for both cTEC and mTEC could be due to the crucial role of PRC2 at the developmental stage where progenitors, that have attained a cTEC phenotype, asymmetrically differentiate to adopt the mTEC fate. In the absence of PRC2, cTEC are less likely to assume the medullary (mTEC) phenotype. The partial restriction, in turn, impacts on the absolute cellularity and maturation of mTEC.

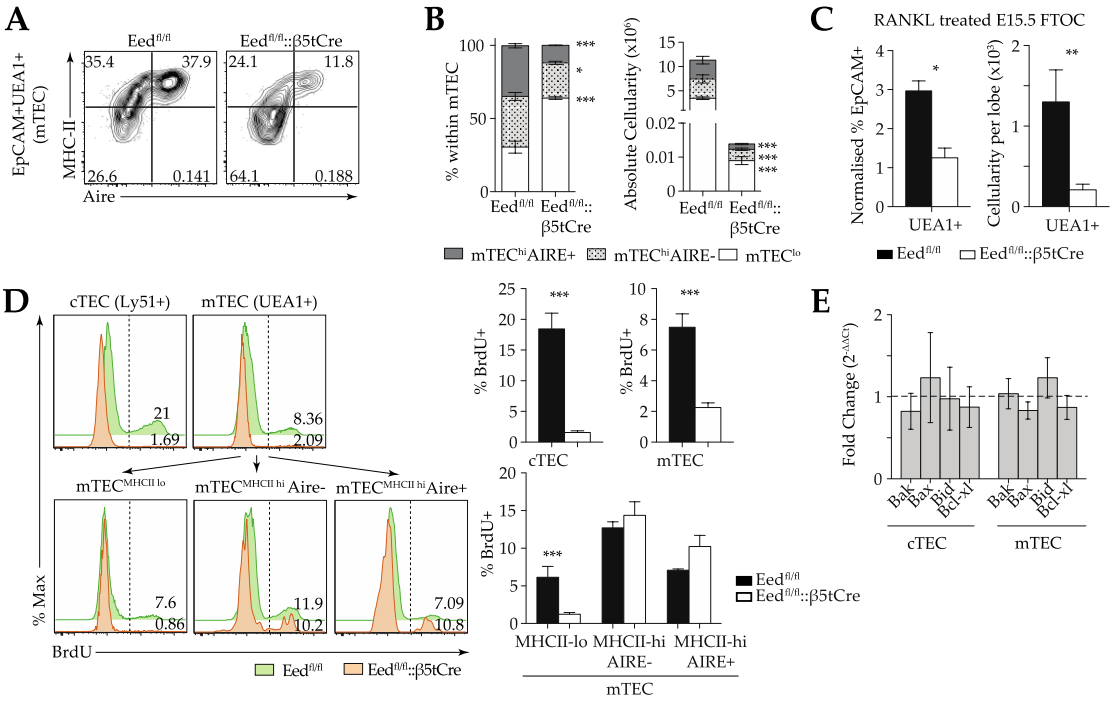

Figure 10. *Altered mTEC maturation in 4-weeks-old Eed$^{fl/fl}$::β5tCre mice*. (**A**) Gating strategy to analyse mTEC maturation stages with flow cytometry. The immature mTEC, defined by the low expression level of MHC-II, matures and up-regulates MHC-II and subsequently expresses Aire. (**B**) Frequency (*left panel*) and cellularity (*right panel*) of mTEC subpopulations within the medullary epithelia (EpCAM+, UEA1+, Ly51-). (**C**) Inability of *in vitro* RANKL stimulation to restore mTEC cellularity in Eed$^{fl/fl}$::β5tCre thymus. Thymocyte depleted E15.5 thymic lobes were cultured with 10µg/ml of RANKL for 5 days and the frequency of mTEC was measured by flow cytometric analysis was then normalised to the frequency of mTEC present in the non-RANKL-treated control (*left panel*). The cellularity of mTEC measured per lobe in RANKL treated thymic lobes is presented on the *right panel*. (**D**) The flow cytometric analysis (*left panel*) and frequencies (*right panel*) of various TEC subpopulations incorporating BrdU during 16 hours following i.p. injection (1mg per mouse). (**E**) Expression of apoptosis-associated genes (*Bak, Bax, Bid, Bcl-xl*) in cTEC and mTEC of Eed$^{fl/fl}$::β5tCre and Eed$^{fl/fl}$ control mice. Expression levels of each apoptosis-associated gene were normalised to GAPDH expression and fold changes in the expression levels of each genes were related to the corresponding gene expression level in the Eed$^{fl/fl}$ control TEC, where fold change was set to an arbitrary value of 1. Data are representative of at least 2 independent experiments (except E which displays data from one experiment) with 3 to 5 4-weeks-old mice per group. * p<0.05, *** p<0.001, two-tailed paired Student's T test.

4.2.4. TEC double deficient for Ezh1/2 display comparable defects in TEC cellularity and maturation

To ensure that the observed TEC phenotype of $Eed^{fl/fl}$::β5tCre mice was directly related to the loss of the methyltransferase activity of the PRC2, the TEC phenotype was also determined in the case of deletion of the subunits containing the catalytic domains, Ezh1/2. Therefore, I generated mice that are devoid of either one of these PRC2 components (designated $Ezh1^{KO}$ and $Ezh2^{fl/fl}$::β5tCre). Due to partial redundancy of Ezh1 and Ezh2 (*108*), single deletion of either Ezh1 or Ezh2 resulted only in mild phenotypes (**Figure 11A, C-F**). For this reason, double knockout mice were bred in which a constitutive loss of *Ezh1* was paired with TEC-targeted loss of *Ezh2* (designated $Ezh1^{KO}$::$Ezh2^{fl/fl}$::β5tCre). These double deficient mice, displayed significant changes in the frequency and absolute cellularity of mTEC and cTEC, as highlighted by a reduction in the former and an increase in the latter (**Figure 11A, E, F**). The population of mutant mTEC contained also a small mTEC population that seemingly maintain regular level of H3K27me marks (**Figure 11B**), a finding comparable to what was observed in mTEC isolated from $Eed^{fl/fl}$::β5tCre mice. In contrast to the unchanged TEC cellularity in $Eed^{fl/fl}$::β5tCre mice, total TEC cellularity was significantly reduced in 4-weeks-old $Ezh1^{KO}$::$Ezh2^{fl/fl}$::β5tCre mice as compared to the controls or single mutants (**Figure 11D**). In $Ezh1^{KO}$::$Ezh2^{fl/fl}$::β5tCre mice, the lineage specific differentiation into separate mTEC populations was skewed with a lower frequency of $mTEC^{hi}$, with or without Aire expression (**Figure 11G**). The striking similarity (albeit not identical) in the phenotype following changes in the composition of the canonical PRC2 complex reinforced the conclusion that PRC2 function is essential for regular TEC lineage differentiation and maintenance.

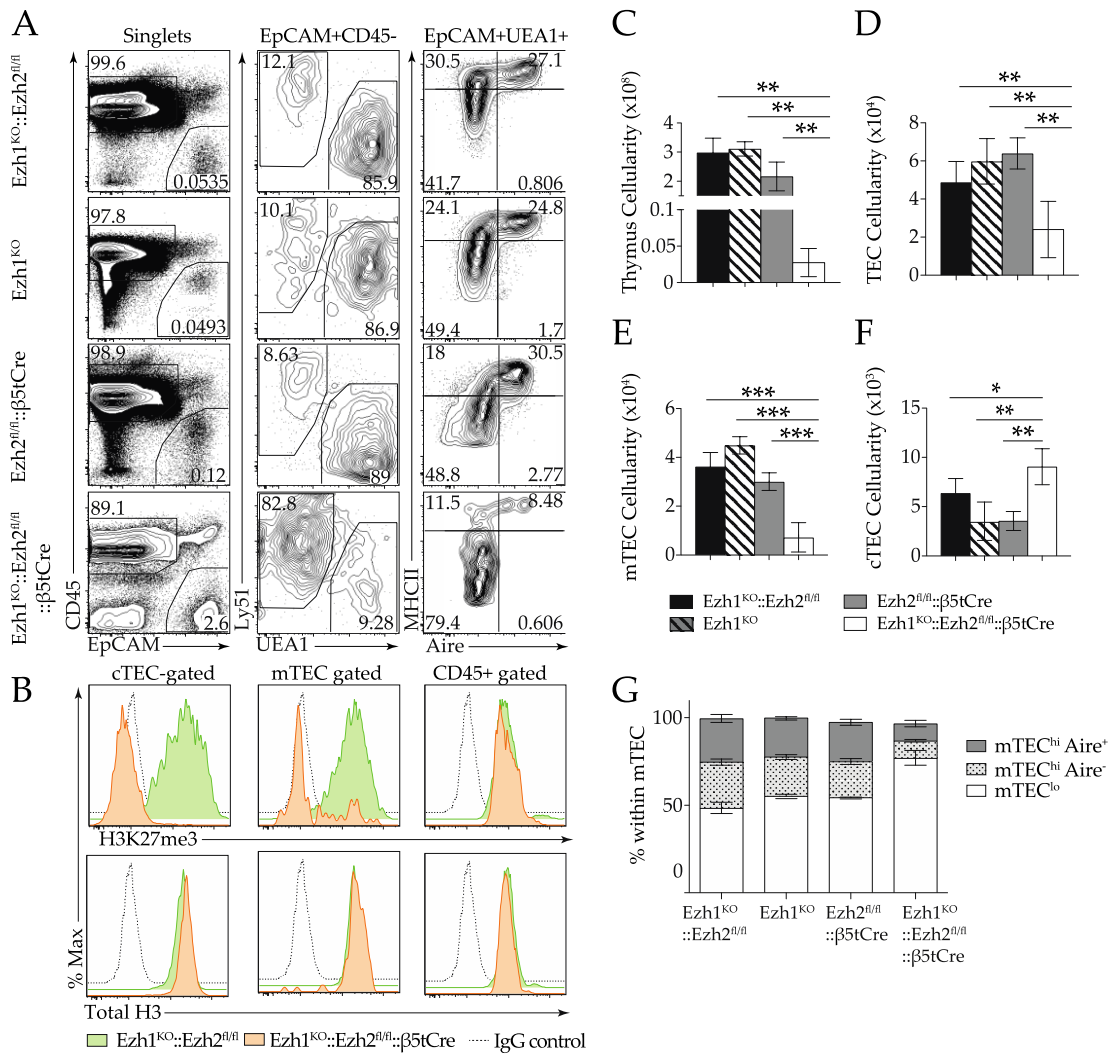

Figure 11. *Reduced TEC cellularity and defective mTEC maturation in 4-weeks-old Ezh1^{KO}::Ezh2$^{fl/fl}$::β5tCre mice result from a loss of the PRC2 catalytic activity*. (**A**) Only the combined knockout of *Ezh1* and *Ezh2* homologs but not the single knockouts altered TEC differentiation. (**B**) Loss of methyltransferase activity of PRC2 reduces H3K27me3 marks in all cTEC and the majority of mTEC. (**C - F**) Plots of the absolute cellularity of thymus, TEC and TEC subpopulations in the single knockout mice, double knockout and Cre negative control mice. Significant changes in the cellularity were observed only in loss of both Ezh1 and Ezh2 expression. (**G**) Partial maturational block of mTEC devoid of Ezh1/2 expression with a decrease in cells with a mature phenotype. Data are representative of at least 2 independent experiments with 3 to 4 mice per group. ** p< 0.01, *** p<0.001, two-tailed paired Student's T test.

4.3. Thymocyte Development

4.3.1. PRC2 is involved in recruitment of early T-lineage progenitors

The loss of PRC2 function in TEC resulted in a hypocellular thymus despite a stromal scaffold composed of TEC that were identical in number to that of control mice. I, therefore, investigated next the quality and quantity of thymopoiesis in a microenvironment made up of Eed-deficient epithelia. Staining B cell-, erythroid and myeloid lineage negative thymocytes for the cell surface expression of CD4 and CD8 revealed a normal maturational progression as the frequency of DN, CD8ISP, DP, CD4SP or CD8SP remained unchanged (**Figure 12A**). Moreover, a detailed analysis of the individual DN subpopulations, using the differential cell surface expression of CD44 and CD25, demonstrated normal frequencies for each of these stages in early thymocyte development (**Figure 12B**). Therefore, a specific and especially early but partial intrathymic block in thymocyte differentiation could be excluded as an explanation for the hypocellularity of thymocytes in the thymus of $Eed^{fl/fl}$::β5tCre mice.

Since the reduced thymocytes cellularity in $Eed^{fl/fl}$::β5tCre mice could not be explained by blockages in the thymocyte differentiation, earlier stages of the thymocyte development were being investigated. The T cell progenitors are attracted to the thymus by a set of well-characterised chemokines, including CXCL12 and CCL25, typically expressed by the cTEC (*27*). $Eed^{fl/fl}$::β5tCre mice demonstrated a significantly reduced relative frequency and absolute cellularity (2,670 ± 864.2 vs. 50 ± 15.6) of ETP (Lineage-, CD44+, c-Kit+) (**Figure 12C**). This decrease in ETP recruitment correlated with a reduced number of transcripts in cTEC for the chemokines CXCL12 and CCL25 (**Figure 12D**), which may have caused the reduced efficiency of Eed-deficient TEC to recruit ETP into the thymus. As a result, subsequent

thymocyte development in Eed$^{fl/fl}$::β5tCre mice drew from a smaller pool of the earliest detectable population of thymocyte precursors.

4.3.2. Unaffected initiation of thymocyte selection

During thymopoiesis, maturational progression beyond the DN stages requires the productive rearrangement and expression of a TCRβ chain (*34*). Subsequently, thymocytes acquire the concomitant expression of CD4 and CD8 and begin to express a complete TCR complex competent to scan MHC-peptide complexes and initiate signaling upon the engagement with these ligands that is of sufficient affinity (*34*). Activation of TCR above a developmentally set threshold and the consequent selection of these cells for further survival and differentiation coincide with the transient expression of CD69 (*39*, *129*). The frequency of CD69-positive thymocytes was comparable for Eed$^{fl/fl}$::β5tCre and Eed$^{fl/fl}$ control mice (**Figure 12E**) which indicates an undisturbed capacity of cTEC to initiate thymocyte selection.

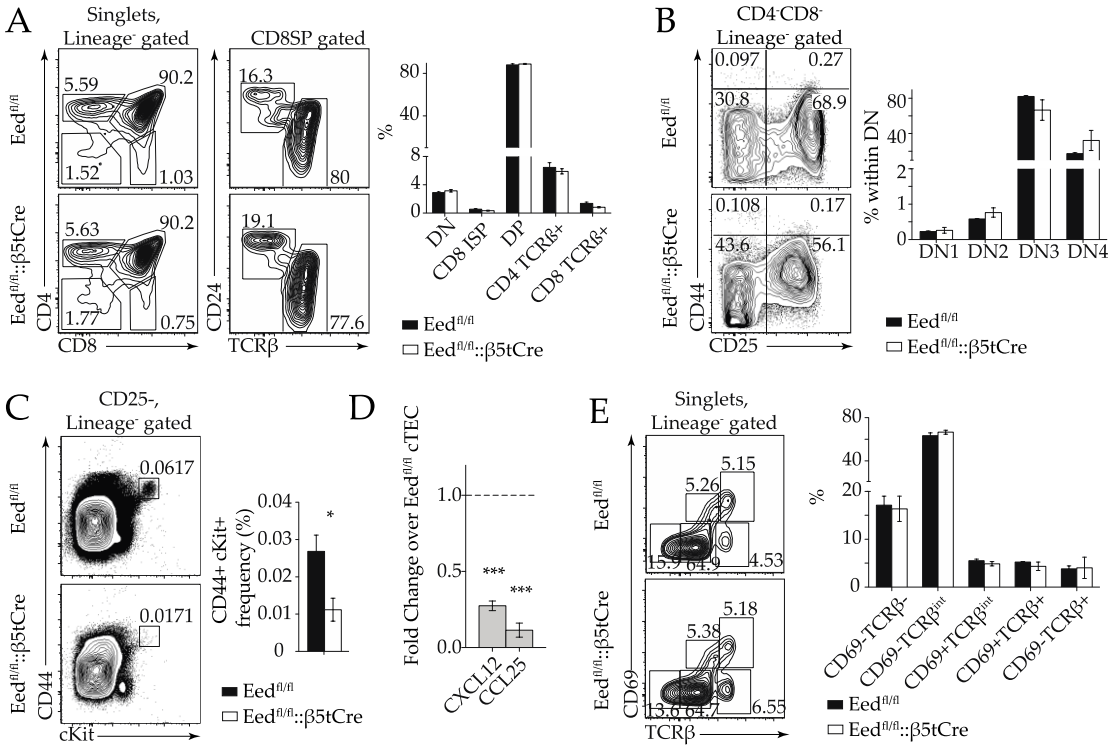

Figure 12. *Reduced early T-lineage progenitor frequency but unperturbed initial selection of thymocytes in 4-weeks-old Eed$^{fl/fl}$::β5tCre mice*. (**A**) Analysis of major thymocyte developmental stages as marked by the expression of CD4 and CD8 on lineage negative cells (i.e. B cells, myeloid cells and red blood cells). CD8 SP cells were further characterised to distinguish between immature (TCRβ^{-}, CD24^{+}) and mature cells (TCRβ^{+}, CD24^{-}). (**B**) The relative frequency of DN thymocytes. (**C**) The frequency of ETP (c-Kit^{+}, CD44^{+}) among cells excluded of non-lymphoid and T_{reg} cells (lineage negative, CD25^{-}). (**D**) qPCR analysis of cTEC for CXCL12 and CCL25 transcripts in Eed$^{fl/fl}$::β5tCre mice when compared to Eed$^{fl/fl}$ control mice where the fold change values were set to an arbitrary value of 1. cDNA amounts were normalised with housekeeping gene GAPDH. (**E**) CD69 and TCRβ expression on total thymocytes. Data are representative of at least 2 independent experiments with 3 to 4 mice per group. *p<0.05, ***p<0.001, two-tailed paired Student's T test.

4.3.3. Defective Negative Selection

Thymocytes expressing TCR specificities directed against the host's own cells and molecules (self antigens) hold the risk to initiate and maintain an autoimmune response to peripheral organs and their products should these cells be allowed to mature and exit the thymus without any form of selection. A system of TCR quality control is therefore in place during intrathymic T cell maturation to secure a repertoire of mature, functional T cells that are tolerant to self-antigens but responsive to foreign antigens. This process is referred to as thymocyte negative selection which deletes maturing thymocytes whose TCRs have a sufficiently high affinity for MHC/self-antigen complexes presented on surface the cTEC, mTEC, and antigen presenting cells (dendritic cells, B cells, macrophages). Cortical thymocytes (CCR7-) undergoing negative selection are identified by a co-expression of the cell surface markers Helios and PD-1 (*42*). The frequency of Helios+PD-1+ cortical thymocytes was significantly reduced in $Eed^{fl/fl}$::β5tCre mice (**Figure 13A**) and these cells displayed a higher avidity for MHC/self-antigen complexes as measured by the geometric mean fluorescence intensity (gMFI) expression of CD5 (*130*). Thus, cTEC rendered deficient of a functional PRC2 complex displayed a defective capacity for cortical negative selection.

The cell surface acquisition of CCR7 expression marks the capacity of thymocytes to migrate into the medulla where the second opportunity for negative selection is provided by interaction with mTEC and other antigen presenting cells. Within the population of medullary (CCR7+) CD4 SP cells, negatively selected cells are identified by the expression of Helios (*42*). The frequencies of Helios positive thymocytes among medullary immature (CD24+) and mature (CD24-) CD4 SP cells were both reduced in $Eed^{fl/fl}$::β5tCre mice when compared to $Eed^{fl/fl}$ control mice (**Figure 13A**). The CD5 gMFI values were also increased in each of these CD4SP population

(**Figure 13B**) indicating the negative selection of cells in Eed$^{fl/fl}$::β5tCre mice that display a higher average TCR avidity. Hence, mTEC lacking PRC2 activity also fail to enforce normal negative selection.

To confirm the conclusion that PRC2 function is required for regular thymocyte selection of high avidity thymocytes in both the cortex and medulla, an alternative approach was also used to quantify negative selection in both compartments. Using the differential expression of cell surface markers PD1, CD24, and Ox40, two separate waves of negative selection can be identified (*43*). The first wave occurs in the cortex and is characterised by the parallel expression of PD1 and CD24 on CCR7-TCRβ+ thymocytes. The second wave takes place in the medulla and is marked by the expression of Ox40, a member of the tumor necrosis factor receptor superfamily (S. Daley, *personal communication*). The frequencies of cells subject to negative selection were decreased in both waves (**Figure 13C**). Based on two different flow cytometric analyses to assess the extent of negative selection, both approaches demonstrated that cTEC and mTEC are indeed limited in their capacity to induce negative selection in the absence of physiological PRC2 expression as in Eed$^{fl/fl}$::β5tCre mice.

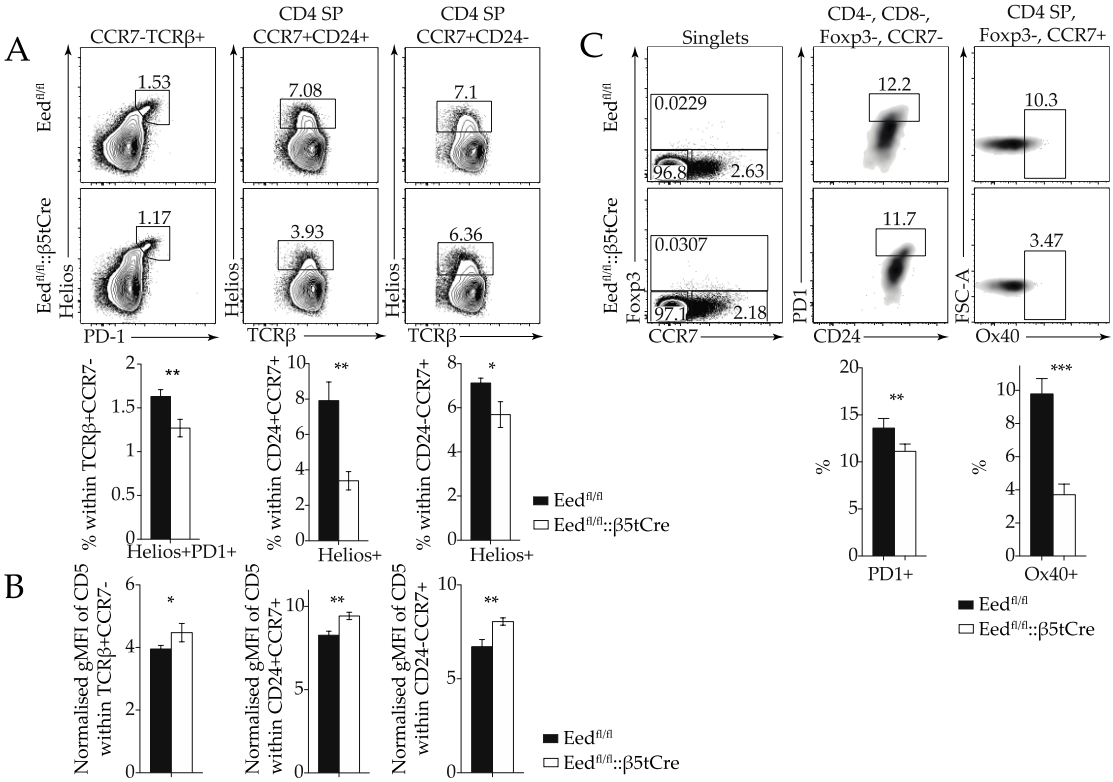

Figure 13. *Reduced negative selection of cortical and medullary thymocytes in 4-weeks-old Eed$^{fl/fl}$::β5tCre mice*. (A) Detection of negatively selected thymocytes in the cortex (CCR7-, TCRβ+) and immature (CD24+) and mature CD4SP cells (CD24-) in the medulla (CCR7+) using the co-expression of PD1 and Helios in the former and only Helios in the latter. (B) Determination of TCR avidity as per mean fluorescence intensity (gMFI) values of CD5 among negatively selected thymocytes in cortex and and medulla as per panel A. (C) Cortical thymocytes undergoing negative selection are identified by expression of PD-1 while the negatively selected medullary thymocytes are identified by the expression of Ox40. (C) Detection of negatively selected DP thymocytes in the cortex (CCR7-, Foxp3-, TCRβ+) and medulla (CCR7+ CD4SP) using the co-expression of PD1 and CD24 in the former and Ox40 in the latter. Data are representative of at least 2 independent experiments with 3 to 5 mice per group. *p<0.05, **p<0.01, *** p<0.001, two-tailed paired Student's T test.

4.3.4. Detection of negative selection efficiency

Effective negative selection of thymocytes requires the expression and presentation of a complete repertoire of TRA. Having demonstrated the capacity of negative selection is reduced in PRC2-deficient TEC, I seek further to demonstrate a direct measure of the functional loss of negative selection by PRC2-deficient TEC. Tetramer assay is an efficient way to identify and quantify T cells with specific antigen specificity. This method relies on several MHC molecules each presenting a known antigenic peptide that are bound to a fluorescence-tagged streptavidin to form a multimeric complex that displays a high binding avidity to circumvent the problem of dissociation. T cells positively stained with these tetramers thus represent cells with TCR specificity for the antigenic peptide used in the tetramer complexes. This method has been successfully used to quantify the efficiency of thymic selection by quantifying the absolute number of antigen-specific (i.e. tetramer-positive staining) T cells at distinct development stages (*46*, *131*, *132*). This method is therefore employed to probe the efficiency of negative selection in the presence or absence of PRC2 function in TEC. Since Cre is expressed in $Eed^{fl/fl}$::β5tCre mice under the transcriptional control of β5t promoter, all cTEC would be positive for the recombinase. On the other hand, a subpopulation of mature mTEC in $Eed^{fl/fl}$::β5tCre mice should also be expressing Cre recombinase based on available transcriptomic data that indicated the presence of β5t expression in a subpopulation of mature mTEC (*unpublished data from Holländer lab*). Nevertheless, this assumption remained to be experimentally proven. Therefore, the Cre recombinase was used as a surrogate self-antigen to probe for the efficiency of negative selection(*46*). The frequency of Cre-tetramer^{+} cortical thymocytes not undergoing negative selection ($CCR7^{-}PD1^{-}Helios^{-}$) was lower in mice that expressed Cre transgene, suggesting that the negative selection in cortex is apparently undisturbed for

this surrogate self-antigen (**Figure 14A**). In contrast, and despite a lower thymocyte to mTEC ratio, Cre-tetramer$^+$ thymocytes were observed to at a higher frequency in Eed$^{fl/fl}$::β5tCre mice when compared to PRC2-proficient, Cre-expressing transgenic mice (**Figure 14B**). Of note, a higher frequency of Cre-tetramer$^+$ thymocytes was also observed in PRC2-proficient Eed$^{fl/fl}$ control mice that lack Cre transgene. The absolute cellularity of Cre-tetramer$^+$ thymocyte was, however, greatly diminished in keeping with the hypocellularity of the Eed$^{fl/fl}$::β5tCre thymus (**Figure 14B**). These data independently verify that thymocyte negative selection is compromised in the absence of Eed expression in mTEC.

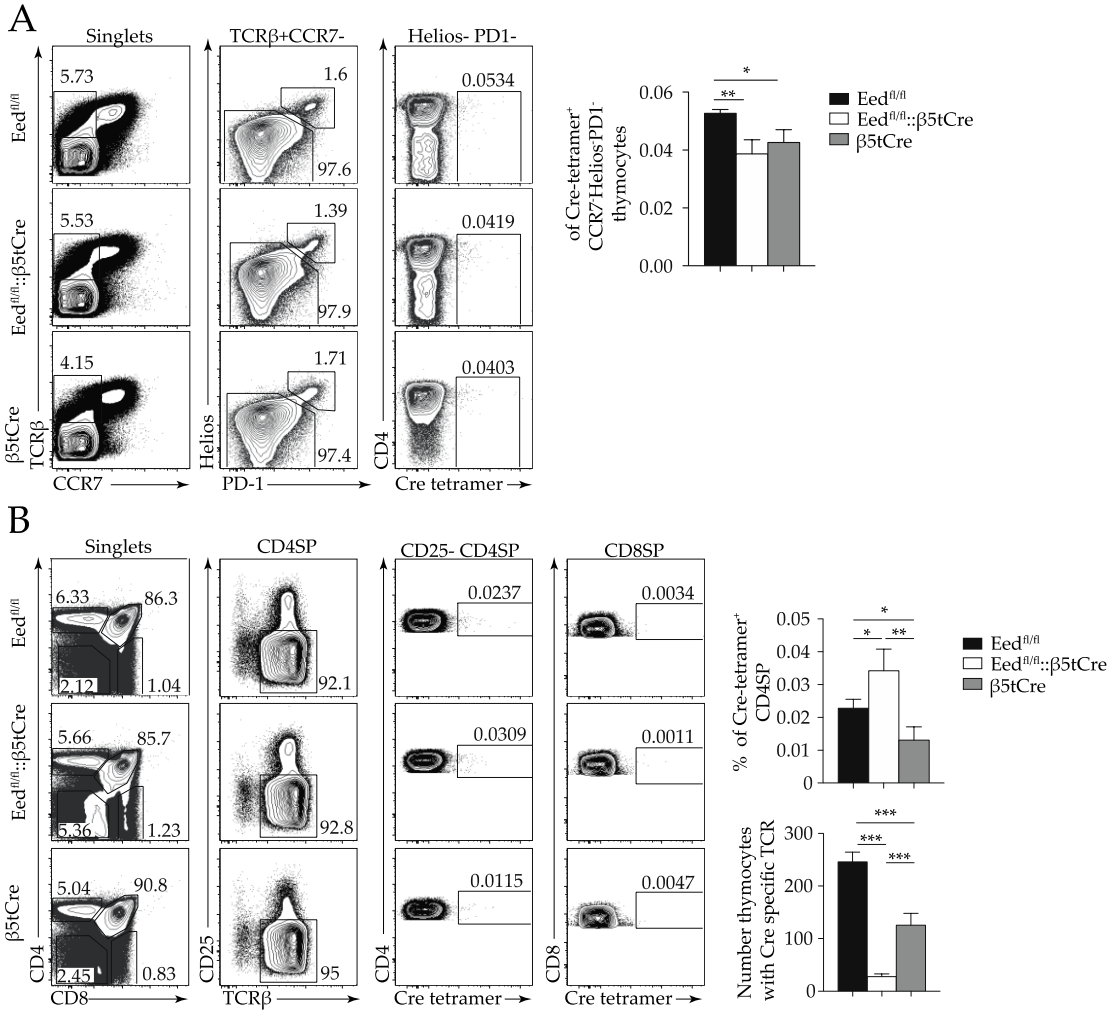

Figure 14. *Compromised negative selection of medullary thymocytes with reactivity to the Cre recombinase.* (**A**) Decreased frequencies of cortical (CCR7$^-$) Cre-tetramer$^+$ CD4 SP thymocytes in Cre-expressing transgenic mouse lines but unchanged in the absence

of PRC2 function. Flow cytometric analysis (*left panel*) and frequencies (*right panel*) of Cre-tetramer^{+} CD4 SP thymocytes within the population of non-negatively selected (PD1^{-}Helios^{-}) cortical (CCR7^{-}) thymocytes. (**B**) Increased frequency of Cre-tetramer^{+} CD4 SP thymocytes in PRC2-deficient. The gating strategy of the flow cytometric analysis of CD4SP thymocytes for reactivity to Cre tetramers is presented on the *left panel*. CD8 SP cells staining for Cre-tetramer were used as a negative control to set the threshold for the gates. The *right panel* shows the frequency (*top*) and cellularity (*bottom*) of Cre-tetramer-positive CD4 SP thymocytes in the indicated mouse strains. Data are representative of at least 2 independent experiments with 4 4-weeks-old mice per group. *p<0.05, **p<0.01, *** p<0.001, two-tailed paired Student's T test.

4.3.5. Thymic T_{reg} are reduced in Eed$^{fl/fl}$::β5tCre mice

Thymocyte negative selection is a mechanism of central T cell tolerance induction that is neither sufficiently comprehensive under physiological conditions nor fully effective. Therefore, an additional fail-safe mechanism needs to be in place to control self-reactive thymocytes that have escaped both the cortical and medullary negative selections. The non-deletional mechanism in controlling auto-reactive T cells in the periphery (i.e. outside of the thymus) relies on the generation of T_{reg}. These cells can either be generated by conversion of peripheral T effector cells or, alternatively, are formed in the thymic medulla after negative selection has been imposed. The mTEC play an essential role in generating T_{reg} by providing necessary developmental niches (*43*). In the thymus of Eed$^{fl/fl}$::β5tCre mice, an increased frequency but reduced cellularity of T_{reg} (Foxp3^{+}CD25^{+}) was observed among CD4SP cells (**Figure 15A**). The pool of T_{reg} from the thymus of the Eed$^{fl/fl}$::β5tCre mice also express TCR of unchanged avidity based on the similar level of CD5 gMFI values (**Figure 15A**). However, T_{reg} cells found in the thymus with this phenotype can either be derive within the thymus (thymic T_{reg}) or, alternatively, constitute a population of T_{reg} that have re-circulated from the periphery back to the thymus (recirculating T_{reg}) (*133*). Recirculating T_{reg} can be phenotypically identified as cells that are CCR7- but express high surface

level of CD44 (CCR7^{-}CD44^{high}). Applying these markers to the intrathymic T_{reg}, both the relative frequency and absolute cellularity of thymic T_{reg} were significantly reduced whereas the population of recirculating T_{reg} was increased in frequency but unchanged in absolute cellularity in comparison to the Eed$^{fl/fl}$ control mice (**Figure 15A, B**). The TCR avidity of only the recirculating T_{reg} pool but not the thymic T_{reg} was increased (**Figure 15B**). These findings suggested that the niches supporting thymic T_{reg} development were affected by the paucity of mTEC cellularity and/or the functional impairment of mTEC due to a loss of Eed expression.

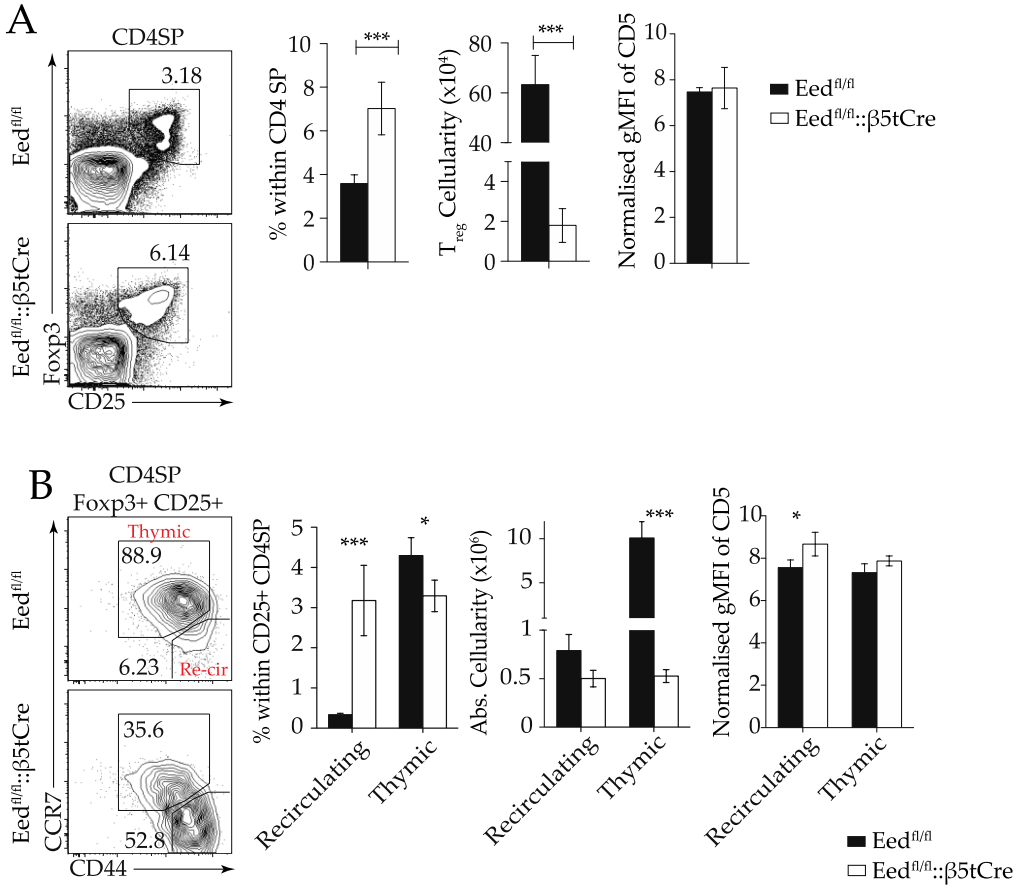

Figure 15. *Reduced thymic T_{reg} frequency and cellularity in 4-weeks-old Eed$^{fl/fl}$::β5tCre mice*. (**A**) Frequency and cellularity of total T_{reg} (Foxp3+CD25+CD4SP) in the thymus. The TCR avidity of the total T_{reg} is reflected by the mean fluorescence intensity (gMFI) values of CD5. (**B**) Detection of thymic T_{reg} (CCR7+CD44^{lo}) and re-circulating T_{reg} (CCR7-CD44^{hi}). TCR avidity values of both T_{reg} subpopulations are reflected by the mean fluorescence intensity (gMFI) values of CD5. Data are representative of at least 2 independent experiments with 3 to 4 mice per group. **<0.01, *** p<0.001, two-tailed paired Student's T test.

4.3.6. Thymic hypocellularity of Eed$^{fl/fl}$::β5tCre mice results in peripheral T cell lymphopenia

The peripheral T cell pool is in mice largely maintained by the efficient export of mature naïve T cells from the thymus. Therefore, the extent to which the thymic hypocellularity of Eed$^{fl/fl}$::β5tCre mice had compromised the establishment of the peripheral T cell pool was accessed. Analysing the spleen, fewer T cells could be recovered while both total splenic and B cellularity were not altered (**Figure 16A**). Hence, a significantly hypocellular thymus (**Figure 8B**) correlated with a contracted peripheral T cell pool suggesting a diminished naïve T cell output resulted, at least in part, in significantly fewer peripheral T cells.

The lack of competition in T lymphopenic hosts increases the access of naïve T cells to growth factors including interleukin-7 (IL7) and IL-15 and heightens the chance to encounter cognate MHC/peptide complexes on antigen presenting cells. As a consequence, tonic stimuli are abound to drive the homeostatic expansion of naïve T cells that consequently acquire a memory phenotype as characterised by an up-regulation of CD44 expression (*167, 168*). Peripheral CD4 and CD8 T cells of Eed$^{fl/fl}$::β5tCre mice displayed significantly higher frequencies of cells with phenotypes of memory cells (**Figure 16B**). Moreover, purified anti-CD3 stimulated naïve CD4 T cells displayed *in vitro* a heightened proliferation response as quantified by the faster dilution of CFSE-labeling (**Figure 16C, left panel**). As a consequence, increased IL2 concentrations were recovered from the supernatant of the cell culture (**Figure 16C, bottom right panel**). Taken together, these results suggest that both the phenotype and the mitogenic response of T cells had changed in Eed$^{fl/fl}$::β5tCre mice in comparison to Eed$^{fl/fl}$ control mice reflecting the animals' lymphopenic state.

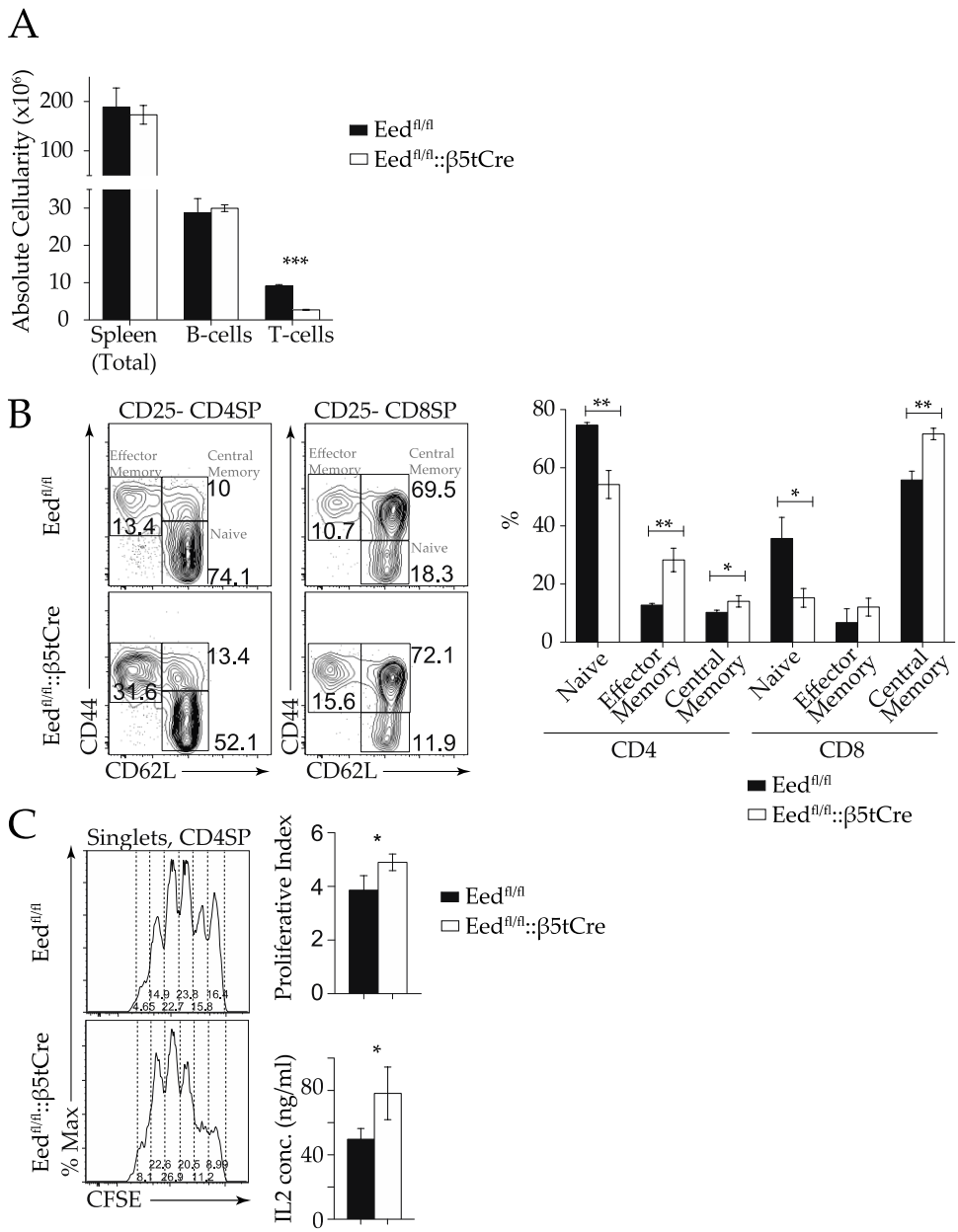

Figure 16. *Peripheral lymphopenia in 4-weeks-old Eed$^{fl/fl}$::β5tCre.* (**A**) Absolute cellularity of splenic total cells, T cells and B cells. (**B**) Increased frequencies of peripheral T cells with memory phenotype. Flow cytometric analysis (***left panel***) and frequencies (***right panel***) of spleen cells for the cell surface markers identifying naïve, effector and central memory T cells. (**C**) Increased proliferation rate upon *in vitro* stimulation with 1μg/ml of anti-CD3 for 72hours. Flow cytometric analysis on the CFSE signal in CD4 peripheral naïve T cells displayed the serial dilution after each successive round of replication (***left panel***). The proliferation index (***right top panel***; *refer to Materials and Methods section for calculation method*) and supernatant IL-2 concentrations (*right bottom panel; determined by ELISA*) of *in vitro* stimulated peripheral naïve CD4SP T cells. The CD4 peripheral naïve T cells were first purified by the flow cytometer then cultured for 72 hours *in vitro* with 1μg/ml of anti-CD3 antibody and irradiated splenocytes isolated from Rag2-deficient mice. Data are representative of at least 3 independent experiments with 3 to 4 4-weeks-old mice per group. **p<0.01, *** p<0.001, two-tailed paired Student's T test.

4.3.7. Increased frequency of anergic T cells in the periphery of Eed$^{fl/fl}$::β5tCre mice

Eed$^{fl/fl}$::β5tCre mice display a defect in their capacity to negatively select thymocytes (**Figure 17**) and were therefore investigated for signs of spontaneous autoimmunity, characterised either by premature death or the presence of mononuclear organ infiltration. Investigating mice as old as 40-weeks-old did not reveal any overt signs of ill health and histological analysis of tissues that are characteristically targeted by autoimmunity also failed to identify cellular signs of organ-related autoimmunity (*data not shown*). Next, to exclude the possibility that a repertoire of T_{reg} selected in the first week of life may have dominantly suppressed auto-reactive T cells escaping negative selection, T cells were depleted in 2-weeks-old Eed$^{fl/fl}$::β5tCre and Eed$^{fl/fl}$ control mice. This T cell depletion procedure involved 3 doses of *in vivo* i.p. injection with a concoction of complement-activating (anti-Thy1.1, anti-CD4 and anti-CD8) antibodies resulting in a virtual complete depletion of T cells 3 days after the final dose (**Figure 17B**). Following the treatment, peripheral T cell pool was subsequently repopulated with cells that were now educated and selected in a thymic microenvironment characterised by a progressive loss in regular cellular composition and reduced functionality (**Figure 9D, E & 10B**). The mice were then sacrificed 20 weeks after the T cell depletion and analysed for histological signs of autoimmunity. Again, both the Eed$^{fl/fl}$::β5tCre and Eed$^{fl/fl}$ control mice failed to display any mononuclear infiltration in characteristically targeted by autoimmunity (i.e. eye, salivary glands, liver, pancreas, kidney) (**Figure 17A, C**). Hence, T cell selection in Eed$^{fl/fl}$::β5tCre mice at the age of 2 weeks or older did not result in a repertoire of T cells capable of eliciting tissue infiltration.

Since overt autoimmunity was not be detected in Eed$^{fl/fl}$::β5tCre mice spontaneously or after depletion and recovery of the periphery T cell pool, I

next investigated whether an increased frequency of anergic cells could be detected in the T cell repertoire of $Eed^{fl/fl}$::β5tCre mice. T cell anergy constitutes an essential mechanism by which lymphocytes are rendered functionally inactive to avoid activation of an adaptive immune response following the recognition of their cognate antigen. Anergic T cells will be hypo-responsive for an extended period of time despite an adequate stimulation of their TCR and co-stimulatory molecules upon re-encounter of their specific antigen (*134*). This state of anergy is either attained following incomplete T cell activation or, alternatively, is effected in an environment lacking adequate co-stimulatory signals or marked by a heightened presence of co-inhibitory signals. Given that impaired negative selection of thymocyte may result in the survival of auto-reactive T cells, the induction of anergy is one of the fail-safe mechanisms to avoid autoimmunity. In this analysis, $Foxp3^{-}$ CD4 SP cells were probed for the up-regulation of CD73 (*Nt5e*) and folate receptor 4 (FR4, *Izumo1r*), two cell surface markers associated with the functional state of anergy (*135*, *136*). $Eed^{fl/fl}$::β5tCre mice displayed a higher frequency of $CD73^{+}FR4^{+}$ CD4 SP T cells in both the naïve and effector memory T cell pool when compared to $Eed^{fl/fl}$ control mice (**Figure 17E**). Overall, these results suggested that induction of anergy served as an effective mechanism to prevent improperly selected T cells from initiating an autoimmune response.

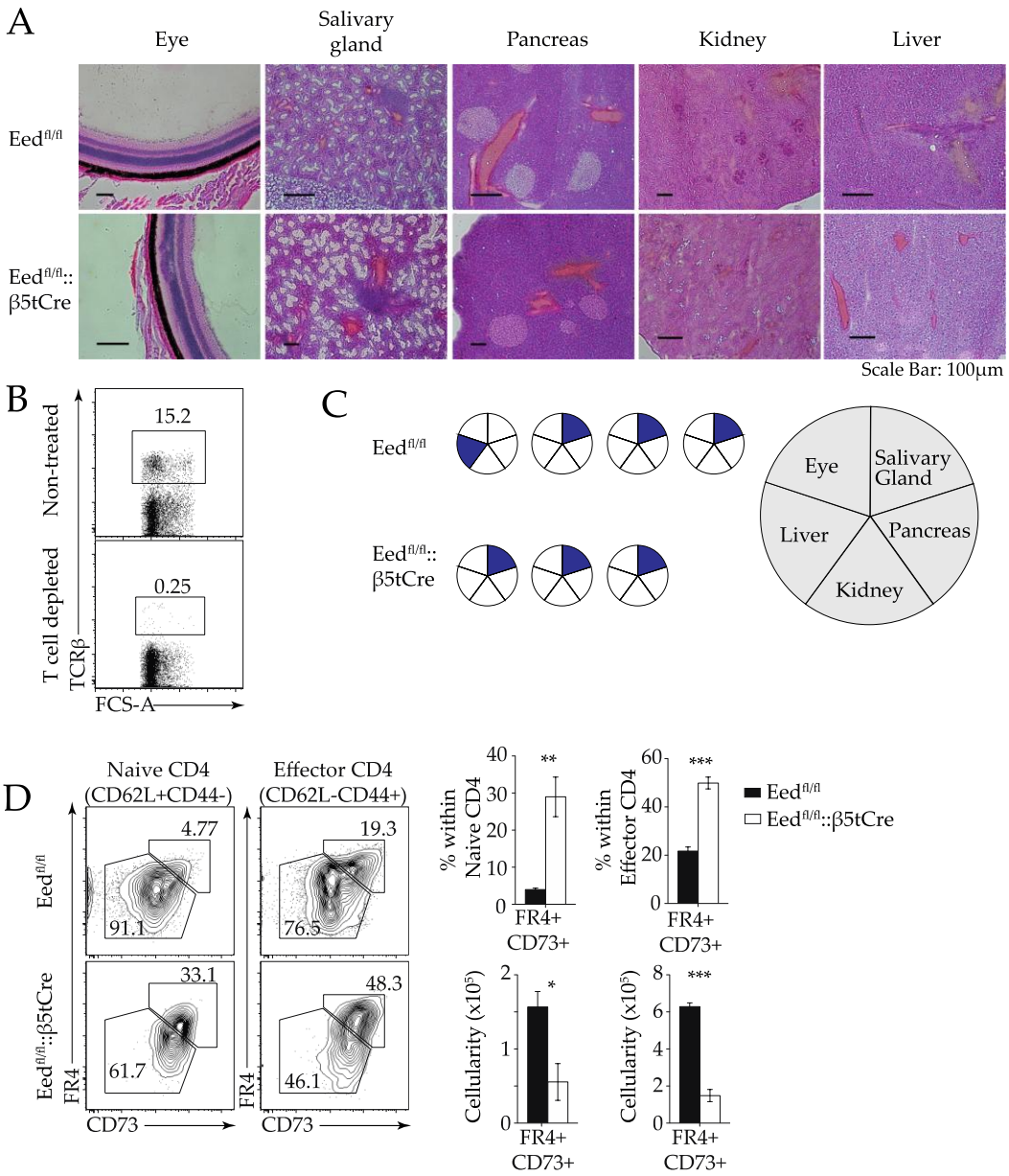

Figure 17. *Lack of autoimmunity in T cell depleted accompanied with increased frequency of anergic peripheral CD4 T cells in Eed$^{fl/fl}$::β5tCre mice.* (**A**) Representative images from the H&E analysis of peripheral tissues of both Eed$^{fl/fl}$::β5tCre and Eed$^{fl/fl}$ mice. Organs were isolated from both mutant and wild type mice 20 weeks after T cell depletion at the age of 2-weeks using anti-CD4/CD8/Thy1.1 antibody concoction i.p. injected *in vivo*. (**B**) Effective depletion of peripheral T cells by triple dosage of anti-CD4/CD8/Thy1.1 antibody concoction. Analysis of the spleenocytes 3 days after the final dosages showed drastically reduced frequency of T cells in the periphery (*bottom panel*). (**C**) Incidence of lymphocytic infiltrates in selected target tissues of Eed$^{fl/fl}$::β5tCre (n=4) and Eed$^{fl/fl}$ (n=3) mice. Coloured segments indicated histologically verified infilatration of an organ indicated in the larger pie chart to the right. (**D**) Frequency of anergic CD4 SP cell were reduced in Eed$^{fl/fl}$::β5tCre mice. Quantification of anergic peripheral CD4 SP T cells based on their expression of both FR4 and CD73. Data in (**D**) are representative of at least 2 independent experiments with 3 4-weeks-old mice per group. **p<0.01, *** p<0.001, two-tailed paired Student's T test.

4.4. Evidences for the presence of β5t-independent mTEC

4.4.1. Detection of an mTEC lineage derived via a β5t-independent developmental pathway in Eed$^{fl/fl}$::β5tCre mice

Tissue targeted gain or loss of function mutations using the Cre-loxP system critically depend not only on the "tightness" and efficiency of Cre expression under a chosen transcriptional control but are also influenced by the chromatin accessibility of the loxP-flanked target sequence. The Cre expression driven by the *Psmb11* locus, encoding the proteasome component β5t, results in a highly efficient (>99%) recombination of loxP sites (*122*). Under physiological conditions, all TEC in cortex and medulla are derived from a common precursor in which *Psmb11* (β5t) is transcriptionally active (*21*). Therefore, all cortical and medullary TEC are expected to reveal Cre-mediated deletions of loxP-flanked target genes (*21*, *122*).

The interrogation of Eed$^{fl/fl}$::β5tCre mice for their functional loss of PRC2-mediated methylation of H3K27me3 revealed a complete loss of these marks in the nuclei of cTEC but two different patterns of H3K27me3 marks in the mTEC population (**Figure 9B**). The majority of mTEC (70%) in 4-weeks-old mutant animals displayed the expected loss of H3K27me3 marks when analysed by flow cytometry whereas a minority of mTEC (30%) appeared to maintain these post-translational modifications (**Figure 18A**). Further analysis of the "escapees" (i.e. cells that had seemingly not rearranged their conditional *Eed* locus) demonstrated that H3K27me marks were more frequently observed in mature vs. immature mTEC (mTEC^{hi}: 55% vs. mTEC^{lo}: 20%) inferring an advantage for the process of TEC maturation where physiological PRC2 activity is maintained. This finding was mirrored in Ezh1^{KO}::Ezh2$^{fl/fl}$::β5tCre mice where PRC2 function is ablated due to the loss of

its catalytically active subunits Ezh1/2. In these mice, as much as 80% of mTEC^{hi} maintained a wild type H3K27me3 level (**Figure 18B**).

The most probable explanation for the persistence of mTEC with a normal H3K27me3 complementation in Eed$^{fl/fl}$::β5tCre mice implied that these cells were derived from a TEC precursor which, contrary to wild type conditions, did not express β5t as part of their transcriptome and thus lack Cre expression. As a consequence, these cells and their progeny would not have deleted the *Eed* gene locus. However, other reasons to be considered including the possibility that Cre was expressed but that the *Eed* locus was inaccessible. To test this assertion directly, a strong green fluorochrome *ZsGreen* transgene was introduced as a reporter into the genetic background of Eed$^{fl/fl}$::β5tCre mice. This allowed TEC and their progeny to express ZsGreen from the *Rosa26* locus after Cre-loxP driven excision of a stop cassette containing multiple stop codons. Again not all mTEC in these triple transgenic mice appeared to express Cre with as many as 30% of all mTEC lacking ZsGreen expression (**Figure 18C**) and hence being derived from epithelial precursors that had not transcribed Cre from the *Psmb11* locus. In contrast, more than 99% of cTEC were green fluorescent (**Figure 18C**). Further analysis of immature and mature mTEC demonstrated that, as previously observed in double transgenic mice at comparable frequency, a higher relative frequency of mature mTEC not expressing Cre (**Figure 18D**). Importantly, the lack of wild type levels of H3K27me3 marks in ZsGreen^{+} cTEC showed that Cre activity had not only successfully removed the stop cassette upstream of the *ZsGreen* transgene but had also deleted exons 3 to 6 of *Eed* rendering the catalytic activity of PRC2 inoperative (**Figure 18E**). Conversely, mTEC that remained ZsGreen^{-} retained a wild type H3K27me3 expression pattern (**Figure 18E**). The loss of PRC2 activity did not change the amount of total histone 3 in both the cTEC and mTEC (**Figure 18E**). Taken together, these data strongly implied the existence of an mTEC lineage

derived from precursors that did not express β5t. Moreover, the progressive increase in the relative frequency of PRC2 competent mTEC parallel to the cells' maturation would argue for a growth advantage of these cells when compared to Eed-deficient mTEC.

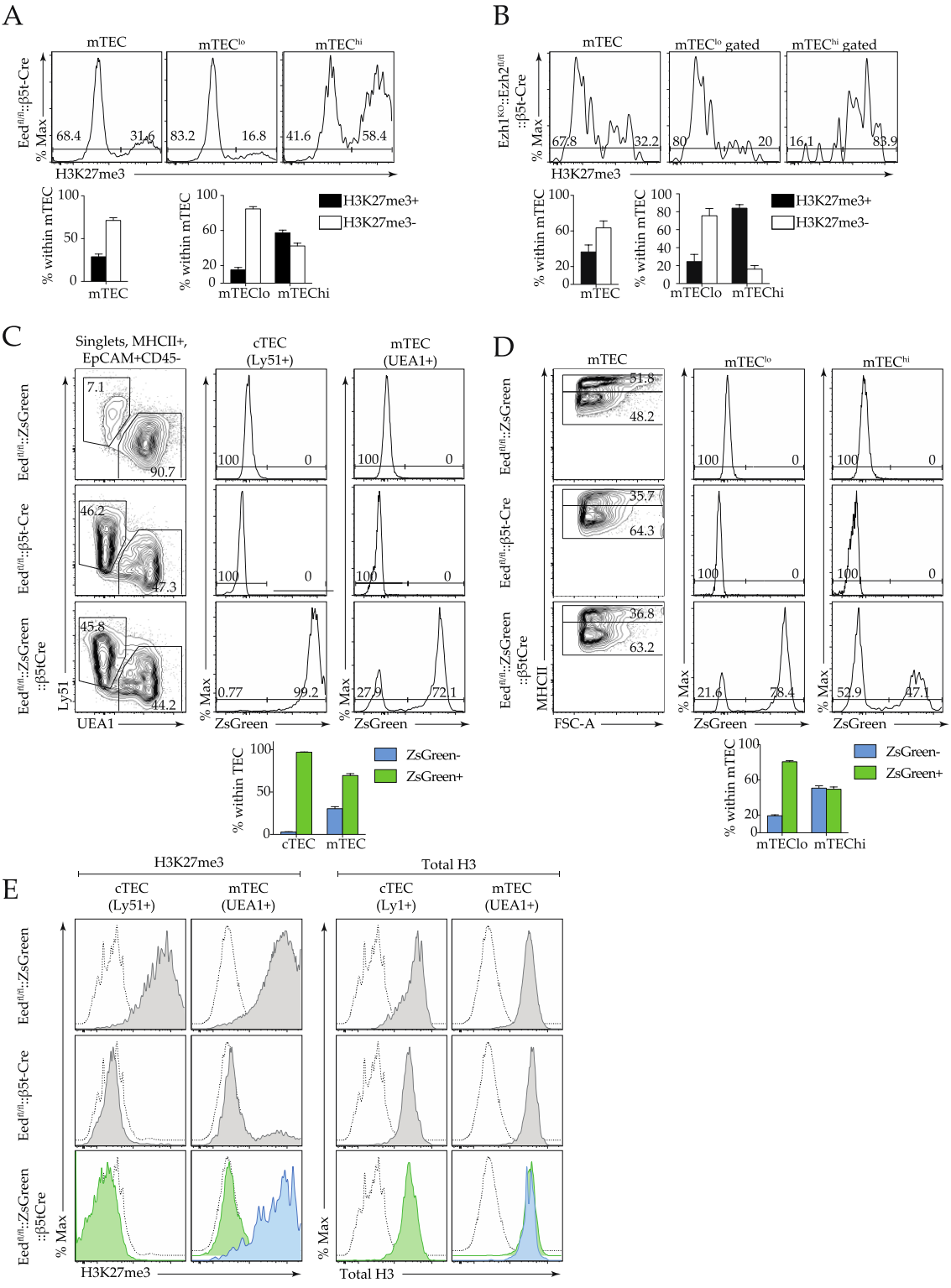

Figure 18. *Psmb11-mediated Cre expression spares a population of mTEC from loss of Eed in 4-weeks-old mice*. (**A**) Top panels: Flow cytometric analysis of H3K27me3 expression in individual TEC subpopulations isolated from 4-weeks-old Eed$^{fl/fl}$::β5tCre mice. Lower panels: Relative frequency of individual TEC subpopulations containing wild type level (*black*) or lacking (*white*) H3K27me3. (**B**) Top panels: Flow cytometric analysis of H3K27me expression in individual TEC subpopulations isolated from 4-weeks-old Ezh1^{KO}::Ezh2$^{fl/fl}$::β5tCre mice. Lower panels: Relative frequency of

individual TEC subpopulations containing wild type level (*black*) or lacking (*white*) H3K27me3. (**C**) ZsGreen expression in cTEC (Ly51+) and mTEC (UEA1+) of 4-weeks-old $Eed^{fl/fl}$:: ZsGreen::β5tCre mice. The lower panels show the relative frequencies of each individual phenotype. (**D**) ZsGreen expression in immature mTEC (expressing low MHC-II level, $mTEC^{lo}$) and mature mTEC (expressing high MHC-II level, $mTEC^{hi}$) of $Eed^{fl/fl}$::ZsGreen::β5tCre mice. The lower panels show the relative frequencies of each individual phenotype. (**E)** Flow cytometric analysis of H3K2me3 (left) and total H3 (right) expression in cTEC and mTEC isolated from $Eed^{fl/fl}$::ZsGreen::β5tCre mice. The individual histograms are colour-coded for the expression of ZsGreen (*green*) or its absence (*blue*). Data are representative of at least 2 independent experiments with 3-4-weeks-old mice per group.

4.4.2. Persistence of Eed-expressing mTEC in $Eed^{fl/fl}$:: β5tCre

I next wished to independently confirm the two separate mTEC populations using additional methods. For this purpose, the population of mTEC isolated from $Eed^{fl/fl}$::β5tCre mice was being analysed for their Eed expression at genomic, transcriptomic and protein level. Populations with and without the expected genomic deletion of exons 3-6 were observed in the separate mTEC populations indicating the lack of recombination in a significant proportion of both immature and mature mTEC ($mTEC^{lo}$ and $mTEC^{hi}$, respectively) (**Figure 19A**). Though the difference in genomic DNA excision between these two subpopulations could mirror the flow cytometric findings, a precise quantification of the observed loss of *Eed* exons 3-6 could, however not be calculated given the dissimilar kinetics of amplifying genomic sequences of different length. At the transcriptional level, changes in the detection of *Eed* exon 3 to 6 were noted whereby cDNA for these targeted exons could not be amplified in cTEC but partially detected in the two separate mTEC populations (**Figure 19B**). Again, an exact resolution of the relative frequency of TEC with a recombined *Eed* locus was not possible. Nevertheless, the differences in the detection of amplicons for the targeted sequences correlated with the results obtained from genomic and flow cytometric analyses. Finally, Eed protein expression was analysed with

immunohistology of TEC that had been sorted and then cytospun onto glass slides (**Figure 19C, left panel**). The presence of Eed could not be detected in any of the cTEC isolated from the Eed$^{fl/fl}$::β5tCre mice. In contrast, mTEC subpopulations contained cells that still expressed the Eed protein. Their frequencies (**Figure 19C, right panel**) were largely comparable to that observed by the flow cytometric analysis (**Figure 18D**). Taken together, the deletion of *Eed* exons 3-6 was complete in cTEC whereas this was only partially observed in mTEC further supporting the contention that Eed-proficient mTEC did not recombine their targeted locus.

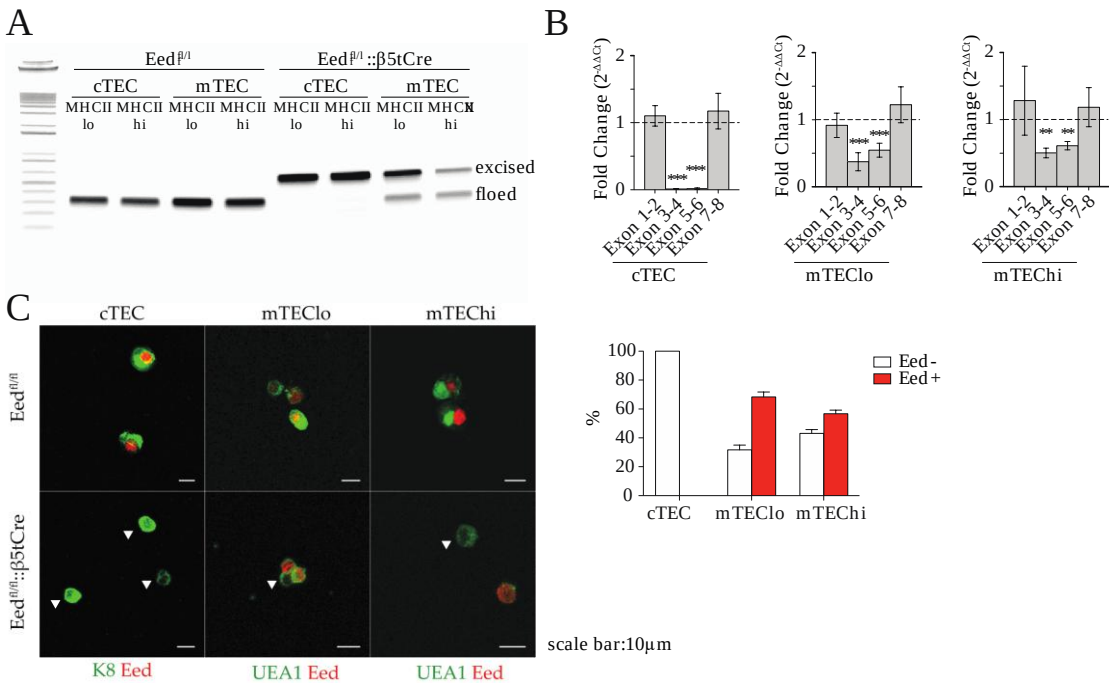

Figure 19. *Analysis of Eed expression at genomic, transcriptomic and protein level in 4-weeks-old Eed$^{fl/fl}$::β5tCre mice*. (**A**) Genomic PCR analysis of *Eed* locus in separate TEC subpopulations sorted by flow cytometry. (**B**) qPCR analysis of the expression of separate *Eed* exons in the indicated TEC subpopulations sorted by flow cytometry where the corresponding value was arbitrarily set to 1. cDNA amounts were normalised using the housekeeping gene GAPDH. **p<0.01, *** p<0.001, two-tailed paired Student's T test. (**C**) Immuno-histology for Eed (*red*) and anti-keratin 8 or UEA-1 reactivity (each in *green*) in FACS-sorted TEC placed onto glass slides by cytospin centrifugation (*left panel*). The white arrows indicate the cells that lack Eed protein detection. Relative frequency of TEC populations expressing (*red*) or lacking (*white*) Eed protein (*right panel*). Data are representative of 2 independent experiments with 3 4-weeks-old mice per group.

4.4.3. Differences in the transcriptome of mTEC proficient or deficient in Eed expression

The identification of a subpopulation of mTEC that apparently defied *Eed* deletion under the experimental conditions used in $Eed^{fl/fl}$::β5tCre mice was unexpected but inferred that the genetic pressure of a loss of PRC2 function allowed for the generation of mTEC via an alternative lineage pathway that did not rely on β5t-expressing TEC progenitors. To confirm this assertion, single mTEC from $Eed^{fl/fl}$::β5tCre and $Eed^{fl/fl}$ control mice were investigated for their respective transcriptomes. The single cell data set (when combined) was observed to show a good correlation in gene expression profile to the transcriptome data obtained from bulk cell analysis (*50,* **Figure 20A**). This demonstrated the robust quality of the single cells transcriptomic data. Next, the mTEC isolated from $Eed^{fl/fl}$::β5tCre mice were confirmed to be indeed Eed-proficient mTEC with the detection of loxP flanked exons in the transcriptome at the same level as the wild type control (**Figure 20B**). The overall pattern of both gene expression and gene copy number (as measured by Fragments per kilobase of transcript per million mapped reads, FPKM) of expressed tissue-restricted antigens were largely comparable for the PRC2-proficient mTEC isolated from $Eed^{fl/fl}$::β5tCre mice and wild type control mice (**Figure 20C**). To further interrogate the differences in expression levels of TRA, an analysis combining single transcriptomic data from multiple mTEC was carried out. This analysis aimed to recapitulate the nature of TRA expression in mTEC whereby individual mTEC expresses incomplete sets of TRA and represent the entire TRA repertoire collectively at the population level (*57*). The number of genes with detectable expression (FPKM > 1) was determined from the combined transcriptomic data amassed from multiple cells. This analysis showed that PRC2 proficient mTEC in $Eed^{fl/fl}$::β5tCre mice expressed fewer Aire-dependent genes per single cell when compared to the

wild type mTEC of the same phenotype (**Figure 20D**). In contrast, the expression of all TRA collectively, including the Aire-independent genes, was affected to a lesser extend.

A t-SNE clustering analysis was carried to further investigate the differences in expression patterns between the transcriptome of PRC2-proficient mTEC from $Eed^{fl/fl}$:: β5tCre and wild type mice. This analysis aimed to identify gene expression patterns in multi-dimensional datasets, the expression levels of many genes, by reducing them into 2 dimensional projections composing of principal component 1 (PC1) against PC2. The PC compresses multi-dimensional data in way to highlight their similarities and differences. This analysis showed that a distinct group of mTEC isolated from $Eed^{fl/fl}$::β5tCre clustered separately from other mTEC from the wild type control within the expression pattern of both Aire-enhanced genes (expression up-regulated by Aire) and the other TRA (**Figure 20E**). However, this separate clustering pattern was not observed in the expression pattern of Aire-dependent TRA in mTEC from the $Eed^{fl/fl}$:: β5tCre and wild type mice. The differences within the t-SNE clustering patterns of gene expression highlighted the innate differences of the biology of the mTEC from the mutant and wild type mouse strains.

Next, a differential gene expression analysis was conducted to probe further for differences between transcriptomes of PRC2-proficient mTEC from $Eed^{fl/fl}$::β5tCre and wild type mice. In the PRC2-proficient mTEC isolated from $Eed^{fl/fl}$::β5tCre mice, 144 genes were down-regulated while 408 genes were up-regulated in comparison to those from wild type controls. Gene annotation analyses revealed that PRC2-deficient mTEC of $Eed^{fl/fl}$::β5tCre expressed significant lower levels of genes associated to cell stress and with interaction with extracellular matrix (**Figure 20F, G**). Therefore, the functional transcriptomic makeup of PRC2-proficient mTEC in $Eed^{fl/fl}$::β5tCre mice differed from the corresponding cell type in wild type mice.

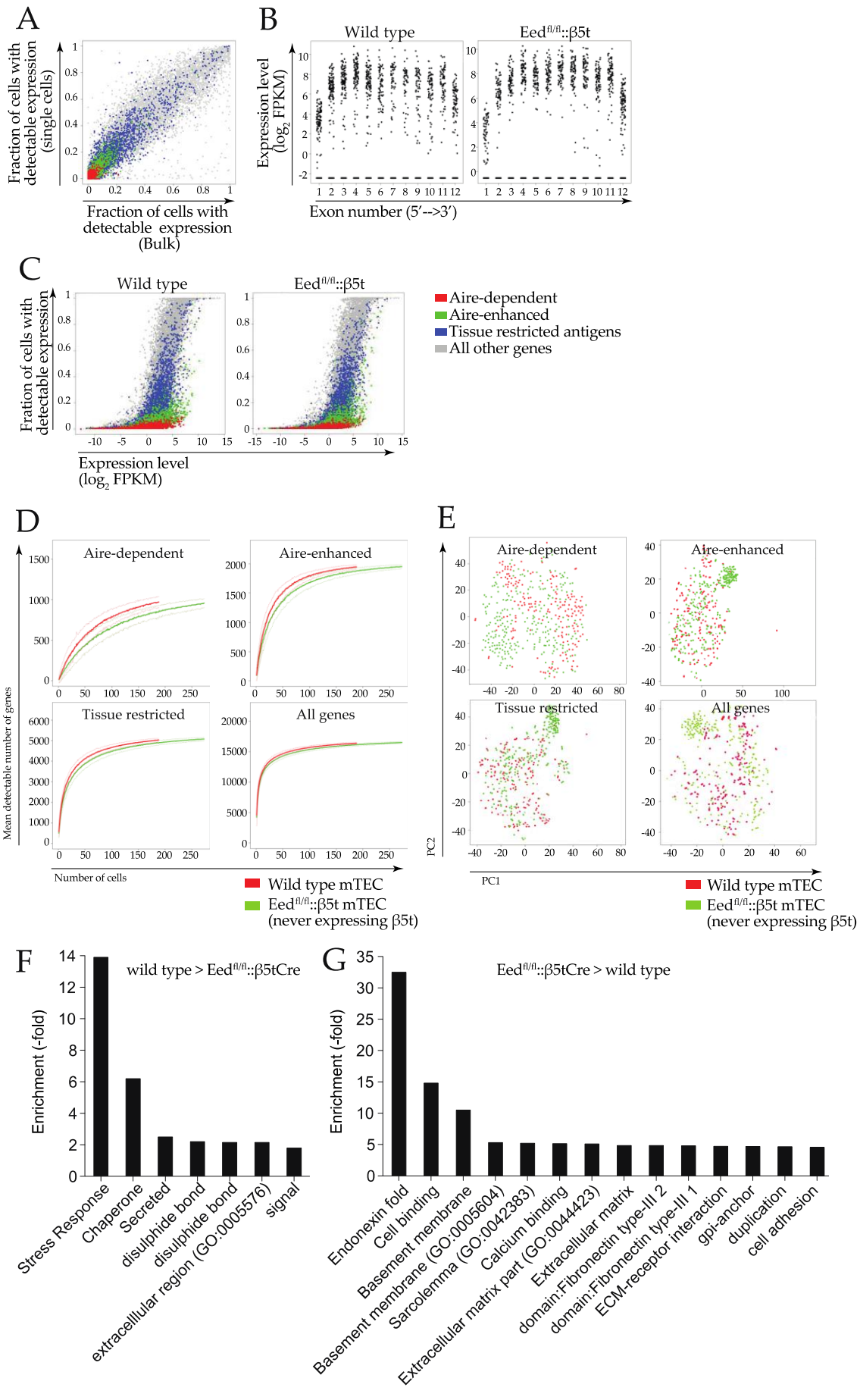
A
Fraction of cells with detectable expression (single cells)
Fraction of cells with detectable expression (Bulk)
B
Wild type
Eed^fl/fl::β5t
Expression level (log2 FPKM)
Exon number (5'-->3')
C
Wild type
Eed^fl/fl::β5t
Fration of cells with detectable expression
Expression level (log2 FPKM)
Aire-dependent
Aire-enhanced
Tissue restricted antigens
All other genes
D
Aire-dependent
Aire-enhanced
Tissue restricted
All genes
Mean detectable number of genes
Number of cells
Wild type mTEC
Eed^fl/fl::β5t mTEC (never expressing β5t)
E
Aire-dependent
Aire-enhanced
Tissue restricted
All genes
PC2
PC1
Wild type mTEC
Eed^fl/fl::β5t mTEC (never expressing β5t)
F
wild type > Eed^fl/fl::β5tCre
Enrichment (-fold)
Stress Response
Chaperone
Secreted
disulphide bond
disulphide bond
extracelllular region (GO:0005576)
signal
G
Eed^fl/fl::β5tCre > wild type
Enrichment (-fold)
Endonexin fold
Cell binding
Basement membrane
Basement membrane (GO:0005604)
Sarcolemma (GO:0042383)
Calcium binding
Extracellular matrix part (GO:0044423)
Extracellular matrix
domain:Fibronectin type-III 2
domain:Fibronectin type-III 1
ECM-receptor interaction
gpi-anchor
duplication
cell adhesion

Figure 20. *Single cell transcriptomic analysis of β5t-independent mTEC from 4-weeks-old Eed$^{fl/fl}$::β5tCre*. (**A**) Correlation of data from single cell compared to previous bulk RNA-sequencing data. The proportion of mTEC with detectable expression from the bulk sequencing was plotted against proportion of single mTEC with each gene detectable. The genes were classified into Aire-dependent (*red*), Aire-enhanced (*green*), TRA (*blue*), and all other genes (*grey*). (**B**) All mTEC isolated from Eed$^{fl/fl}$::β5tCre used in this set of analyses retained Eed expression. The exon coverage (1 to 12) of *Eed* gene locus with mTEC from Eed$^{fl/fl}$::β5tCre (***right panel***) and wild type control (***left panel***). (**C**) Plot of mean expression (log_2 FPKM) against the proportion of cells showing detectable gene expression with mTEC from Eed$^{fl/fl}$::β5tCre (***right panel***) and the wild type control (***left panel***). (**D**) The mean number of genes detectable when combining different number of mTEC. The mean number of genes with expression level (FPKM) of at least 1 upon combining different number of cells (*x-axis*) of mTEC from Eed$^{fl/fl}$::β5tCre (*green*) and control (*blue*). Genes are categorised into Aire-dependent genes (*top left*), Aire-enhanced genes (*top right*), tissue-restricted genes (*bottom left*) or all protein-encoding genes (***bottom right***). The dotted line represented the 95% confidence interval of each corresponding sample. (**E**) t-SNE clustering analysis of mTEC from Eed$^{fl/fl}$::β5tCre (*green*) and wild type control (*red*). Genes are categorised into Aire-dependent genes (***top left***), Aire-enhanced genes (***top right***), tissue-restricted genes (***bottom left***) or all protein-encoding genes (***bottom right***). (**F**) Gene ontology analysis of differentially expressed genes. The genes expressed in a higher amount in PRC2-proficient mTEC from Eed$^{fl/fl}$::β5tCre as compared to the wild type control are plotted on the *right panel* and vice versa (***left panel***). Data presented in this figure were obtained from a single experiment and included 273 mTEC from Eed$^{fl/fl}$:: β5tCre and 184 mTEC from the wild type control that passed the quality control. Please refer to the Materials and Methods section for detailed description of the methodology used for the analyses.

5. DISCUSSIONS

Recent progress in the field of thymus biology demonstrated that, within the mTEC, regions of chromatin encoding for TRA contained higher levels of repressive histone marks. In particular to the interest of this thesis, elevated level of H3K27me3 was found to be present at the transcription start sites of TRA transcriptionally controlled by Aire in mTEC with high level of MHC-II expression (*50*). Albeit the correlation of epigenetic marks in TRA expression, there is a lack of in depth understanding of the functional significance of H3K27me3 modification in TEC. This thesis addresses the paucity in the knowledge pertaining to the role of H3K27me3 marks in TEC differentiation and development, including the capacity of TEC to support the negative selection of thymocytes.

The PRC2 is primarily responsible in creating and maintaining the H3K27me3 marks on the chromatin and its core components includes Eed and Ezh1/2 (*98*). Mouse models with specific deletion of Polycomb repressive complex 2 (PRC2) in TEC, and hence altered H3K27me3 marks on the chromatin, were generated to achieve the aims of this study. Previous studies showed that the ablation of Eed precluded the H3K27me3 marks without affecting the level of H3K4me3 (*102*). However, when targeting the other core subunits of PRC2, simultaneous ablation of both Ezh1 and Ezh2 are required to achieve the same effect as eliminating only Eed due to the partial redundancy of the 2 Ezh homologs (*94*, *102*). In this study, β5t promoter is chosen as the TEC-specific promoter of Cre recombinase to specifically delete the chromatin section encoding the subunits of PRC2, which were modified to be flanked by loxP sequences.

5.1. Summary of findings

The thymi in the $Eed^{fl/fl}$::β5tCre mice were severely hypocellular despite unaltered TEC cellularity up to the age of 4 weeks (**Figure 8B**). Despite the severe reduction of thymocyte cellularity, TEC cellularity was unchanged and the hypocellular thymus also maintained a clear cortico-medullary segregation (**Figure 8C, D**). In the mutant mice, the cTEC to mTEC ratio was increased (**Figure 9D, E**) and the maturation of mTEC was also hindered (**Figure 10A, B**). The Eed-deficient cTEC expressed reduced levels of chemokines CXCL12 and CCL25 (**Figure 12D**) that coincided with the reduced number of ETP recruited to the thymus (**Figure 12C**). The reduced ETP recruitment most likely led to the drastically reduced thymocyte cellularity, as the later stages of thymocyte development were unaffected (**Figure 12A**). Although the lack of Eed did not have any effect on the positive selection process, the efficiency of negative selection of potentially harmful thymocytes was significantly reduced (**Figure 13**). The cellularity of thymic T_{reg} was also reduced corresponding to the reduced mTEC pool (**Figure 15B**) that provides niches to foster the development of T_{reg} (*138*). As a consequence of the reduced thymocytes cellularity, the mutant mice were lymphopenic in the periphery (**Figure 16**). However, the mutant mice did not develop autoimmune diseases spontaneously or upon T cell depletion (**Figure 17A**). This lack of autoimmunity could partially be explained by the increased frequency of anergic CD4 T cells in the periphery of mutant mice (**Figure 17D**), possibly including the potentially auto-reactive T cells.

Another main finding of this study is an unreported mTEC population derived from progenitors independent of β5t expression. In wild type mouse virtually all TEC are derived from a common progenitor expressing β5t (*21*, *122*). In this study, the regular mTEC differentiation pathway was disturbed by PRC2 deficiency and the alternative mTEC development pathway

involving β5t-independent progenitors came into play. In mouse models lacking PRC2 function in the majority of the total TEC, this unique mTEC population derived from β5t-independent progenitors composed about 30% of the mTEC population at the age of 4 weeks (**Figure 18A, B**) and these cells also possessed a unique transcription profile. These mTEC derived from β5t-independent progenitors expressed fewer TRA and lower expression level of genes related to cell stress and extra-cellular matrix (**Figure 20**).

5.2. Tissue specificity and timing of Cre recombinase expression

The *Foxn1* promoter is the conventional choice to achieve TEC specificity in Cre recombinase expression (*125*). However, in addition to the thymic epithelial, *Foxn1* promoter activity is also significantly active within the skin keratinocytes (*123*). Recently, Foxn1Cre activity was reported in the male germ cells and resulted in all offsprings from Foxn1Cre male mice to possess recombined loxP flanked gene locus indiscriminately in all tissues (*139*). An ideally designed Cre-lox system achieves specific deletion in only the desired cell types so as to determine the physiological effects without influences from defects in other organs of the host system. In light of the caveats of utilising the *Foxn1* promoter to achieve TEC-specific targeting, an alternative model was used instead to circumvent these potential problems mentioned. β5t is a proteasome subunit expressed in virtually all the TEC progenitors and maintained only within the cTEC population (*122*). As such, the *β5t* promoter activity is highly specific to only TEC with activity found only in TEC progenitors and cTEC. Therefore, the *Psmb11* (*β5t*) promoter is able to replace *Foxn1* promoter and function as the driver of Cre recombinase expression specifically only in the TEC (*122*).

An important factor to be considered when using *Psmb11* (*β5t*) promoter instead of *Foxn1* promoter to drive the Cre recombinase is the time

point at which the promoter's activity is initiated. The transcriptional activity of *Foxn1* locus is detectable by E11.25 (*12*), while the β5t, a target of Foxn1 (*124*), is first expressed in TEC only approximately a day later at E12.5 (*140*). Preliminary data from experiments on $Eed^{fl/fl}$::Foxn1Cre mice reported that at the age of 4 weeks the thymus was highly cystic and the TEC cellularity was diminished with a greater effect on the cTEC population (*141*). In contrast, the hypocellular thymus of a 4-weeks-old $Eed^{fl/fl}$::β5tCre mouse was neither cystic nor had a lower total TEC cellularity as compared to control mice (**Figure 8**). The differences in TEC phenotype between the usages of different promoters indicated that the timing of deletion of PRC2 has a profound effect on the TEC development. On E11.25, besides the up-regulation of Foxn1, another hallmark in thymic organogenesis is the initial seeding of haematopoietic cells via chemotaxis (*24*, *142*). The time point at which Foxn1Cre induces the inactivation of PRC2 coincides with the initial seeding of haematopoietic cells. The additional day of development after the initial recruitment of haematopoietic cells in $Eed^{fl/fl}$::β5tCre could provide sufficient time for the TEC progenitors to attain a more determined cell fate and thus permit the formation of a non-cystic thymus containing unaltered TEC cellularity up to the age of 4 weeks. Therefore, this suggests that PRC2 probably plays a critical role during the early stages, in particular from E11.25 to E12.5, of the thymus development.

During E11 to E11.5, the thymic primordia detach from the pharynx and embryonic TEC proliferate intensively under the support from growth factors produced by the mesenchymal cells (*7*, *143*). The development of the thymic primordia requires complex signaling pathways involving fibroblast growth factors, bone morphogenetic proteins and homeobox proteins (*7*, *143*). Since the expression of homeobox proteins is under the regulation of PRC2 (*90*), the earlier inactivation of PRC2 initiated by Foxn1Cre could disturb the organogenesis to a greater extent by disabling the signaling pathways

involving homeobox proteins in less mature thymic primordia. Therefore, the differences in the phenotypes resulting from different timing of PRC2 inactivation highlight the critical role played by PRC2 in the early stages of thymus organogenesis.

5.3. Specificity of PRC2 inactivation

The effect of PRC2 deficiency in TEC was mainly studied in the $Eed^{fl/fl}$::β5tCre mice. In addition to this mouse model, the double knockout mouse model ($Ezh1^{KO}$::$Ezh2^{fl/fl}$::β5tCre) was used to confirm that the phenotype observed in $Eed^{fl/fl}$::β5tCre mice was indeed specifically due to PRC2 deficiency. The Ezh1/2 subunit of PRC2 interacts with Eed to activate the catalytic SET domain in order to carry out its function (*98*). Hence, deleting only *Eed* is sufficient to eliminate the catalytic function of PRC2 completely (*102*). On the other hand, the partial redundancy of the homologs *Ezh1* and *Ezh2* requires the deletion of both genes to achieve the same effect of the single Eed deficiency (*94*). The deletion of Eed or Ezh1/2 in HSC did not change the levels of other post-translational modifications on the histone 3 (*102*). Thus, the predominant effect of knocking out PRC2 is the preclusion of H3K27me3 mark on the chromatin.

Besides catalysing the trimethylation of H3K27, Ezh2 methylates both Gata4 and Stat3 to repress the function of the former while activating the latter (*111*, *144*). While there has been no report of cellular processes dependent on Gata4 in TEC, Stat3 was shown to be crucial for the postnatal maintenance of thymic architecture and function (*111*). However, TEC-specific loss of Stat3 does not result in any observable phenotype in mice before the age of 5 weeks (*145*). In TEC-specific Stat3-deficient mice older than 5 weeks of age, the thymus is severely hypocellular accompanied by altered tissue architecture and a great loss of thymocyte cellularity. This late onset

phenotype is beyond the time frame relevant for this study and off-target effects should not be significant in young mice. Moreover, in particular to the activation of Stat3 via methylation, Ezh2 specifically methylates Stat3 only on the lysine residue at the 180th position. This post-translational modification increases the activity of Stat3 in cellular signaling specifically within glioblastoma cells (*111*). Thus, the potential contribution of altered Stat3 is highly unlikely to influence TEC physiology in Eed$^{fl/fl}$::β5tCre mice. Therefore, the deletion of either *Eed* of *Ezh1/2* would serve as essential tools to investigate the physiological outcome of eliminating PRC2 function and consequently the lack of H3K27me3 mark on the chromatin. Nevertheless, one should keep in mind about the potential pitfalls of off-target effects of PRC2 while drawing conclusions. In this study, the concurrence of PRC2-deficient phenotypes from two independent mouse models (**Figure 11**) demonstrated the specificity of the phenotype to the inactivation of the primary function of PRC2 instead of off-target effects that the mouse models might inherently habour.

5.4. Defective maturation process of PRC2-deficienct mTEC

Both the cTEC and mTEC are derived from a common source of progenitor cells that first attain a cTEC-like phenotype and later diverge via asymmetrical differentiation into mTEC (*122*, *146*). At E12.5, the thymic primordia consist of undifferentiated epithelial cells surrounded by a capsule of mesenchyme derived from neural crest cells (*147*). These undifferentiated epithelial cells express classical cTEC markers, such as β5t, and are capable to give rise to both cTEC and mTEC (*20*). PRC2 plays a crucial role in the regulation of gene expression during both early embryogenesis (*90*) and the process of homeostasis in various tissues. In the context of skin epithelia, the double deletion of Ezh1/2 accelerated the differentiation of epidermal

progenitor cells into Merkel cells due to the repression of Sox2 expression (*149*). In the intestinal epithelium, PRC2 deficiency resulted in a reduced capacity of stress-induced regeneration (*148*). In these mice, the lack of PRC2 led to the failure in repressing *Cdkn2a* within the intestinal stem cell and subsequently reduced the ability of the stem cell to differentiate into mature intestinal epithelial cells for the process of regeneration. Although the role of Cdkn2a has not been investigated in TEC, similar effects on cellular plasticity of mTEC progenitors could possibly explain the reduced mTEC subpopulation in $Eed^{fl/fl}$::β5tCre mice. In the $Eed^{fl/fl}$::β5tCre mice, the decreased cellularity of PRC2-deficient mTEC was demonstrated to be an intrinsic incompetency and not solely due to the lack of thymocytes. This was shown by the failure of *in vitro* RANKL stimulation to rescue the mTEC frequency and cellularity in thymocyte-depleted fetal thymus organ culture (**Figure 10C**). The decreased mTEC frequency was also not due to the increased turnover rate of PRC2-deficient mTEC (**Figure 10E**). In comparison to the reported instances of PRC2's role in the differentiation program of other cell types, PRC2 seems likely to also play crucial roles in the regulation of mTEC differentiation. Furthermore, the importance of PRC2 in the maturation of mTEC is also highlighted by the over-representation (75%) of PRC2-deficient mTEC within the $mTEC^{lo}$ population (immature phenotype), with the remaining 25% being PRC2-proficient. In contrast, only 50% of the $mTEC^{hi}$ (mature phenotype) are PRC2-deficient (**Figure 18D**). Therefore, these data indicate that PRC2 plays an important role in the differentiation of mTEC.

The development of mTEC involves multiple signaling pathways and the signaling mechanisms involved differ at different developmental stages. The process of mTEC development depends on the availability of RANKL, lymphotoxinβ and CD40L that are provided by single positive thymocytes in the thymus (*128*, *150*, *151*). The presence of mTEC ($UEA1^{+}$) is first observed at

E15.5 (*152*) and subsequently Aire^{+} mTEC appear on E16 (*153*). However, at this stage of thymus development, the single positive (CD4/8^{+}TCRβ^{hi}) thymocytes are not yet present and the developing mTEC are dependent on lymphoid tissue inducer (LTi) cells as a source for RANKL and lymphotoxinβ (*153*, *154*). In the postnatal thymus, a population of β5t^{+} mTEC progenitors resides in the cortico-medullary junction and contributes to the mTEC population albeit at a reduced rate with increasing age (*21*). The development of Aire^{+} mTEC is dependent on the availability of RANKL as highlighted by the void of Aire^{+} mTEC in adult RANKL-deficient mice (*154*). The deficiency of CD40, on the other hand, resulted in a reduction of frequency of Aire^{+} mTEC (*153*). The reduction of Aire^{+} mTEC indicated that CD40-CD40L interaction is not crucial for the development of Aire^{+} mTEC but probably does play a role in regulating the turnover rate of the mTEC.

In relation to the differences of tissue homeostasis with age, the function of PRC2 can be exerted in a differential and age-sensitive fashion. In haematopoietic stem cells (HSC), targeted deletion of Eed showed that PRC2 is crucial for the maintenance of adult bone marrow HSC but has no role in the production of fetal liver HSC (*102*). While the other subunit of PRC2, Ezh2 is crucial for fetal but dispensable for adult HSC (*110*). The reduction of mTEC cellularity from 1 week to 4 weeks old Eed$^{fl/fl}$::β5tCre mice (**Figure 9D**) could suggest that PRC2 also plays an important role in the postnatal homeostasis of the mTEC pool.

PRC2 catalyses the deposition of H3K27me3 mark on histone 3 and, in doing so, increases the degree of chromatin compaction. As such, PRC2 is able to regulate the chromatin's accessibility to transcriptional factors thereby regulating the expression of genes (*155*). It is plausible that PRC2 exerts its control over mTEC development through regulating the expression of proteins crucial to mTEC development. The changes in expression levels of genes involved in mTEC development including Aire (*154*) CD40, CD80 (*22*),

and markers used to define mTEC maturation such as involucrin (*156*), claudin3 and caludin4 (*157*) could be determined in PRC2-deficient mTEC to better understand the molecular mechanisms regulating mTEC development. These data could be extracted from single cell transcriptomic data that is projected to be completed in the near future.

5.5. PRC2 regulates chemokine production by cTEC

The recruitment of ETP is dependent on the expression of chemokines by the cTEC (*27*). Indeed there was a reduced expression levels of CXCL12 and CCL25 by the PRC2-deficient cTEC (**Figure 12D**) that coincided with the reduced number of ETP recruited to the thymus (**Figure 12C**). Defects in chemokine expression were also observed in mouse model with defective β-catenin function in TEC (*29*, *125, 158*). In mutant mice with TEC-specific constitutive activation of β-catenin, the recruitment of ETP was restricted due to the failure to express sufficient chemokines (CCL25) by the cTEC (*125*). Similarly, a different mouse line lacking β-catenin in the cTEC also presented a downregulation of chemokines CXCL12, CCL19, CCL25 (158). Interestingly, the mutant mice with β-catenin deficiency within the cTEC have hypocellular thymi composed of an increased frequency of cTEC ($Ly51^{+}$) and decreased frequency of mTEC ($UEA1^{+}$) (*158*), which resembles the observations made in the $Eed^{fl/fl}$:: β5tCre mice (**Figure 9D, E**). However, unlike in the $Eed^{fl/fl}$:: β5tCre mice, cTEC with defective β-catenin function are unable to support normal thymopoiesis (*125*, *158*). Upon further analysis, both the mutant mice lacking normal β-catenin function in cTEC were found to express reduced level of Foxn1. Being a master regulator of TEC, Foxn1 regulates the expression of key target genes that are essential not only for TEC development but also those that enable TEC to support T cell development (*124*). Recently, it was experimentally proven that Foxn1 directly regulates the expression of the

chemokines CXCL12 and CCL25 in cTEC (*124*). To relate these observations to the PRC2-deficient mice, the level of Foxn1 expression in PRC2-deficient cTEC needs to be determined to ascertain if the reduced chemokine expression is caused by insufficient amount of Foxn1.

Alternatively, the reduced ETP recruitment could be a consequence of a reduced T cell progenitor cell pool in the periphery. Even though the deficiency of PRC2 is assumed to be restricted to TEC in $Eed^{fl/fl}$::β5tCre mice, the possibility of a reduced cellularity of T cells progenitors in the peripheral blood and bone marrow, that are yet to be recruited to the thymus, could not be completely eliminated. Further experiments would be necessary to address this aspect so as to draw a clearer conclusion to the phenomenon of the reduced ETP recruitment in thymus of $Eed^{fl/fl}$::β5tCre mice. Although there is no definite conclusion on the mechanism resulting in the reduced ETP recruitment, the deficiency of PRC2 in cTEC was shown to result in reduced chemokine expression but without compromising TEC's ability to support thymopoiesis.

5.6. PRC2 regulates the efficacy of negative selection

The process of negative selection deletes thymocytes expressing self-reactive TCR that are capable of eliciting autoimmunity (*115*). Deletion of self-reactive thymocytes constitutes part of central tolerance induction in the thymus and is dependent on the expression of TRA that are presented on the surface of TEC. The range of TRA expressed by TEC at the population level is capable of representing almost the entire repertoire of self-antigens in the periphery of the host organism (*50*). The lack of expression of Aire-dependent TRA in Aire-deficient mice resulted in the development of multi-organ autoimmunity (*159*) and defective deletion of auto-reactive T cells (*160*). One possible postulation of the reduced frequency of negatively selected

thymocytes in Eed$^{fl/fl}$:: β5tCre mice (**Figure 13**) could be that there is an altered efficiency of TRA expression in the TEC due to the PRC2-deficiency that subsequently altered the H3K27me3 landscape. Alternatively, the expression of TRA is also dependent on the maturation of TEC (*161*). Hence, the deficiency of PRC2 in TEC could possibly lead to a reduced expression of TRA in mTEC by either disturbing the maturation of mTEC and/or the expression of TRA in mature mTEC. Nevertheless, these postulations could not yet be verified without the single cell transcriptome data that will provide information on the changes in TRA expression by the TEC.

In the Eed$^{fl/fl}$::β5tCre mice, the reduction of efficiency in negative selection is more apparent in thymocytes residing in the medulla (CCR7^{+}) than those in the cortex (CCR7^{-}) (**Figure 13C**). Since a wider array of TRA is being expressed by the mTEC (*161*), the extent of altered TRA expression as a result of PRC2-deficiency could potentially have a stronger impact within the mTEC. Therefore, this could consequently result in the negative selection being affected to a greater extend in the medulla than the cortex. Similarly, the validation of these postulations would require quantification of alteration of the TRA expression levels in PRC2-deficient cTEC and mTEC from single cell transcriptome data.

The other factor that could play a part in the reduced negative selection of thymocytes is the TEC to thymocyte ratio in the hypocellular thymus of the Eed$^{fl/fl}$::β5tCre mice. Since the thymocyte cellularity was drastically reduced while TEC cellularity remained unchanged (**Figure 8B, 9C**), there was a much higher TEC to thymocyte ratio in the mutant mice. Despite a greater availability of TEC to provide interaction interface to facilitate the negative selection process, the efficiency of negative selection was still reduced. Hence, the altered negative selection could not be an attribute of the availability of TEC to facilitate the process.

Yet another factor to consider would be the presence of PRC2-proficient mTEC in the Eed$^{fl/fl}$::β5tCre mice. These PRC2-proficient mTEC were however unable to compensate for the reduced functionality of PRC2-deficient mTEC. These PRC2-proficient mTEC in the Eed$^{fl/fl}$::β5tCre mice expressed reduced number of TRA per cell (**Figure 20D**) and did not expand to completely replace the mTEC cellularity observed in the control mice (**Figure 9D**). Hence, these PRC2-proficient mTEC in the Eed$^{fl/fl}$::β5tCre mice were possibly less efficient in negative selection compared to PRC2-proficient mTEC found in wild type mice.

In addition to the approaches presented in this thesis to demonstrate the reduced negative selection efficiency, changes in the quality of negative selection can be further interrogated through the analysis of the composition of various TCRα/β chains in thymocytes undergoing negative selection in the mutant mice. The TCRα/β gene loci undergo gene rearrangement to give rise to receptors with unique composition of TCRα/β based on the usage of different V(D)J gene segments. The T cell pool generated within individual mouse from a given strain contains consistent compositions of TCRα/β chains (*162*). Hence, the specific composition of TCRα/β chains of the T cell pool is dependent on the genetic makeup that in turn influences the development of thymocytes in the thymus of the host. The analysis proposed here aims to detect the shift in compositions of TCRα/β chain in T cells undergoing negative selection in the mutant mice. The changes in composition of TCRα/β chain within the population of thymocytes undergoing negative selection can be determined via gene expression sequencing analysis. Due to the immense combinations of various V(D)J gene segments possible in the TCRα/β chains, the complexity of TCR V(D)J gene segment usage has to be reduced. This can be achieved by transplanting bone marrow from a transgenic mouse strain, with a fixed TCRβ-chain transgene (e.g. YAe62β) and only one locus of TCRα chain undergoing rearrangement, into lethally irradiated Eed$^{fl/fl}$::β5tCre mice.

Hence, effectively only the TCRα chain composition would be variable and the TCRα composition of the thymocytes undergoing negative selection can then be determined. This approach would provide a direct qualitative measure of the alteration in negative selection in the $Eed^{fl/fl}$::β5tCre mice.

5.7. Increased anergic peripheral CD4 T cells

Despite the reduced negative selection of thymocytes, there is no onset of autoimmune diseases in mice over 20-weeks-old spontaneously or upon T cell depletion at the age of 2-weeks-old (**Figure 17A**). A possible explanation for this phenomenon could be the higher frequency of anergic ($CD73^{+}FR4^{+}$) CD4 T cells in the periphery (**Figure 17D**). These CD4 T cells co-expressing CD73 and FR4 are found in higher frequency within the periphery of Aire-deficient and Bim-deficient mice, both of which exhibit defects in the induction of central tolerance (*163*). The imperfect negative selection in the thymus could thus possibly be counteracted by the gain of anergic phenotype by the self-reactive cells upon entering the periphery. To further confirm that these cells are indeed anergic cells, the $CD73^{+}FR4^{+}CD4^{+}$ T cells could be sorted and stimulated *in vitro* with anti-CD3 to determine the level of proliferative response. If the cell were indeed anergic, the cells should have limited proliferation and IL2 production. To further confirm the phenotype of these anergic cells, the levels of expression of markers associated with development of anergy T cells, such as CBL-B (an E3 ubiquitin-protein ligase) and diacylglycerol kinase-α, could be also determined (*164, 165*).

The lack of signs of autoimmunity (i.e. lymphocyte infiltration and autoimmune diseases) contradicted the reduced efficiency of negative selection in $Eed^{fl/fl}$::β5tCre mice. In the case of $Eed^{fl/fl}$::β5tCre mice, these compensatory mechanisms from the peripheral tolerance appeared to be sufficient in counteracting the potential of the onset of autoimmune diseases

resulting from declined negative selection unlike in Aire-deficient mice (*166*). One hypothesis would be that the degree of alteration of TRA expression in PRC2-deficiency is insufficient to induce autoimmunity. However, this hypothesis requires data from single cell transcriptomic analysis of PRC2-deficient versus PRC2-proficient mTEC. Nevertheless, several independent experiments using different approaches demonstrated consistently that negative selection is indeed less efficient in $Eed^{fl/fl}$::β5tCre mice.

5.8. Population of mTEC derived from β5t-independent progenitors

TEC progenitors express β5t and first attain a cTEC-like phenotype but some of the cells later differentiate asymmetrically to give rise to mTEC (*20*). In the embryonic thymus, undifferentiated progenitor cells in the thymic primordia express β5t as early as E12.5 (*20*). The TEC progenitors exist also in the postnatal thymus residing in the cortico-medullary junction (*21*). Upon TEC differentiation into the mTEC lineage, the expression of β5t is ceased. Hence, the utilisation of *Psmb11* (*β5t*) promoter to achieve TEC specific gene deletion is possible as virtually all TEC are derived from a common source of β5t-expressing progenitors. However, in both $Eed^{fl/fl}$::β5tCre and $Ezh1^{KO}$:: $Ezh2^{fl/fl}$::β5tCre mice, approximately 30% of mTEC retain the expression of Eed and subsequently contain the same H3K27me3 levels as the typical mTEC found in wild type mice (**Figure 18E**). This phenomenon could be explained by either the inaccessibility of *Eed* gene locus to Cre recombinase or that these mTEC are derived from progenitors that have never expressed β5t (β5t-independent). An aspect supporting the latter is the discrepancy of percentage of reported negative cells in $Eed^{fl/fl}$::ZsGreen::β5tCre and ZsGreen:: β5tCre mice. Both mouse lines were generated from the same stock of mice carrying the transgene ZsGreen and thus the efficiency of Cre-driven excision of stop cassette in the ZsGreen transgene locus should be comparable. Despite

this, the ZsGreen::β5tCre mice have less than 1% of ZsGreen$^-$ mTEC (*20*) while the absence of PRC2 function dramatically increased ZsGreen$^-$ mTEC frequency to 30%, (**Figure 18A, B**). Furthermore, the percentage of ZsGreen$^-$ mTEC also coincide with the frequency of the lesser population of mTEC in Eed$^{fl/fl}$::β5tCre mice that retaining wild type levels of H3K27me3 (**Figure 18A-C**). These scenarios would not have been statistically possible if the presence of PRC2-proficieint mTEC in Eed$^{fl/fl}$::β5tCre mice is merely due to the inaccessibility of the *Eed* gene locus for Cre-driven recombination. The increase in the frequency of PRC2-proficient/ZsGreen$^-$ mTEC is also unlikely a consequence of decreased survival rate of PRC2-deficient/ZsGreen$^+$ mTEC as the expression levels of apoptosis-related genes is not elevated in PRC2-deficient mTEC (**Figure 10E**). Furthermore, the reduced number of TRA expressed per cell and distinct t-SNE clustering pattern (**Figure 18D, E**) indicate a unique biological makeup that would argue for the presence of mTEC derived from β5t-independent progenitors. Thus, these observations highlight the biological significance and support the hypothesis that these PRC2-proficient mTEC in Eed$^{fl/fl}$::β5tCre mice are most probably derived from β5t-independent progenitors.

Yet, mTEC derived from these β5t-independent progenitors are not found in significant numbers, not more than 1%, in the thymus of the wild type mouse (*20*). Similar to the reduced frequency and impaired maturation process of PRC2-deficient mTEC observed in this study, the deficiency of PRC2 in the intestinal epithelium also impedes the differentiation of the epithelial cells (*148*). With the importance of PRC2 in the differentiation of cells, PRC2-deficient mTEC could have a lower efficiency to develop via asymmetrical differentiation to diverge from the progenitors that have gained the cTEC phenotype. However, β5t-independent progenitors having escaped *Eed* deletion preserve PRC2 function and thus gain developmental advantages in filling up the cellular niches. This allows the otherwise

negligible mTEC population to expand and make up 30% of the mTEC pool. Nevertheless, the frequency and cellularity of the total mTEC is still reduced and the functions of mTEC in supporting negative selection (**Figure 13**) and T_{reg} production (**Figure 15B**) are compromised. Therefore, mTEC derived from β5t-independent progenitors are present in elevated frequency probably due to greater developmental advantage within the $Eed^{fl/fl}$::β5tCre mice but is insufficient to compensate for the defective mTEC function.

Unlike the mTEC compartment, there is an absence of any cTEC retaining Eed expression (**Figure 18, 19**). Therefore, PRC2 seems to be dispensable in the commitment of TEC progenitors to a cTEC phenotype but crucial for the subsequent stage of asymmetrical differentiation to form mTEC. Even though the TEC progenitors are able to give rise to the cTEC ($Ly51^{+}$), the efficiency of cTEC to attract ETP and foster the first round of negative selection are rendered sub-optimal.

Using the triple transgenic mouse model ($Eed^{fl/fl}$::ZsGreen::β5tCre), PRC2-deficient mTEC can be conveniently identified based on the positivity of the expression of the ZsGreen gene reporter. These cells can be isolated and sorted individually and be used for single cell transcriptomic analysis. The single cell transcriptomic data are required to demonstrate, if any, the effect of PRC2-deficiency upon TRA expression.

5.9. Relevance and Impact

This thesis addresses the functional significance of PRC2 in both TEC development and function. With regards to TEC development, this study provides experimental data demonstrating the differential role of PRC2 in different TEC subpopulations. The deficiency of PRC2 does not affect the ability of TEC progenitors to gain cTEC phenotype. But progress of development of the progenitors into mTEC lineage and subsequently the

maturation of mTEC is significantly hindered in the absence of PRC2. Besides TEC development, PRC2 is also needed for TEC to function efficiently. PRC2 function is important for cTEC to produce chemokines effectively and for mTEC to carry out negative selection efficiently. The significance of PRC2 in the efficacy of negative selection by the mTEC was consistently demonstrated through different approaches in this study.

Furthermore, a unexpected finding also suggested the existence of a previously unreported population of mTEC in $Eed^{fl/fl}$::β5tCre mice derived from progenitors that never expressed β5t. This unique pool of mTEC expresses fewer TRA per cell and is unable to compensate for the PRC2-deficient mTEC derived from β5t-expressing progenitors in the thymus of $Eed^{fl/fl}$::β5tCre mice. Nevertheless, this opens up a new area of investigations to gain deeper understanding of the biology, importance, and role of this unique mTEC population.

The thymus is fundamental in the establishment of a functional but self-tolerant T cell repertoire in the host. This study contributes to a better understanding in the molecular mechanisms exerted by PRC2 in thymus biology and will help unravel the molecular causes of diseases involving thymic stromal deficiencies. In addition, a more extensive comprehension of the molecular basis of normal thymus organogenesis, maintenance and function is equally crucial to develop therapies and treatments to thymic defects. Overall, the findings reported in this thesis specifically enhance the role of PRC2 in thymus biology and hence provides invaluable knowledge that might be applied to both translation and clinical medicine.

6. REFERENCES

1. Lavini, C., Moran, C., Uliano, and Schönhuber, R. (2008) Thymus Gland Pathology, Springer.
2. Miller, J. F. (2004) Events that led to the discovery of T-cell development and function-a personal recollection, *Tissue Antigens 63*, 509–17.
3. Miller, J. (1962) Effect of neonatal thymectomy on the immunological responsiveness of the mouse, *Proceedings of the Royal Society 156*, 415–428.
4. Bevan, M. J. (1977) In a radiation chimaera, host H–2 antigens determine immune responsiveness of donor cytotoxic cells, *Nature 269*, 417–8.
5. Kappler, J. W., Roehm, N., and Marrack, P. (1987) T cell tolerance by clonal elimination in the thymus, *Cell 49*, 273–80.
6. Jordan, M. S., Boesteanu, A., Reed, A. J., Petrone, A. L., Holenbeck, A. E., Lerman, M. A., Naji, A., and Caton, A. J. (2001) Thymic selection of CD4+CD25+ regulatory T cells induced by an agonist self-peptide, *Nature Immunology 2*, 301–6.
7. Blackburn, C. C., and Manley, N. R. (2004) Developing a new paradigm for thymus organogenesis, *Nature Reviews Immunology 4*, 278–89.
8. Sarang, Z., Garabuczi, É., Joós, G., Kiss, B., Tóth, K., Rühl, R., and Szondy, Z. (2013) Macrophages engulfing apoptotic thymocytes produce retinoids to promote selection, differentiation, removal and replacement of double positive thymocytes, *Immunobiology 218*, 1354–60.
9. Brocker, T. (1999) The role of dendritic cells in T cell selection and survival, *Journal of Leukocyte Biology 66*, 331–5.
10. Hubert, F.-X. X., Kinkel, S. A., Davey, G. M., Phipson, B., Mueller, S. N., Liston, A., Proietto, A. I., Cannon, P. Z., Forehan, S., Smyth, G. K., Wu, L., Goodnow, C. C., Carbone, F. R., Scott, H. S., and Heath, W. R. (2011) Aire regulates the transfer of antigen from mTECs to dendritic cells for induction of thymic tolerance, *Blood 118*, 2462–72.
11. Skogberg, G., Lundberg, V., Berglund, M., Gudmundsdottir, J., Telemo, E., Lindgren, S., and Ekwall, O. (2015) Human thymic epithelial primary cells produce exosomes carrying tissue-restricted antigens, *Immunology and Cell Biology 93*, 727–34.
12. Balciunaite, G., Keller, M. P., Balciunaite, E., Piali, L., Zuklys, S., Mathieu, Y. D., Gill, J., Boyd, R., Sussman, D. J., and Holländer, G. A. (2002) Wnt glycoproteins regulate the expression of FoxN1, the gene defective in nude mice, *Nature Immunology 3*, 1102–8.
13. Gordon, J., Bennett, A. R., Blackburn, C. C., and Manley, N. R. (2001) Gcm2 and Foxn1 mark early parathyroid- and thymus-specific domains in the developing third pharyngeal pouch, *Mechanisms of Development 103*, 141–3.
14. Foster, K. E., Gordon, J., Cardenas, K., Veiga-Fernandes, H., Makinen, T.,

Grigorieva, E., Wilkinson, D. G., Blackburn, C. C., Richie, E., Manley, N. R., Adams, R. H., Kioussis, D., and Coles, M. C. (2010) EphB-ephrin-B2 interactions are required for thymus migration during organogenesis, *Proceedings of the National Academy of Sciences of the United States of America. 107*, 13414–9.
15. Gordon, J., Wilson, V. A., Blair, N. F., Sheridan, J., Farley, A., Wilson, L., Manley, N. R., and Blackburn, C. C. (2004) Functional evidence for a single endodermal origin for the thymic epithelium, *Nature Immunology 5*, 546–53.
16. Blackburn, C. C., Augustine, C. L., Li, R., Harvey, R. P., Malin, M. A., Boyd, R. L., Miller, J. F., and Morahan, G. (1996) The nu gene acts cell-autonomously and is required for differentiation of thymic epithelial progenitors, *Proceedings of the National Academy of Sciences of the United States of America 93*, 5742–6.
17. Klug, D. B., Carter, C., Crouch, E., Roop, D., Conti, C. J., and Richie, E. R. (1998) Interdependence of cortical thymic epithelial cell differentiation and T-lineage commitment, *Proceedings of the National Academy of Sciences of the United States of America 95*, 11822–7.
18. Rossi, S. W., Jenkinson, W. E., Anderson, G., and Jenkinson, E. J. (2006) Clonal analysis reveals a common progenitor for thymic cortical and medullary epithelium, *Nature 441*, 988–91.
19. Bleul, C. C., Corbeaux, T., Reuter, A., Fisch, P., Mönting, J. S. S., and Boehm, T. (2006) Formation of a functional thymus initiated by a postnatal epithelial progenitor cell., *Nature 441*, 992–6.
20. Ohigashi, I., Zuklys, S., Sakata, M., Mayer, C. E., Zhanybekova, S., Murata, S., Tanaka, K., Holländer, G. A., and Takahama, Y. (2013) Aire-expressing thymic medullary epithelial cells originate from β5t-expressing progenitor cells, *Proceedings of the National Academy of Sciences of the United States of America 110*, 9885–90.
21. Mayer, C. E., Žuklys, S., Zhanybekova, S., Ohigashi, I., Teh, H.-Y. Y., Sansom, S. N., Shikama-Dorn, N., Hafen, K., Macaulay, I. C., Deadman, M. E., Ponting, C. P., Takahama, Y., and Holländer, G. A. (2016) Dynamic spatio-temporal contribution of single β5t+ cortical epithelial precursors to the thymus medulla, *European Journal of Immunology 46*, 846–56.
22. Shakib, S., Desanti, G. E., Jenkinson, W. E., Parnell, S. M., Jenkinson, E. J., and Anderson, G. (2009) Checkpoints in the development of thymic cortical epithelial cells, *Journal of Immunology 182*, 130–7.
23. Gäbler, J., Arnold, J., and Kyewski, B. (2007) Promiscuous gene expression and the developmental dynamics of medullary thymic epithelial cells., *European Journal of Immunology 37*, 3363–72.
24. Luis, T. C., Luc, S., Mizukami, T., Boukarabila, H., Thongjuea, S., Woll, P. S., Azzoni, E., Giustacchini, A., Lutteropp, M., Bouriez-Jones, T., Vaidya, H., Mead, A. J., Atkinson, D., Böiers, C., Carrelha, J., Macaulay, I. C., Patient, R., Geissmann, F., Nerlov, C., Sandberg, R., de Bruijn, M. F. T. R., Blackburn, C.

C., Godin, I., and Jacobsen, S. E. (2016) Initial seeding of the embryonic thymus by immune-restricted lympho-myeloid progenitors, *Nature Immunology 17*, 1424–35.
25. Schwarz, B. A., and Bhandoola, A. (2004) Circulating hematopoietic progenitors with T lineage potential, *Nature Immunology 5*, 953–60.
26. Calderón, L., and Boehm, T. (2011) Three chemokine receptors cooperatively regulate homing of hematopoietic progenitors to the embryonic mouse thymus, *Proceedings of the National Academy of Sciences of the United States of America 108*, 7517–22.
27. Zlotoff, D. A., Sambandam, A., Logan, T. D., Bell, J. J., Schwarz, B. A., and Bhandoola, A. (2010) CCR7 and CCR9 together recruit hematopoietic progenitors to the adult thymus, *Blood 115*, 1897–905.
28. Rossi, F. M., Corbel, S. Y., Merzaban, J. S., Carlow, D. A., Gossens, K., Duenas, J., So, L., Yi, L., and Ziltener, H. J. (2005) Recruitment of adult thymic progenitors is regulated by P-selectin and its ligand PSGL-1, *Nature Immunology 6*, 626–34.
29. Gossens, K., Naus, S., Corbel, S. Y., Lin, S., Rossi, F., Kast, J., and Ziltener, H. J. (2009) Thymic progenitor homing and lymphocyte homeostasis are linked via S1P-controlled expression of thymic P-selectin/CCL25, *The Journal of Experimental Medicine 206*, 761–778.
30. Prockop, S. E., and Petrie, H. T. (2004) Regulation of thymus size by competition for stromal niches among early T cell progenitors, *Journal of Immunology 173*, 1604–11.
31. Sambandam, A., Maillard, I., Zediak, V., Xu, L., Gerstein, R., Aster, J., Pear, W., and Bhandoola, A. (2005) Notch signaling controls the generation and differentiation of early T lineage progenitors, *Nature Immunol*ogy *6*, 663–70.
32. Radtke, F., Wilson, A., Stark, G., Bauer, M., van Meerwijk, J., MacDonald, H. R., and Aguet, M. (1999) Deficient T cell fate specification in mice with an induced inactivation of Notch1, *Immunity 10*, 547–58.
33. Von Freeden-Jeffry, U., Vieira, P., Lucian, L. A., McNeil, T., Burdach, S. E. G., and Murray, R. (1995) Lymphopenia in interleukin (IL)-7 gene-deleted mice identifies IL-7 as a nonredundant cytokine, *The Journal of Experimental Medicine 181*, 1519–26.
34. Dudley, E. C., Petrie, H. T., Shah, L. M., Owen, M. J., and Hayday, A. C. (1994) T cell receptor beta chain gene rearrangement and selection during thymocyte development in adult mice, *Immunity 1*, 83–93.
35. Paterson, D. J., and Williams, A. F. (1987) An intermediate cell in thymocyte differentiation that expresses CD8 but not CD4 antigen, *The Journal of Experimental Medicine 166*, 1603–8.
36. Rothenberg, E. V., Moore, J. E., and Yui, M. A. (2008) Launching the T-cell-lineage developmental programme, *Nature Review Immunology 8*, 9–21.
37. Kisielow, P., Teh, H. S., Blüthmann, H., and von Boehmer, H. (1988) Positive selection of antigen-specific T cells in thymus by restricting MHC

molecules, *Nature 335*, 730–3.
38. Grossman, Z., and Singer, A. (1996) Tuning of activation thresholds explains flexibility in the selection and development of T cells in the thymus, *Proceedings of the National Academy of Sciences of the United States of America 93*, 14747–52.
39. Barthlott, T., Kohler, H., and Eichmann, K. (1997) Asynchronous coreceptor downregulation after positive thymic selection: prolonged maintenance of the double positive state in CD8 lineage differentiation due to sustained biosynthesis of the CD4 coreceptor, *The Journal of Experimental Medicine 185*, 357–62.
40. Suzuki, H., Punt, J., Granger, L., and Singer, A. (1995) Asymmetric signaling requirements for thymocyte commitment to the CD4+ versus CD8+ T cell lineages: A new perspective on thymic commitment and selection, *Immunity 2*, 413–25.
41. Ashton-Rickardt, P. G., Bandeira, A., Delaney, J. R., Van Kaer, L., Pircher, H. P., Zinkernagel, R. M., and Tonegawa, S. (1994) Evidence for a differential avidity model of T cell selection in the thymus, *Cell 76*, 651–63.
42. Daley, S. R., Hu, D. Y., and Goodnow, C. C. (2013) Helios marks strongly autoreactive CD4+ T cells in two major waves of thymic deletion distinguished by induction of PD-1 or NF-κB, *The Journal of Experimental Medicine 210*, 269–85.
43. Hu, D. Y., Yap, J. Y., Wirasinha, R. C., Howard, D. R., Goodnow, C. C., and Daley, S. R. (2016) A timeline demarcating two waves of clonal deletion and Foxp3 upregulation during thymocyte development, *Immunology and Cell Biology 94*, 357–66.
44. Daniels, M. A., Teixeiro, E., Gill, J., Hausmann, B., Roubaty, D., Holmberg, K., Werlen, G., Holländer, G. A., Gascoigne, N. R., and Palmer, E. (2006) Thymic selection threshold defined by compartmentalization of Ras/MAPK signalling, *Nature 444*, 724–9.
45. Huesmann, M., Scott, B., Kisielow, P., and von Boehmer, H. (1991) Kinetics and efficacy of positive selection in the thymus of normal and T cell receptor transgenic mice, *Cell 66*, 533–40.
46. Legoux, F. P., Lim, J.-B. B., Cauley, A. W., Dikiy, S., Ertelt, J., Mariani, T. J., Sparwasser, T., Way, S. S., and Moon, J. J. (2015) CD4+ T cell tolerance to tissue-restricted self antigens is mediated by antigen-specific regulatory T cells rather than deletion, *Immunity 43*, 896–908.
47. Nishizuka, Y., and Sakakura, T. (1969) Thymus and reproduction: sex-linked dysgenesia of the gonad after neonatal thymectomy in mice, *Science 166*, 753–5.
48. Bautista, J. L., Lio, C.-W. J. W., Lathrop, S. K., Forbush, K., Liang, Y., Luo, J., Rudensky, A. Y., and Hsieh, C.-S. S. (2009) Intraclonal competition limits the fate determination of regulatory T cells in the thymus, *Nature Immunology 10*, 610–7.

49. Matloubian, M., Lo, C. G., Cinamon, G., Lesneski, M. J., Xu, Y., Brinkmann, V., Allende, M. L., Proia, R. L., and Cyster, J. G. (2004) Lymphocyte egress from thymus and peripheral lymphoid organs is dependent on S1P receptor 1, *Nature 427*, 355–60.
50. Sansom, S. N., Shikama-Dorn, N., Zhanybekova, S., Nusspaumer, G., Macaulay, I. C., Deadman, M. E., Heger, A., Ponting, C. P., and Holländer, G. A. (2014) Population and single-cell genomics reveal the Aire dependency, relief from Polycomb silencing, and distribution of self-antigen expression in thymic epithelia, *Genome Research 24*, 1918–31.
51. Marrack, P., and Kappler, J. (1987) The T cell receptor, *Science 238*, 1073–79.
52. Murata, S., Sasaki, K., Kishimoto, T., Niwa, S.-I., Hayashi, H., Takahama, Y., and Tanaka, K. (2007) Regulation of CD8+ T cell development by thymus-specific proteasomes, *Science 316*, 1349–53.
53. Honey, K., Nakagawa, T., Peters, C., and Rudensky, A. (2002) Cathepsin L regulates CD4+ T cell selection independently of its effect on invariant chain: a role in the generation of positively selecting peptide ligands, *The Journal of Experimental Medicine 195*, 1349–58.
54. Nakagawa, T., Roth, W., Wong, P., Nelson, A., Farr, A., Deussing, J., Villadangos, J. A., Ploegh, H., Peters, C., and Rudensky, A. Y. (1998) Cathepsin L: critical role in Ii degradation and CD4 T cell selection in the thymus, *Science 280*, 450–3.
55. Gommeaux, J., Grégoire, C., Nguessan, P., Richelme, M., Malissen, M., Guerder, S., Malissen, B., and Carrier, A. (2009) Thymus-specific serine protease regulates positive selection of a subset of CD4+ thymocytes, *European Journal of Immunology 39*, 956–64.
56. Takaba, H., Morishita, Y., Tomofuji, Y., Danks, L., Nitta, T., Komatsu, N., Kodama, T., and Takayanagi, H. (2015) Fezf2 Orchestrates a Thymic Program of Self-Antigen Expression for Immune Tolerance, *Cell 163*, 975–87.
57. Pinto, S., Michel, C., Schmidt-Glenewinkel, H., Harder, N., Rohr, K., Wild, S., Brors, B., and Kyewski, B. (2013) Overlapping gene coexpression patterns in human medullary thymic epithelial cells generate self-antigen diversity., *Proceedings of the National Academy of Sciences of the United States of America 110*, 3497–505.
58. Brennecke, P., Reyes, A., Pinto, S., Rattay, K., Nguyen, M., Küchler, R., Huber, W., Kyewski, B., and Steinmetz, L. M. (2015) Single-cell transcriptome analysis reveals coordinated ectopic gene-expression patterns in medullary thymic epithelial cells., *Nature Immunology 16*, 933–41.
59. Meredith, M., Zemmour, D., Mathis, D., and Benoist, C. (2015) Aire controls gene expression in the thymic epithelium with ordered stochasticity, *Nature Immunology 16*, 942–9.
60. Tollervey, J. R., and Lunyak, V. V. (2012) Epigenetics: judge, jury and executioner of stem cell fate, *Epigenetics 7*, 823–40.
61. Egger, G., Liang, G., Aparicio, A., and Jones, P. A. (2004) Epigenetics in

human disease and prospects for epigenetic therapy, *Nature 429*, 457–63.
62. Gaetani, M., Matafora, V., Saare, M., Spiliotopoulos, D., Mollica, L., Quilici, G., Chignola, F., Mannella, V., Zucchelli, C., Peterson, P., Bachi, A., and Musco, G. (2012) AIRE-PHD fingers are structural hubs to maintain the integrity of chromatin-associated interactome, *Nucleic Acids Research 40*, 11756–68.
63. Abramson, J., Giraud, M., Benoist, C., and Mathis, D. (2010) Aire's partners in the molecular control of immunological tolerance, *Cell 140*, 123–35.
64. Waterfield, M., Khan, I. S., Cortez, J. T., Fan, U., Metzger, T., Greer, A., Fasano, K., Martinez-Llordella, M., Pollack, J. L., Erle, D. J., Su, M., and Anderson, M. S. (2014) The transcriptional regulator Aire coopts the repressive ATF7ip-MBD1 complex for the induction of immunotolerance, *Nature Immunology 15*, 258–65.
65. Musselman, C. A., Mansfield, R. E., Garske, A. L., Davrazou, F., Kwan, A. H., Oliver, S. S., O'Leary, H., Denu, J. M., Mackay, J. P., and Kutateladze, T. G. (2009) Binding of the CHD4 PHD2 finger to histone H3 is modulated by covalent modifications, *Biochemical Journal 423*, 179–87.
66. Mansfield, R. E., Musselman, C. A., Kwan, A. H., Oliver, S. S., Garske, A. L., Davrazou, F., Denu, J. M., Kutateladze, T. G., and Mackay, J. P. (2011) Plant homeodomain (PHD) fingers of CHD4 are histone H3-binding modules with preference for unmodified H3K4 and methylated H3K9, *The Journal of Biological Chemistry 286*, 11779–91.
67. Xie, W., Ling, T., Zhou, Y., Feng, W., Zhu, Q., Stunnenberg, H. G., Grummt, I., and Tao, W. (2012) The chromatin remodeling complex NuRD establishes the poised state of rRNA genes characterized by bivalent histone modifications and altered nucleosome positions, *Proceedings of the National Academy of Sciences of the United States of America 109*, 8161–6.
68. Alfonso, R., Lutz, T., Rodriguez, A., Chavez, J. P., Rodriguez, P., Gutierrez, S., and Nieto, A. (2011) CHD6 chromatin remodeler is a negative modulator of influenza virus replication that relocates to inactive chromatin upon infection, *Cellular Microbiology 13*, 1894–906.
69. Tong, J. K., Hassig, C. A., Schnitzler, G. R., Kingston, R. E., and Schreiber, S. L. (1998) Chromatin deacetylation by an ATP-dependent nucleosome remodelling complex, *Nature 395*, 917–21.
70. Urquhart, A. J., Gatei, M., Richard, D. J., and Khanna, K. K. (2011) ATM mediated phosphorylation of CHD4 contributes to genome maintenance, *Genome Integrity 2*.
71. Williams, C. J., Naito, T., Arco, P. G., Seavitt, J. R., Cashman, S. M., De Souza, B., Qi, X., Keables, P., Von Andrian, U. H., and Georgopoulos, K. (2004) The chromatin remodeler Mi-2beta is required for CD4 expression and T cell development, *Immunity 20*, 719–33.
72. Meissner, A. (2010) Epigenetic modifications in pluripotent and differentiated cells., *Nature Biotechnology 28*, 1079–88.

73. Margueron, R., Trojer, P., and Reinberg, D. (2005) The key to development: interpreting the histone code?, *Current Opinion in Genetics & Development 15*, 163–76.
74. Voigt, P., Tee, W.-W. W., and Reinberg, D. (2013) A double take on bivalent promoters., *Genes & Development 27*, 1318–38.
75. Hirahara, K., Vahedi, G., Ghoreschi, K., Yang, X.-P. P., Nakayamada, S., Kanno, Y., O'Shea, J. J., and Laurence, A. (2011) Helper T-cell differentiation and plasticity: insights from epigenetics., *Immunology 134*, 235–45.
76. Floess, S., Freyer, J., Siewert, C., Baron, U., Olek, S., Polansky, J., Schlawe, K., Chang, H.-D. D., Bopp, T., Schmitt, E., Klein-Hessling, S., Serfling, E., Hamann, A., and Huehn, J. (2007) Epigenetic control of the foxp3 locus in regulatory T cells., *PLoS Biology 5*, e38.
77. Mukasa, R., Balasubramani, A., Lee, Y. K., Whitley, S. K., Weaver, B. T., Shibata, Y., Crawford, G. E., Hatton, R. D., and Weaver, C. T. (2010) Epigenetic instability of cytokine and transcription factor gene loci underlies plasticity of the T helper 17 cell lineage, *Immunity 32*, 616–27.
78. Pasini, D., Bracken, A. P., Jensen, M. R., Lazzerini Denchi, E., and Helin, K. (2004) Suz12 is essential for mouse development and for EZH2 histone methyltransferase activity., *The EMBO Journal 23*, 4061–71.
79. Faust, C., Schumacher, A., Holdener, B., and Magnuson, T. (1995) The eed mutation disrupts anterior mesoderm production in mice, *Development 121*, 273–85.
80. O'Carroll, D., Erhardt, S., Pagani, M., Barton, S. C., Surani, M. A., and Jenuwein, T. (2001) The polycomb-group gene Ezh2 is required for early mouse development, *Molecular and Cellular Biology 21*, 4330–6.
81. Sanulli, S., Justin, N., Teissandier, A., Ancelin, K., Portoso, M., Caron, M., Michaud, A., Lombard, B., da Rocha, S. T., Offer, J., Loew, D., Servant, N., Wassef, M., Burlina, F., Gamblin, S. J., Heard, E., and Margueron, R. (2015) Jarid2 Methylation via the PRC2 Complex Regulates H3K27me3 Deposition during Cell Differentiation, *Molecular Cell 57*, 769–83.
82. Kim, H., Kang, K., and Kim, J. (2009) AEBP2 as a potential targeting protein for Polycomb Repression Complex PRC2., *Nucleic Acids Research 37*, 2940–50.
83. Walker, E., Chang, W. Y., Hunkapiller, J., Cagney, G., Garcha, K., Torchia, J., Krogan, N. J., Reiter, J. F., and Stanford, W. L. (2010) Polycomb-like 2 associates with PRC2 and regulates transcriptional networks during mouse embryonic stem cell self-renewal and differentiation, *Cell Stem Cell 6*, 153–66.
84. Cai, L., Rothbart, S. B., Lu, R., Xu, B., Chen, W.-Y. Y., Tripathy, A., Rockowitz, S., Zheng, D., Patel, D. J., Allis, C. D., Strahl, B. D., Song, J., and Wang, G. G. (2013) An H3K36 methylation-engaging Tudor motif of polycomb-like proteins mediates PRC2 complex targeting, *Molecular Cell 49*, 571–82.
85. Margueron, R., and Reinberg, D. (2011) The Polycomb complex PRC2 and

its mark in life, *Nature 469*, 343–9.
86. Margueron, R., Justin, N., Ohno, K., Sharpe, M. L., Son, J., Drury, W. J., Voigt, P., Martin, S. R., Taylor, W. R., De Marco, V., Pirrotta, V., Reinberg, D., and Gamblin, S. J. (2009) Role of the polycomb protein EED in the propagation of repressive histone marks, *Nature 461*, 762–7.
87. Lee, M. G., Villa, R., Trojer, P., Norman, J., Yan, K.-P. P., Reinberg, D., Di Croce, L., and Shiekhattar, R. (2007) Demethylation of H3K27 regulates polycomb recruitment and H2A ubiquitination, *Science 318*, 447–50.
88. Kalb, R., Latwiel, S., Baymaz, H. I., Jansen, P. W., Müller, C. W., Vermeulen, M., and Müller, J. (2014) Histone H2A monoubiquitination promotes histone H3 methylation in Polycomb repression, *Nature Structural & Molecular Biology 21*, 569–71.
89. Kahn, T. G., Dorafshan, E., Schultheis, D., Zare, A., Stenberg, P., Reim, I., Pirrotta, V., and Schwartz, Y. B. (2016) Interdependence of PRC1 and PRC2 for recruitment to Polycomb Response Elements, *Nucleic Acids Research 44*, 10132–49.
90. Wang, J., Mager, J., Schnedier, E., and Magnuson, T. (2002) The mouse PcG gene eed is required for Hox gene repression and extraembryonic development, *Mammalian Genome 13*, 493–503.
91. Boyer, L. A., Plath, K., Zeitlinger, J., Brambrink, T., Medeiros, L. A., Lee, T. I., Levine, S. S., Wernig, M., Tajonar, A., Ray, M. K., Bell, G. W., Otte, A. P., Vidal, M., Gifford, D. K., Young, R. A., and Jaenisch, R. (2006) Polycomb complexes repress developmental regulators in murine embryonic stem cells, *Nature 441*, 349–53.
92. Landeira, D., Sauer, S., Poot, R., Dvorkina, M., Mazzarella, L., Jørgensen, H. F., Pereira, C. F., Leleu, M., Piccolo, F. M., Spivakov, M., Brookes, E., Pombo, A., Fisher, C., Skarnes, W. C., Snoek, T., Bezstarosti, K., Demmers, J., Klose, R. J., Casanova, M., Tavares, L., Brockdorff, N., Merkenschlager, M., and Fisher, A. G. (2010) Jarid2 is a PRC2 component in embryonic stem cells required for multi-lineage differentiation and recruitment of PRC1 and RNA Polymerase II to developmental regulators, *Nature Cell Biology 12*, 618–24.
93. Wang, L., Jin, Q., Lee, J.-E. E., Su, I. H., and Ge, K. (2010) Histone H3K27 methyltransferase Ezh2 represses Wnt genes to facilitate adipogenesis., *Proceedings of the National Academy of Sciences of the United States of America 107*, 7317–22.
94. Su, I.-H. H., Basavaraj, A., Krutchinsky, A. N., Hobert, O., Ullrich, A., Chait, B. T., and Tarakhovsky, A. (2003) Ezh2 controls B cell development through histone H3 methylation and Igh rearrangement, *Nature Immunology 4*, 124–31.
95. Caretti, G., Di Padova, M., Micales, B., Lyons, G. E., and Sartorelli, V. (2004) The Polycomb Ezh2 methyltransferase regulates muscle gene expression and skeletal muscle differentiation, *Genes & Development 18*, 2627–38.

96. Ezhkova, E., Pasolli, H. A., Parker, J. S., Stokes, N., Su, I. H., Hannon, G., Tarakhovsky, A., and Fuchs, E. (2009) Ezh2 orchestrates gene expression for the stepwise differentiation of tissue-specific stem cell, *Cell 136*, 1122–35.
97. Han, Z., Xing, X., Hu, M., Zhang, Y., Liu, P., and Chai, J. (2007) Structural basis of EZH2 recognition by EED, *Structure*, Structure *15*, 1306–15.
98. Ciferri, C., Lander, G. C., Maiolica, A., Herzog, F., Aebersold, R., and Nogales, E. (2012) Molecular architecture of human polycomb repressive complex 2., *Elife 1*, e00005.
99. Shen, X., Liu, Y., Hsu, Y.-J., Fujiwara, Y., Kim, J., Mao, X., Yuan, G.-C., and Orkin, S. H. (2008) EZH1 mediates methylation on histone H3 lysine 27 and complements EZH2 in maintaining stem cell identity and executing pluripotency, *Molecular Cell 32*, 491–502.
100. Akasaka, T., van Lohuizen, M., van der Lugt, N., Mizutani-Koseki, Y., Kanno, M., Taniguchi, M., Vidal, M., Alkema, M., Berns, A., and Koseki, H. (2001) Mice doubly deficient for the Polycomb group genes Mel18 and Bmi1 reveal synergy and requirement for maintenance but not initiation of Hox gene expression, *Development 128*, 1587–97.
101. Van der Lugt, N. M. T., Alkema, M., Berns, A., and Deschamps, J. (1996) The Polycomb-group homolog Bmi-1 is a regulator of murine Hox gene expression, *Mechanisms of Development 58*, 153–64.
102. Xie, H., Xu, J., Hsu, J. H., Nguyen, M., Fujiwara, Y., Peng, C., and Orkin, S. H. (2014) Polycomb repressive complex 2 regulates normal hematopoietic stem cell function in a developmental-stage-specific manner, *Cell Stem Cell 14*, 68–80.
103. Stassen, M. J., Bailey, D., Nelson, S., Chinwalla, V., and Harte, P. J. (1995) The Drosophila trithorax proteins contain a novel variant of the nuclear receptor type DNA binding domain and an ancient conserved motif found in other chromosomal proteins, *Mechanisms of Development 52*, 209–23.
104. Jones, R. S., and Gelbart, W. M. (1993) The Drosophila Polycomb-group gene Enhancer of zeste contains a region with sequence similarity to trithorax, *Molecular and Cellular Biology 13*, 6357–66.
105. Tschiersch, B., Hofmann, A., Krauss, V., Dorn, R., Korge, G., and Reuter, G. (1994) The protein encoded by the Drosophila position-effect variegation suppressor gene Su(var)3-9 combines domains of antagonistic regulators of homeotic gene complexes, *The EMBO Journal 13*, 3822–31.
106. Czermin, B., Melfi, R., McCabe, D., Seitz, V., Imhof, A., and Pirrotta, V. (2002) Drosophila enhancer of Zeste/ESC complexes have a histone H3 methyltransferase activity that marks chromosomal Polycomb sites, *Cell 111*, 185–96.
107. Rea, S., Eisenhaber, F., O'Carroll, D., Strahl, B. D., Sun, Z.-W., Schmid, M., Opravil, S., Mechtler, K., Ponting, C. P., Allis, C. D., and Jenuwein, T. (2000) Regulation of chromatin structure by site-specific histone H3 methyltransferases, *Nature 406*, 593–9.

108. Ezhkova, E., Lien, W.-H., Stokes, N., Pasolli, H. A., Silva, J. M., and Fuchs, E. (2011) EZH1 and EZH2 cogovern histone H3K27 trimethylation and are essential for hair follicle homeostasis and wound repair, *Genes & Development 25*, 485–98.
109. Margueron, R., Li, G., Sarma, K., Blais, A., Zavadil, J., Woodcock, C. L., Dynlacht, B. D., and Reinberg, D. (2008) Ezh1 and Ezh2 maintain repressive chromatin through different mechanisms, *Molecular Cell 32*, 503–18.
110. Hidalgo, I., Herrera-Merchan, A., Ligos, J. M., Carramolino, L., Nuñez, J., Martinez, F., Dominguez, O., Torres, M., and Gonzalez, S. (2012) Ezh1 is required for hematopoietic stem cell maintenance and prevents senescence-like cell cycle arrest, *Cell Stem Cell 11*, 649–62.
111. Kim, E., Kim, M., Woo, D.-H. H., Shin, Y., Shin, J., Chang, N., Oh, Y. T., Kim, H., Rheey, J., Nakano, I., Lee, C., Joo, K. M., Rich, J. N., Nam, D.-H. H., and Lee, J. (2013) Phosphorylation of EZH2 activates STAT3 signaling via STAT3 methylation and promotes tumorigenicity of glioblastoma stem-like cells, *Cancer Cell 23*, 839–52.
112. Koh, A. S., Kuo, A. J., Park, S. Y., Cheung, P., Abramson, J., Bua, D., Carney, D., Shoelson, S. E., Gozani, O., Kingston, R. E., Benoist, C., and Mathis, D. (2008) Aire employs a histone-binding module to mediate immunological tolerance, linking chromatin regulation with organ-specific autoimmunity, *Proceedings of the National Academy of Sciences of the United States of America 105*, 15878–83.
113. Org, T., Chignola, F., Hetényi, C., Gaetani, M., Rebane, A., Liiv, I., Maran, U., Mollica, L., Bottomley, M. J., Musco, G., and Peterson, P. (2008) The autoimmune regulator PHD finger binds to non-methylated histone H3K4 to activate gene expression, *EMBO Reports 9*, 370–6.
114. Guerau-de-Arellano, M., Mathis, D., and Benoist, C. (2008) Transcriptional impact of Aire varies with cell type., *Proceedings of the National Academy of Sciences of the United States of America 105*, 14011–6.
115. Peterson, P., Nagamine, K., Scott, H., Heino, M., Kudoh, J., Shimizu, N., Antonarakis, S. E., and Krohn, K. J. E. (1998) APECED: a monogenic autoimmune disease providing new clues to self-tolerance, *Immunology Today 19*, 384–6.
116. Jiang, W., Anderson, M. S., Bronson, R., Mathis, D., and Benoist, C. (2005) Modifier loci condition autoimmunity provoked by Aire deficiency, *The Journal of Experimental Medicine 202*, 805–15.
117. Picelli, S., Björklund, Å. K. K., Faridani, O. R., Sagasser, S., Winberg, G., and Sandberg, R. (2013) Smart-seq2 for sensitive full-length transcriptome profiling in single cells, *Nature Methods 10*, 1096–8.
118. Brennecke, P., Anders, S., Kim, J. K., Kołodziejczyk, A. A., Zhang, X., Proserpio, V., Baying, B., Benes, V., Teichmann, S. A., Marioni, J. C., and Heisler, M. G. (2013) Accounting for technical noise in single-cell RNA-seq experiments, *Nature Methods 10*, 1093–5.

119. Kharchenko, P. V., Silberstein, L., and Scadden, D. T. (2014) Bayesian approach to single-cell differential expression analysis, *Nature Methods 11*, 740–2.
120. Huang, D. W. a W., Sherman, B. T., and Lempicki, R. A. (2009) Systematic and integrative analysis of large gene lists using DAVID bioinformatics resources, *Nature Protocol 4*, 44–57.
121. Lewandoski, M. (2001) Conditional control of gene expression in the mouse, *Nature Review Genetic 2*, 743–55.
122. Ohigashi, I., Zuklys, S., Sakata, M., Mayer, C. E., Hamazaki, Y., Minato, N., Holländer, G. A., and Takahama, Y. (2015) Adult thymic medullary epithelium is maintained and regenerated by lineage-restricted cells rather than bipotent progenitors, *Cell Reports 13*, 1432–43.
123. Nehls, M., Pfeifer, D., Schorpp, M., Hedrich, H., and Boehm, T. (1994) New member of the winged-helix protein family disrupted in mouse and rat nude mutations, *Nature 372*, 103–7.
124. Zuklys, S., Handel, A., Zhanybekova, S., Govani, F., Keller, M., Maio, S., Mayer, C. E., Teh, H. Y., Hafen, K., Gallone, G., Barthlott, T., Ponting, C. P., and Holländer, G. A. (2016) Foxn1 regulates key target genes essential for T cell development in postnatal thymic epithelial cells, *Nature Immunology 17*, 1206–15.
125. Zuklys, S., Gill, J., Keller, M. P., Hauri-Hohl, M., Zhanybekova, S., Balciunaite, G., Na, K.-J. J., Jeker, L. T., Hafen, K., Tsukamoto, N., Amagai, T., Taketo, M. M., Krenger, W., and Holländer, G. A. (2009) Stabilized beta-catenin in thymic epithelial cells blocks thymus development and function, *Journal of Immunology 182*, 2997–3007.
126. Gray, D., Abramson, J., Benoist, C., and Mathis, D. (2007) Proliferative arrest and rapid turnover of thymic epithelial cells expressing Aire, *The Journal of Experimental Medicine 204*, 2521–2528.
127. Alves, N. L., Huntington, N. D., Rodewald, H.-R. R., and Di Santo, J. P. (2009) Thymic epithelial cells: the multi-tasking framework of the T cell "cradle", *Trends Immunology 30*, 468–74.
128. Akiyama, T., Shimo, Y., Yanai, H., Qin, J., Ohshima, D., Maruyama, Y., Asaumi, Y., Kitazawa, J., Takayanagi, H., Penninger, J. M., Matsumoto, M., Nitta, T., Takahama, Y., and Inoue, J.-I. (2008) The tumor necrosis factor family receptors RANK and CD40 cooperatively establish the thymic medullary microenvironment and self-tolerance, *Immunity 29*, 423–37.
129. Yamashita, I., Nagata, T., Tada, T., and Nakayama, T. (1993) CD69 cell surface expression identifies developing thymocytes which audition for T cell antigen receptor-mediated positive selection, *International Immunology 5*, 1139–50.
130. Azzam, H. S., Grinberg, A., Lui, K., Shen, H., Shores, E. W., and Love, P. E. (1998) CD5 expression is developmentally regulated by T cell receptor (TCR) signals and TCR avidity, *The Journal of Experimental Medicine 188*, 2301–

11.
131. Dolton, G., Tungatt, K., Lloyd, A., Bianchi, V., Theaker, S. M., Trimby, A., Holland, C. J., Donia, M., Godkin, A. J., Cole, D. K., Straten, P. T., Peakman, M., Svane, I. M., and Sewell, A. K. (2015) More tricks with tetramers: a practical guide to staining T cells with peptide-MHC multimers, *Immunology 146*, 11–22.
132. Day, C. L., Seth, N. P., Lucas, M., Appel, H., Gauthier, L., Lauer, G. M., Robbins, G. K., Szczepiorkowski, Z. M., Casson, D. R., Chung, R. T., Bell, S., Harcourt, G., Walker, B. D., Klenerman, P., and Wucherpfennig, K. W. (2003) Ex vivo analysis of human memory CD4 T cells specific for hepatitis C virus using MHC class II tetramers, *Journal of Clinlcal Investigation 112*, 831–42.
133. Thiault, N., Darrigues, J., Adoue, V., Gros, M., Binet, B., Perals, C., Leobon, B., Fazilleau, N., Joffre, O. P., Robey, E. A., van Meerwijk, J. P., and Romagnoli, P. (2015) Peripheral regulatory T lymphocytes recirculating to the thymus suppress the development of their precursors, *Nature Immunology 16*, 628–34.
134. Schwartz, R. H. (2003) T cell anergy, *Annu. Rev. Immunol. 21*, 305–34.
135. Martinez, R. J., Zhang, N., Thomas, S. R., Nandiwada, S. L., Jenkins, M. K., Binstadt, B. A., and Mueller, D. L. (2012) Arthritogenic self-reactive CD4+ T cells acquire an FR4hiCD73hi anergic state in the presence of Foxp3+ regulatory T cells, *Journal of Immunology 188*, 170–81.
136. Adler, A. J., Marsh, D. W., Yochum, G. S., Guzzo, J. L., Nigam, A., Nelson, W. G., and Pardoll, D. M. (1998) CD4+ T cell tolerance to parenchymal self-antigens requires presentation by bone marrow-derived antigen-presenting cells, *The Journal of Experimental Medicine 187*, 1555–64.
137. Ucar, O., and Rattay, K. (2015) Promiscuous Gene Expression in the Thymus: A Matter of Epigenetics, miRNA, and More?, *Frontiers in Immunology 6*, 93.
138. Lin, J., Yang, L., Silva, H. M., Trzeciak, A., Choi, Y., Schwab, S. R., Dustin, M. L., and Lafaille, J. J. (2016) Increased generation of Foxp3+ regulatory T cells by manipulating antigen presentation in the thymus, *Nature Communications 7*.
139. Shi, J., Getun, I., Torres, B., and Petrie, H. (2016) Foxn1[Cre] Expression in the Male Germline., *Plos One 11*, e0166967.
140. Ripen, A., Nitta, T., Murata, S., Tanaka, K., and Takahama, Y. (2011) Ontogeny of thymic cortical epithelial cells expressing the thymoproteasome subunit β5t, *European Journal of Immunology 41*, 1278–1287.
141. Singarapu, N., Xie, H., Orkin, S., and Richie, E. (2015) Targeted deletion of Eed arrests thymus development, Conference abstract for The American Association of Immunologists.
142. Delassus, S., and Cumano, A. (1996) Circulation of hematopoietic progenitors in the mouse embryo, *Immunity 4*, 97–106.
143. Jenkinson, W. E., Jenkinson, E. J., and Anderson, G. (2003) Differential

requirement for mesenchyme in the proliferation and maturation of thymic epithelial progenitors, *Journal of Experimental Medicine 198*, 325–32.
144. He, A., Shen, X., Ma, Q., Cao, J., Gise, A., Zhou, P., Wang, G., Marquez, V. E., Orkin, S. H., and Pu, W. T. (2012) PRC2 directly methylates GATA4 and represses its transcriptional activity, *Genes & Development 26*, 37–42.
145. Sano, S., Takahama, Y., Sugawara, T., Kosaka, H., Itami, S., Yoshikawa, K., Miyazaki, J., Ewijk, W., and Takeda, J. (2001) Stat3 in thymic epithelial cells is essential for postnatal maintenance of thymic architecture and thymocyte survival, *Immunity 15*, 261–73.
146. Alves, N. L., Takahama, Y., Ohigashi, I., Ribeiro, A. R., Baik, S., Anderson, G., and Jenkinson, W. E. (2014) Serial progression of cortical and medullary thymic epithelial microenvironments, *European Journal of Immunology 44*, 16–22.
147. Bennett, A. R., Farley, A., Blair, N. F., Gordon, J., Sharp, L., and Blackburn, C. C. (2002) Identification and characterization of thymic epithelial progenitor cells, *Immunity 16*, 803–14.
148. Chiacchiera, F., Rossi, A., Jammula, S., Zanotti, M., and Pasini, D. (2016) PRC2 preserves intestinal progenitors and restricts secretory lineage commitment, *The EMBO Journal 35*, 2301–14.
149. Bardot, E. S., Valdes, V. J., Zhang, J., Perdigoto, C. N., Nicolis, S., Hearn, S. A., Silva, J. M., and Ezhkova, E. (2013) Polycomb subunits Ezh1 and Ezh2 regulate the Merkel cell differentiation program in skin stem cells, *The EMBO Journal 32*, 1990–2000.
150. Hikosaka, Y., Nitta, T., Ohigashi, I., Yano, K., Ishimaru, N., Hayashi, Y., Matsumoto, M., Matsuo, K., Penninger, J. M., Takayanagi, H., Yokota, Y., Yamada, H., Yoshikai, Y., Inoue, J., Akiyama, T., and Takahama, Y. (2008) The cytokine RANKL produced by positively selected thymocytes fosters medullary thymic epithelial cells that express autoimmune regulator, *Immunity 29*, 438–50.
151. Boehm, T., Scheu, S., Pfeffer, K., and Bleul, C. C. (2003) Thymic medullary epithelial cell differentiation, thymocyte emigration, and the control of autoimmunity require lympho-epithelial cross talk via LT-R, *The Journal of Experimental Medicine 198*, 757–69.
152. Nowell, C. S., Bredenkamp, N., Tetélin, S., Jin, X., Tischner, C., Vaidya, H., Sheridan, J. M., Stenhouse, F. H., Heussen, R., Smith, A. J., and Blackburn, C. C. (2011) Foxn1 regulates lineage progression in cortical and medullary thymic epithelial cells but is dispensable for medullary sublineage divergence., *PLoS Genetic 7*, e1002348.
153. White, A. J., Withers, D. R., Parnell, S. M., Scott, H. S., Finke, D., Lane, P. J., Jenkinson, E. J., and Anderson, G. (2008) Sequential phases in the development of Aire-expressing medullary thymic epithelial cells involve distinct cellular input, *European Journal of Immunology 38*, 942–7.
154. Rossi, S. W., Kim, M.-Y., Leibbrandt, A., Parnell, S. M., Jenkinson, W. E.,

Glanville, S. H., McConnell, F. M., Scott, H. S., Penninger, J. M., and Jenkinson, E. J. (2007) RANK signals from CD4+ 3- inducer cells regulate development of Aire-expressing epithelial cells in the thymic medulla, *Journal of Experimental Medicine 204*, 1267–72.
155. Cao, R., Wang, L., Wang, H., Xia, L., Erdjument-Bromage, H., Tempst, P., Jones, R. S., and Zhang, Y. (2002) Role of histone H3 lysine 27 methylation in Polycomb-group silencing, *Science 298*, 1039–43.
156. White, A. J., Nakamura, K., Jenkinson, W. E., Saini, M., Sinclair, C., Seddon, B., Narendran, P., Pfeffer, K., Nitta, T., Takahama, Y., Caamano, J. H., Lane, P. J., Jenkinson, E. J., and Anderson, G. (2010) Lymphotoxin signals from positively selected thymocytes regulate the terminal differentiation of medullary thymic epithelial cells, *Journal of Immunology 185*, 4769–76.
157. Hamazaki, Y., Fujita, H., Kobayashi, T., Choi, Y., Scott, H. S., Matsumoto, M., and Minato, N. (2007) Medullary thymic epithelial cells expressing Aire represent a unique lineage derived from cells expressing claudin, *Nature Immunology 8*, 304–11.
158. Liang, C.-C., You, L.-R., Yen, J., Liao, N.-S., Yang-Yen, H.-F., and Chen, C.-M. (2013) Thymic epithelial β-catenin is required for adult thymic homeostasis and function, *Immunology & Cell Biology 91*, 511–523.
159. Ramsey, C., Winqvist, O., Puhakka, L., Halonen, M., Moro, A., Kämpe, O., Eskelin, P., Pelto-Huikko, M., and Peltonen, L. (2002) Aire deficient mice develop multiple features of APECED phenotype and show altered immune response, *Human Molecular Genetics 11*, 397–409.
160. Liston, A., Lesage, S., Wilson, J., Peltonen, L., and Goodnow, C. C. (2003) Aire regulates negative selection of organ-specific T cells, *Nature Immunology 4*, 350–354.
161. Derbinski, J., Gäbler, J., Brors, B., Tierling, S., Jonnakuty, S., Hergenhahn, M., Peltonen, L., Walter, J., and Kyewski, B. (2005) Promiscuous gene expression in thymic epithelial cells is regulated at multiple levels, *Journal of Experimental Medicine 202*, 33–45.
162. Heeger, P. S., Smoyer, W. E., Jones, M., Hopfer, S., and Neilson, E. G. (1996) Heterogeneous T cell receptor V gene repertoire in murine interstitial nephritis, *Kidney International 49*, 1222–1230.
163. Kalekar, L. A., Schmiel, S. E., Nandiwada, S. L., Lam, W. Y., Barsness, L. O., Zhang, N., Stritesky, G. L., Deepali, Pauken, K. E., Linehan, J. L., O'Sullivan, M. G., Fife, B. T., Hogquist, K. A., Jenkins, M. K., and Müller, D. L. (2016) CD4+ T cell anergy prevents autoimmunity and generates regulatory T cell precursors, *Nature Immunology 17*, 304–15.
164. Jeon, M.-S. S., Atfield, A., Venuprasad, K., Krawczyk, C., Sarao, R., Elly, C., Yang, C., Arya, S., Bachmaier, K., Su, L., Bouchard, D., Jones, R., Gronski, M., Ohashi, P., Wada, T., Bloom, D., Fathman, C. G., Liu, Y.-C. C., and Penninger, J. M. (2004) Essential role of the E3 ubiquitin ligase Cbl-b in T cell anergy induction., *Immunity 21*, 167–77.

165. Zha, Y., Marks, R., Ho, A. W., Peterson, A. C., Janardhan, S., Brown, I., Praveen, K., Stang, S., Stone, J. C., and Gajewski, T. F. (2006) T cell anergy is reversed by active Ras and is regulated by diacylglycerol kinase-alpha., *Nature Immunology 7*, 1166–73.
166. Anderson, M. S., Venanzi, E. S., Klein, L., Chen, Z., Berzins, S. P., Turley, S. J., von Boehmer, H., Bronson, R., Dierich, A., Benoist, C., and Mathis, D. (2002) Projection of an immunological self shadow within the thymus by the Aire protein, *Science 298*, 1395–401.
167. Jameson, S. C. (2002) Maintaining the norm: T-cell homeostasis., *Nature Review Immunology 2*, 547–56.
168. Kieper, W. C., and Jameson, S. C. (1999) Homeostatic expansion and phenotypic conversion of naïve T cells in response to self peptide/MHC ligands., *Proceedings of the National Academy of Sciences of the United States of America 96*, 13306–11.